SCUOLA DI DOTTORATO

UNIVERSITÀ DEGLI STUDI DI MILANO-BICOCCA

Dipartimento di / Department of

School of Medicine and Surgery

Dottorato di Ricerca in / PhD program **DIMET** Ciclo / Cycle **XXXI**

The multifaceted identity of endothelial cells: the role of Endothelial to Mesenchymal Transition in shifting the balance between vessels and bones

Cognome / Surname **Giovenzana** Nome / Name **Anna**

Matricola / Registration number **722615**

Tutore / Tutor: **Prof. Silvia Brunelli**

Cotutore / Co-tutor: **PhD. Gonzalo Sánchez-Duffhues**

Coordinatore / Coordinator: **Prof. Andrea Biondi**

ANNO ACCADEMICO / ACADEMIC YEAR 2017/2018

TABLE OF CONTENTS

CHAPTER 1

1. General introduction

1.1 Physiological endothelial cells activation in tissue repair

With a turnover of 100 days, endothelial cells (EC) are one of the most static cells of the human body, by lining the entire vascular system with an inner single layer they accomplish several functions, in addition to supply tissues with blood, oxygen and nutrients, they are involved in the regulation of PH, blood pressure, coagulation and host defence (1,2).

Besides being the gatekeeper of blood homeostatic conditions endothelial cells perform other necessary physiological tasks: sustaining the homeostasis of resident stem cells and guiding the regeneration and repair of adult organs without provoking fibrosis.

Tissues belonging to skeletal system, skin, liver and muscle system show an impressive capacity of regeneration, when a damage occurs the restoration of tissue integrity and function comes along and is highly interconnected to the re-establish of vessels network (3).

1.1.1 Angiogenesis

The re-establish of vasculature after a damage occurs through neovascularization and angiogenesis. Angiogenesis is the development of vessels network starting from pre-existing vessels,

while neovascularization is a de novo process mainly present and better characterized in embryo (4).

Usually ECs cells lining blood vessel are in a quiescent state, showing a cobblestone appearance and associated with poor migratory and proliferative activity. Upon damage or in presence of hypoxia signals they turn into an “activated” phenotype that leads to proliferation and migration toward the stimuli released by the demanding tissue. The formation of new vessels requires complex and morphologic changes comprising sprouting morphogenesis, intussusceptive growth, splitting, remodeling, stabilization and differentiation into arterioles, venules and capillaries (5).

1.1.1.1 Tip-stalk model

The cellular and molecular mechanism underlying angiogenic sprouting process have been quite elucidated and described with the tip-stalk model (6).

When sprouting takes place it is possible to distinguish two different types of ECs: tip and stalk, tip cells are the “leaders” cells that start the migration toward the local environmental stimuli and guide the “followers” (stalk cells), that rapidly proliferate and build the physical structure of the vessels.

Leader cells at the front row or in the tip position in a migrating chain of cells (therefore, also called tip cells), show a more polarized morphology and generate more cytoskeletal dynamics than the

follower (to leaders in sheets) or stalk (to tip cells in chains) cells. Leading cells also form a clear lamellipodium and are often less ordered and mesenchyme-like. These differences in polarity are a consequence of a differential expression of surface receptors, like those for chemokines.

Tip and stalk cells do not represent two definitive states of endothelial differentiation, but the shift between the two types is highly dynamic and reversible (6).

Selection of tip cell is the first event of sprouting: it is important that only one cells acquires tip phenotype otherwise the migration would be disorganized and unfunctional. This process is influenced by environmental molecules and mainly governed by VEGF and Notch pathway (7,8).

VEGF is present in the tissue, acts as a chemoattractant by binding VEGFR2 and enhances the expression of Dll4. Dll4 is produced by endothelial cells and binds its receptor Notch1 expressed by neighbouring ECs. Activation of Notch signalling leads to inhibition of VEGFR2 production and indirectly also to a decrease of Dll4. Due to stochastic different levels of VEGF in the environment, regulation of VEGF and Notch pathway results into an unbalance of VEGFR2-Notch pathway activation in adjacent ECs: cells with high Dll4 expression will be selected as tip cells, on the contrary, high Notch activity cells become stalk.

Tip cells are migratory and polarized; they extend long filopodia that scan the environment for attractant or repellent signals, and hence

serve to guide new blood vessels in the direction of the chemotactic stimulus. In order to migrate cytoplasm of migrating cells undergo to spatially and temporal changes that begin with cell polarization (9). Different molecules like, PIP3 and Cdc42 show a particular intracellular localization that induces sub sequential cytoskeleton rearrangements starting with filipodia and lamellipodium formation (10,11), followed by the establishment of adhesion complex between cell and ECM at the leading edge, disruption of focal adhesion at the rear front and contraction of actin and myosin filaments to enable the forward movement (12).

An endothelial tip cell guides the developing capillary sprout through the ECM toward an angiogenic stimulus such as VEGF-A (9). Filopodia secrete large amounts of proteolytic enzymes, which digest a pathway through the ECM for the developing sprout (13). The filopodia of tip cells are heavily endowed with VEGF-A receptors (VEGFR2), allowing them to “sense” differences in VEGF-A concentrations and causing them to align with the VEGF-A gradient. Meanwhile, stalk cells proliferate as they follow behind a tip cell causing the capillary sprout to elongate. Vacuoles develop and coalesce, forming a lumen within a series of stalk cells. These stalk cells become the trunk of the newly formed capillary. When the tip cells of two or more capillary sprouts converge at the source of VEGF-A secretion, the tip cells fuse together creating a continuous lumen through which oxygenated blood can flow. When the local tissues receive adequate amounts of oxygen, VEGF-A levels return to near normal. Maturation and stabilization of

the capillary requires recruitment of pericytes and deposition of ECM along with shear stress and other mechanical signals (14).

1.1.1.2 New players in angiogenesis regulation

A recent work unveiled the role of RNA editing in controlling sprouting angiogenesis in endothelial cells.

The work of Stellos et al. (15), shows that silencing Adar1, an enzyme able to edit RNA by converting adenosine in inosine, causes a significant inhibition of angiogenic sprouting in HUVEC, while overexpression of Adar1 results in an increase in endothelial cell sprouting. The effect is mediated by the increased cathepsin S expression as a result of editing activity. Cathepsin S, is a cysteine protease with elastolytic and collagenolytic activities, is expressed in endothelial cells and various other cell types, and it controls extracellular matrix protein degradation, antigen presentation (16,17) and angiogenesis. Another work (18) demonstrates how A-to-I RNA editing changes the targetoma of microRNA-487b in human vascular cells stimulating multiple proangiogenic pathways.

1.1.1.3 Contribution of macrophages to angiogenesis

The reconstruction of blood vessel network is a complex process in which also non endothelial cells participate at multiple levels. Multiple kind of interactions exist between endothelial cells and macrophages.

Evidences of macrophage-endothelium collaboration in vasculature establishment is found during development, wound healing repair and in cancer (19).

Macrophages are an heterogeneous population of phagocytic cells that vary for their origin, function and spectrum of cytokines. Macrophages can be mainly
divided in two groups depending on the phenotype induced by different cytokines: classical M1 macrophages are stimulated by TLR ligands and IFN-γ, while stimulation with IL-4/IL-13 leads to alternative M2 macrophages (20). The M1 phenotype is characterized by the expression of high levels of proinflammatory cytokines, high production of reactive nitrogen and oxygen intermediates, promotion of Th1 response, and strong microbicidal and tumoricidal activity. In contrast, M2 macrophages are considered to be involved in parasite containment and promotion of tissue remodeling and tumor progression and endowed with immunoregulatory functions. However this classification has been defined on the base of *in vitro* polarization experiments, *in vivo* situation is much more complex and it has been suggested that M1 and M2 phenotypes represents the extremes of a continuum in a universe of activation states (21).
Regarding the role of MP in angiogenesis, MP produce VEGF, but their effect is not only restricted to the production of this proangiogenic factor (22). It has been demonstrated that during hindbrain development, MP promote vascular anastomosis by physically assisting endothelial tip cell fusion through direct cell-to-cell contacts

(23). Similar finding has been shown also for in the developing retina where MP increase the number of numbers of filopodia-bearing sprouts and influence the orientation of sprouts, in macrophage-deficient mice retinal vascular sprouts were fewer and mostly radially-oriented, whereas those of wild-type mice displayed much higher complexity and were both radially- and forward-oriented, thus forming more intersections (24).

MP can influence not only the sprouting and anastomosis but have also been implicated in the post-natal remodeling of the retinal vasculature (25).

Noteworthy, also cancer provides some insights of functions of MP on vasculature, a particular type of MP, named TIE2-expressing macrophages (TEMs), physically interact with tumor blood vessels and promote angiogenesis in mouse tumor models (26).

During wound-healing, studies show that MP recruited during the diverse phases of skin repair (i.e., the inflammatory; tissue formation; and tissue maturation phases) exert distinct functions: in particular, macrophages appear to play an important role in promoting angiogenesis in the granulation tissue during the early phase of skin repair; vascular maturation and stabilization in the subsequent phases (27).

In addition to macrophages, also fibroblasts and pericytes play important role during tissue repair and angiogenesis.

It is known that the deposition of ECM by fibroblasts after a tissue damage constitutes a temporary scaffold, but fibroblasts can also affect angiogenesis by releasing angiopoietin-1 (ANG-1), angiogenin,

hepatocyte growth factor (HGF), transforming growth factor-α (TGFB-α), and tumor necrosis factor (TNFα) and VEGF that increase sprouting, while secretion of collagen I, procollagen C endopeptidase enhancer 1, secreted protein acidic and rich in cysteine, transforming growth factor-β–induced protein ig-h3, and insulin growth factor–binding protein 7 enhance lumen formation (28).

Pericytes are defined morphologically as periendothelial support cells that elongate and wrap along ECs. Through transbasement membrane interactions, pericytes are thought to regulate capillary diameter and physically influence EC behaviour. Regarding the angiogenesis, pericytes have been shown to both stabilize and promote capillary sprouting (29). The prominent signaling pathways are PDGF-B/PDGFR-β, angiopoietin 1 (Ang1)/Tie2 and transforming growth factor-β (TGFβ) (30), which regulate pericyte recruitment, EC viability and mural cell differentiation, respectively. Pericytes can also influence the local extracellular matrix (ECM) to guide endothelial migration by modulating deposition of basement and they have also been shown to lead sprouting ECs and bridge the gaps between two sprouting segments in some cases.

1.1.2 Instructive niche

The importance of circulatory system is not important in tissue regeneration just for supplying nutrients and oxygen, but genetic and biochemical studies have shown that ECs serve as a fertile, instructive

niche that plays key roles in directing organ regeneration in a "perfusion-independent". Angiocrine factors are paracrine factors released by ECs comprising stimulatory and inhibitory growth factors, morphogens, extracellular matrix and chemokines that act on the repopulating cells.

Instructive functions of ECs have been demonstrated in studies showing that the deletion of angiocrine factors in adult ECs disrupts stem-cell homeostasis and impairs organ repair without compromising blood supply (3).

The ability of endothelial cells to model the niche to guide the proper differentiation of surrounding cells relies on the existence of endothelial cells with specific tissue-identity. For example, in bone tissues it is possible to recognizes a type of capillaries with a specific function: capillaries with high expression of CD31 and Endomucin (type H) are found closely associates with osteoprogenitors influencing their proliferation (31).

Mounting evidence show that EC are organ-specific and have a unique profile able to promote proliferation or differentiation of specific stem cells during development and in regenerating conditions (32).

Noteworthy, partial hepatectomy reveals the contribution of liver sinusoidal ECs to regeneration process (33). During the initial angiogenesis-independent inductive phase, which occurs 1–4 days after partial hepatectomy, VEGFR-2–AKT-dependent upregulation of transcription factor Id1 in non-proliferating liver sinusoidal ECs stimulates the expression of Wnt2 and hepatocyte growth factor (HGF). Activation of VEGFR-1 on non-angiogenic liver sinusoidal ECs

also induces the production of HGF and other pro-hepatic factors, such as heparin-binding EGF (HB-EGF), TGF-α and connective tissue growth factor (CTGF), to drive liver regeneration (34). On days 4–12 after partial hepatectomy, liver sinusoidal ECs promote proliferative angiogenesis to meet the metabolic demands of the enlarging liver. Putative bone-marrow-derived ECs that co-express CD133, CD45 and CD31 and have the capacity to produce HGF can also engraft into populations of regenerating liver sinusoidal ECs, which helps to boost regeneration of the liver (35).

1.1.3 A particular regenerating niche: the muscle tissue

Muscle niche is another proof of EC potential in guarding homeostasis and driving regeneration after a damage.
It has been known for more than a century that skeletal muscle, the most abundant tissue of the body, has the ability to regenerate new muscle fibers after it has been damaged by injury or as a consequence of diseases such as muscular dystrophy (36).

The disruption of muscle architecture is followed by a precise multi-phase process in which several cell types, in particular immune cells, fibroblasts, pericytes, fibroadipogenic (FAP) cells and endothelial cells, take part in the repair following a highly complex cascade and with distinct temporal and spatial kinetics (37).

1.1.3.1 Satellite cells

Muscle is composed by multinucleated fibers, syncytial cells that contain several hundred nuclei within a continuous cytoplasm. Fibers regeneration mainly relies on the presence of muscle stem cells: satellite cells (SC), SC are found underneath the basal lamina of muscle fibers, closely juxtaposed to the plasma membrane. Under steady-state conditions SCs are present in adult mammalian muscle as quiescent cells and represent 2.5%–6% of all nuclei of a given muscle fiber. However, when activated by muscle injury, they can generate large numbers of new myofibers within just a few days (38).

Three different basic states can be recognized in SCs: quiescence, proliferation and differentiation. In homeostatic conditions the environment remains essentially static and imposes signals that promote the quiescent stem cell state. Several studies have identified the Notch receptors as being critical for the maintenance of satellite cell quiescence. In these conditions SCs express Pax7 and Pax3 genes (38).

Upon injury the cell niche changes rapidly and leads to the activation and proliferation of SCs. At this stage, they are often referred to as either myogenic precursor cells (mpc) or myoblasts. Several signals, deriving both from damaged fibers and infiltrating cells, are involved in SC activation, including HGF, FGF, IGF, and NO (39,40). The progression of activated SCs toward myogenic differentiation is mainly controlled by Myf5 and MyoD. Once differentiated into myocytes, the cells will align and form new syncytial muscle fibres or fuse to existing

fibres. On completion of this regenerative response, the tissue returns to its homeostatic state and the resident cell populations re-enter a resting state (41).

A pool of undifferentiated SCs is maintained within the muscle, thanks to asymmetrical divisions, one of the daughter cell does not express Myf5, is not primed to myogenic differentiation and returns to quiescent state (42).

1.1.3.2 Immune cells in the muscle regenerating niche

Satellite cells and their progeny are essential for muscle regeneration, but their presence alone is insufficient for muscle regeneration; the cells must have the capacity to proceed through the sequence of activation, proliferation and differentiation, the immune system plays a pivotal role in guiding these sequential stages in multiple ways.

Although they appear scant in histological observations, a surprisingly high number is present within muscle tissue: there are 500 to 2,000 leukocytes per mm^3 of adult, rodent limb muscles, which is equivalent to approximately 10^9 leukocytes per litre of muscle. Although intramuscular leukocytes comprise various cell types, including CD8+ cytotoxic T cells, regulatory T (Treg) cells, neutrophils and eosinophils, each population constitutes a small proportion of the total leukocyte population in healthy muscle. The vast majority of intramuscular leukocytes are monocytes or macrophages located primarily in either

the sheath of connective tissue that surrounds entire muscles or near blood vessels.

Muscle damage triggers a well-orchestrated inflammatory response in which the number of intramuscular leukocytes can rapidly increase more than 100-fold. Within hours after a damage, neutrophils invade damaged muscle and reach maximum numbers at approximately 12 to 24 hours post injury, after which they rapidly return to near-normal numbers (43,44).

In addition to support angiogenesis, as discussed above, macrophages hold specific tasks in muscle regeneration.

Resident macrophages (that express F4/80, LY6C and CD11b, but lack expression of CXC-chemokine receptor 1 (CXCR1)) promote this marked neutrophil influx by releasing the neutrophil chemo attractants CXC- chemokine ligand 1 (CXCL1) and CC-chemokine ligand 2 (CCL2).

Neutrophils invasion contributes to the establishment of a pro-inflammatory environment. Following their invasion, circulating monocytes and macrophages extravasate and enter a muscle tissue that is enriched with pro-inflammatory cytokines, including interferon-γ (IFNγ) and tumour necrosis factor (TNFα). Together, these cytokines can activate macrophages to a pro-inflammatory phenotype (M1 macrophages).

M1 MP number reaches a peak approximately 48 hours after damage and then starts to reduce, 4 days later they are barely detected. It has

been demonstrated that M1 MP phagocyte cellular debris and damaged fibers creating space for new tissue, but they also affect SCs. By promoting a proinflammatory environment they sustain proliferation of myogenic cells and reduces their differentiation and fusion capacity (43).

In particular, the proliferative M1 effect seems to be mediated by IFN-γ: inducing CIITA expression suppresses the expression of myogenin, an essential transcription factor for muscle terminal differentiation. Maintaining myoblasts in a proliferative, non-differentiated state, they expand and support tissue repair. Also the release of insulin-like growth factor 1 (IGF1), a strong mitogen for MPCs in muscle, sustains myoblasts expansions (45).

Histological observations show a shift from M1 to M2 phenotype with the proceeding of muscle regeneration: the peak number of CD68hi CD163−phagocytic M1 macrophages that occurred 2 days post injury was replaced by a population of non-phagocytic CD68low CD163+ M2 macrophages that reached peak numbers approximately 4 to 7 days post injury, coinciding with the expression of genes that are markers of terminal differentiation.

M2 macrophages participate to muscle regeneration by mitigating inflammatory response and promoting myoblasts differentiation.

Transition from M1 to M2 phenotype is controlled by cytokines but is also regulated by muscle cells, remarking again the strict correlation between the two systems during muscle regeneration.

It has been demonstrated that IL-10 induces M1-M2 transition, the loss of the IL-10-mediated phenotype switch caused impairments of regeneration resembling those caused by deletion of F4/80+ or CD11b+ cells42. In addition to IL-10, also IGF1 promotes M1-M2 transition (43).

Also the removal of debris promotes M2 phenotype, macrophage phagocytosis of apoptotic neutrophils suppressed the expression of TNFα, and phagocytosis of necrotic or apoptotic neutrophils increased the expression of TGFβ, which indicates a shift towards an M2-biased phenotype.

CD163, a M2 marker, regulates macrophage phenotype and plays an active role in the late phase of the regeneration. CD163 is a transmembrane glycoprotein, by binding haemoglobin– haptoglobin complexes, enables the complexes to be internalized and degraded. This is important in regeneration because haemolysis in injured tissue causes local and toxic elevations of haemoglobin that amplify damage.

Similarly, CD206 mediates M2 macrophage functions that can lead to a reduction of muscle inflammation and damage. CD206 is a mannose receptor that binds and internalizes sugar moieties on molecules present at high levels in inflamed tissue. In the context of muscle damage and regeneration, MPO is an important ligand for CD206 because it serves a prominent role in muscle membrane lysis that is caused by neutrophils, and its ligation and internalization by M2 macrophages would reduce cytotoxicity. CD206 expression by M2 macrophages is promoted by anti-inflammatory cytokines, and its

binding increases the expression of anti-inflammatory cytokines, leading to positive feedback that can enable M2 macrophages to more rapidly deactivate Th1 cells that are capable of free radical-mediated damage of muscle cells (46).

Supporting role of M2 macrophages on myoblast differentiation is suggested by macrophage depletion between days 2 and 4. Normally, MyoD-expressing muscle cells decrease in number and myogenin-expressing muscle cells increase in numbers between days 2 and 4 , reflecting the withdrawal of myogenic cells from the cell cycle, as they transition to early differentiation. Instead, numbers of MyoD-positive cells remained elevated, and myogenin expression does not increase in the macrophage-depleted muscles (47).

1.1.3.3 Endothelial cells in the muscle regenerating niche

As already mentioned, EC cells are pivotal players in regenerating process, specific mechanisms have been discovered in the muscle niche . The location of SCs suggests that EC are privileged partners: in normal human adult muscle, satellite cells are localized at the proximity of capillaries (88% at less than 21 µm of a capillary) (48).

One of the most important crosstalk between myogenic cells and EC is represented by VEGF signalling. During skeletal muscle regeneration, angiogenesis and myogenesis proceed at the same time as formation of new capillaries and formation of new myofibers are observed concomitantly. The delivery of AAV-VEGF markedly improved muscle

fibre reconstitution in ischemic limb. Inversely, in mice exhibiting delay and impairment of muscle regeneration (CCR2-/-mice), VEGF level is decreased until day 21, time of restoration of maximal capillary density. The authors showed that maximal capillary density developed concurrent with the restoration of tissue VEGF, and observed an inverse relationship between the size of regenerated muscle fibres and the number of capillaries (49).

VEGF has been shown to be expressed by satellite cells, myogenic cells, and particularly by differentiating myogenic cells and regenerating myofibres. Importantly, VEGF secreted by myogenic cells confers an angiogenic activity to the myogenic cells. As myogenic cells bear the VEGF-R, it also acts by stimulating their migration and protecting them from apoptosis. VEGF participates also to the myogenic differentiation programme through its regulation by the myogenic transcription factor MyoD (50).

Also FGF signalling has shown a double effect in muscle repair enhancing both myofibers growth and angiogenesis: myogenic cells express bFGF that leads to angiogenesis in a paracrine fashion to help muscle regeneration in ischemic limb, while introducing FGF2 or FGF6 transgenes into muscle enhances the number of CD31+ structures, i.e., vessels, and muscle repair. (51,52)

Finally, Nerve Growth Factor (NGF) has been demonstrated to enhance angiogenesis and arteriogenesis after ischemia *in vivo* while it protects ECs and myofibres from apoptosis *in vitro* (53).

Another proof of endothelial capacity of promoting muscle repair is the release of factors like: IGF, HGF, and PDGF-BB that promote the growth of myogenic cells (53).

The importance of angiogenesis during muscle repair is not limited to the effect of endothelial cells, also pericytes and SMCs affect the repair. While EC stimulate the proliferation of satellite cells, pericytes and SMCs associated to vessels release Ang1 that acts on myogenic cells expressing its receptor Tie2. Ang1 signalling results in inhibition of their growth, promoting the appearance of the quiescent cell/ self-renewing population and the increase of the expression of markers associated with quiescence (Pax7, p130, M-cadherin, Myf5), while expression of markers associated with differentiation is decreased (MyoD, p57).

Although the effects of vessels and pericytes can appear opposite on myogenic cells: the timing of angiogenesis and fibers regeneration solves the incongruence: nascent vessels are lacking in pericytes and SMCs, in this way the pro-differentiation signals are released in the late phase of muscle regeneration (53).

It is evident how muscle damage activates a complex physiological response that requires the coordination of many different types of cells to re-establish the integrity and the function of the tissue. Endothelial cells carry out important tasks throughout the process, alterations in these cells can seriously compromise the outcome of regenerating process with different consequences.

1.2 Pathological endothelial cells activation: EndMT

1.2.1 Maintenance of endothelial identity

Even if endothelial cells are one of the most inactive cells in the body, they are rapidly activated upon damage and can quickly acquire pathological behaviour. If on the one hand endothelial cells are exposed to a myriad of stimuli that accounts for their marked plasticity, on the other, maintenance of endothelial identity is not a passive behaviour but requires a strong signature .

Endothelial cell-junctions are fundamental, not only to accomplish endothelium barrier function, but also to preserving endothelial identity. VE-Cadherin, the cell specific major organizer of endothelial cell-to-cell adherens junctions (54), through the interaction with a complex network of intracellular partners, transduces intracellular signals that mediate contact inhibition of cell growth, cell polarity and lumen formation. Disruption of VE-cadherin organization leads cells to grow in multiple layers, altering endothelium structure: they are unable to form a correct vascular lumen and establish adhesion contacts with the surrounding pericytes and smooth muscle cells (55).

FGF is the most important gate keeper of endothelial fate, its reduction causes loss of VE-cadherin-p120-catenin association and decreases VEGFR2 transcription leading to a compromised barrier function and to endothelial apoptosis (56,57).

When endothelial identity is threatened, endothelial cells can undergo a pathological process known as Endothelial to Mesenchymal Transition (EndMT) in which they convert into mesenchymal cells. FGF prevents this transition by blocking activation of TGFβ signalling cascade that is central to the induction of EndMT transition both in blood and lymphatic endothelial cells (58,59).

1.2.2 Loss of endothelial identity: EndMT

EndMT is characterized by loss of cell-cell junctions and endothelial markers: CD31, VE-Cadherin, Tie2, von Willebrand Factor with concomitant upregulation of mesenchymal markers like: N-cadherin, αSMA, transgelin, fibroblast specific protein (FSP)-1, vimentin and fibronectin. The acquirement of mesenchymal phenotype results in loss of cobble-stone appearance in favour of spindle morphology, in addition to deposition of ECM and highly migratory potential (60).

EndMT occurs naturally in the embryo as a physiological process of valve formation, but in the adult life is involved in the pathogenesis of several fibrotic diseases (60). The abundant presence of myofibroblasts is the main culprit in fibrosis leading to accumulation of fibrous connective tissue and excess of extracellular matrix (ECM) components, such as collagen and fibronectin in and around inflamed or damaged tissue. The increased expression of these genes is accompanied by a concomitant reduction in the activity of ECM degrading enzymes caused by the heightened production of Tissue

Inhibitors of Metalloproteinases also known as TIMPS. The altered tissue often brings about organ dysfunction and death.

Several theories have been proposed to explain the origin of myofibroblasts. Proliferation of resident fibroblasts was firstly hypothesized, but different works demonstrated alternative origins: bone marrow-derived CD34+ differentiate in myofibroblasts after migrating into the fibrotic area; macrophages and pericytes can also undergo to myofibroblasts differentiation. Finally, it has been shown that endothelial cells can give rise to myofibroblasts (61,62).

Involvement of EndMT has been described in many fibrotic disorders 63, 64, 65, 66, 67, 68) and it takes place also in skeletal muscle (69). In particular it has been demonstrated that in mice, depleting macrophages during muscle repair results in failure of vessels assembly, impairment of muscle repair, accumulation of collagen and αSMA+ cells. By taking advantage of endothelial lineage tracing mice the authors showed that endothelial cells lose CD31 expression and up-regulate Collagen I.

The molecular mechanism underlying this pathological transition in muscle has not been clarified yet, but is evident how macrophages do not just guide endothelial cells during angiogenesis but guard their identity and prevent pathological activation.

Considering the role of inflammation and in inducing EndMT, it is clear how orchestrated participation of immune cells accomplishes physiological functions in tissue repairing, while alterations of

inflammatory muscle environment affect muscle niche derailing the fate of endothelial cells and potentially of the entire tissue.

1.2.2.1 TGFβ pathway in regulating physiological and pathological endothelium

The molecular bases of EndMT encompass several pathways. One of the most studied pathway in driving EndMT is represented by TGFβ.

TGFβ is a multi-functional cytokine involved in the regulation of proliferation, differentiation, migration, and survival of many different cell types (70). The relevance of TGFβ signalling in endothelium is made clear by the number of mutations in TGFβ ligands, receptors or intracellular mediators that leads to embryo death for vascular failure and abnormalities (71). In post-natal life it is required during angiogenesis to induce differentiation of mesenchymal precursors in pericytes and smooth muscle cells.

TGFβ pathway is composed by 3 TGFβ ligands: TGFβ1, TGFβ2, TGFβ3 that in endothelial cells signal mainly through ALK1 or ALK5 receptors. These two receptors both bind TGFβR2 to activate the intracellular mediator: Smad proteins. Once phosphorylated by ALK1 or ALK5 Smad factors translocate into the nucleus where they activate TGFβ target genes (70).

TGFβ signalling in endothelial cells can have opposite effects depending on the cellular contest, the type of the receptor activated and the presence of coreceptors that can modulate the signal. Cellular

proliferation can be both induced and inhibited by TGFβ. Also the induction of protease activity and extracellular matrix remodelling are highly dependent on the source of ECs and culture conditions used (71).

The contrary effect can be in part explained by the fine balance between ALK1 and ALK5 transduced signalling. Whereas the TGFβ-h/ALK5 pathway leads to inhibition of EC migration and proliferation, the TGFβ-h/ALK1 pathway induces EC migration and proliferation. Transcriptional profiling using microarrays with constitutively active forms of ALK1 (caALK1) or ALK5 (caALK5) has demonstrated remarkable differences between the target genes regulated by ALK1 or ALK5 in ECs (72). ALK1 specifically stimulates the expression of Id-1, an inhibitor of basic helix-loop-helix (bHLH) proteins that promotes EC proliferation and migration. ALK5 specifically induces expression of fibronectin expression, an extracellular matrix protein, and the plasminogen activator inhibitor type 1 (PAI-1). PAI-1 is a negative regulator of EC migration *in vitro* (73) and angiogenesis *in vivo*.

The work of Goumans et al. (74) reveals a multilevel interplay between ALK1 and ALK5, since ALK5 is important for ALK1 recruitment in TGFβ receptor complex and kinase activity of ALK5 is essential for efficient ALK1 activation. In addition, ALK1 signalling is not only opposite to ALK5 but directly antagonizes ALK5/Smad2/3 signaling.

The molecular mechanism behind TGFβ induced EndMT involves the Snail family of transcription repressors. In mouse embryonic stem cell derived endothelial cells TGFβ induces EndMT and expression of Snail.

This upregulation of Snail TGFβ was shown to be dependent on the activation of Smad, MEK, PI3K and p38 MAPK by TGFβ (75). Subsequent knockdown of Snail blocked the TGFβ induced EndMT. Although overexpression of Snail was sufficient to induce for EndMT Snail expression alone is insufficient (76). The inhibitor of Snail, GSK-3β, needs to be inhibited by phosphorylation by kinases such as AKT to induce EndMT (75). Also Notch can induce EndMT in endothelial cells *in vitro* in a similar way and the Snail family member Slug has been shown to be play an important part in this pathway. Both Snail and Slug are known to repress the expression of VE-cadherin (77).

It has also been reported that other pathways than TGFβ can lead to EndMT. In myocardial infarction (MI) for example, canonical (β-catenin-dependent) Wnt signaling is induced 4 days after experimental MI in the subepicardial endothelial cells and perivascular cells. Coincidently with canonical Wnt activation EndMT was also triggered after the infarction. In addition, canonical Wnt signaling induced mesenchymal characteristics in cultured endothelial cells, suggesting a direct role of canonical Wnt signaling in EndMT (78).

1.2.2.2 The role of inflammation in EndMT

Accumulating evidence suggests that endothelial to mesenchymal transition (EndMT) represents a key link in the complex interactions between inflammatory stress and endothelial dysfunction (79).

Endothelial dysfunction is characterised by upset of the balance between vasodilation and vasoconstriction, inhibition and promotion of vascular smooth muscle proliferation, and prevention and stimulation of platelet aggregation, thrombogenesis, and fibrolysis by the endothelium. Many of these alterations, found in conditions like: angioplasty, stenting, diabetes, hypertension, and immune-mediated damage come along with inflammatory stress in vascular biology (80). Under conditions of chronic inflammation, sustained activation of ECs by inflammatory stimuli, such as interleukin (IL)-6, tumor necrosis factor-α (TNFα), IL-1β, and pathogens, causes alterations in normal endothelial function, resulting in impaired endothelial-dependent immune response, which is the hallmark of endothelial dysfunction (79).

Indeed, it has been reported that EndMT contributes to endothelial dysfunction during inflammatory conditions, and that some inflammatory mediators, such as IL-1β, TNFα, nuclear factor kappa B (NF-κB) transcription factor, and endotoxins, can activate ECs and convert them to mesenchymal-like cells through the EndMT process (81).

In addition, the above discussed work of Zordan et al, (69) demonstrates how, following macrophage depletion, muscle niche is altered, perturbing the natural inflammatory response to a muscle trauma by depleting macrophages leads to EndMT that comes along with alterations of TNFα, IL10, TGFβ, metalloproteinases and proangiogenic factors.

1.2.2.3 EndMT and pluripotency

It has been suggested that EndMT endows endothelial cells with multipotency. During the initial phase of the process, endothelial cells undergo a dedifferentiation state in which they increase the susceptibility to external factors broadening the spectrum of differentiation fate.

From this point of view myofibroblasts differentiation do not represent the ultimate fate of EndMT. Recent studies have shown the ability of EndMT to generate various different types of connective tissues (82).

Several studies have suggested that in heterotopic ossification disorders, in which bone develops outside physiological sites, pathological osseous lesions have an endothelial origin (83). Lineage tracing and biomarker studies have sustained an endothelial origin of heterotopic cartilage and bone that develop in a rare disease called fibrodysplasia ossificans progressiva (FOP) (84, 85, 86). Patients with this disease carry a gain-of-function mutation in the gene encoding activin-like kinase 2 (ALK2) receptor (87). When endothelial cells express this mutated gene, they undergo EndMT and acquire properties of mesenchymal stem cells with the ability to transform into bone, cartilage, or fat cells (84). A recent study has shown that kidney cells isolated from FOP patients can be transformed into induced pluripotent stem cells (iPSC) and subsequently differentiated into endothelial cells, which spontaneously underwent EndMT in culture (88). The ability of EndMT to generate osteoprogenitor cells

has also been observed in vascular calcifications (89), valvular calcifications (90), and tumor calcifications (91). Another recent study has shown that BMP6 has the capacity to stimulate EndMT and subsequent differentiation to osteoblasts both independently and synergistically with oxidized low-density lipoprotein (92). Tang et al. (93) showed that high glucose levels mediate endothelial differentiation to chondrocytes through EndMT. Lineage tracing studies using VE-cadherin-Cre reporter mice have demonstrated an endothelial origin of white and brown fat cells (94). A recent study that isolated endothelium from vascular tumors showed that these cells spontaneously undergo EndMT in culture and have the ability to form adipocytes and mural cells such as pericytes and smooth muscle cells (95). Endothelial progenitor cells (EPCs) have also been induced to undergo EndMT and transform into smooth muscle cells (96).

Endothelial plasticity has also been linked to generation of skeletal myocytes for muscle repair (97). Furthermore, lineage tracing in Tie1-Cre and VE-cadherin-Cre reporter mice has demonstrated an endothelial origin of cardiomyocytes during cardiac homeostasis, which are proposed to arise by EndMT (98).

1.3 Study the role of EndMT and macrophages in heterotopic ossification. The point of view of the regenerating muscle niche

1.3.1 Clinical aspects of acquired and hereditary heterotopic ossification

Heterotopic ossification (HO) is defined as formation of bone in soft tissues. It is possible to distinguish between acquired and hereditary forms of HO. Acquired forms are by far the most common and arise from severe muscle-skeletal trauma like burns, explosions, fractures, total hip arthroplasty or have a neuro- genic cause (such as spinal cord injury or central nervous system injury) (99). Among hereditary forms, Fibrodysplasia Ossificans Progressiva has the most dramatic outcome leading to life-threatening conditions and extended immobilization.

In the acquired forms, the clinical signs and symptoms of HO may appear as early as 3 weeks or as late as 12 weeks after the muscle-skeletal trauma or a spinal cord injury (99).

The incidence of HO after total hip arthroplasty (THA) ranges between 16% and 53%. Post-traumatic HO formation can occur in any sites, but most frequently in the hip following total hip arthroplasty. The hip is also the most common site of involvement in patients with a traumatic brain or spinal cord injury. The knee is less frequently affected. The incidence of HO following open reduction and internal fixation of acetabular fractures ranges between 18% and 90%.

Also shoulders and elbows are common sites ossification. Loss of joint mobility and resulting loss of function are the principal complications of HO. For example, the hip that has HO may fuse or become ankylosed in a flexed position. Other complications of HO include peripheral nerve entrapment and pressure ulcers (100).

Eighty percent or more of cases of HO run a relatively benign course without any of these complications. In the remaining 10%–20% of cases, significant loss of motion develops, with ankylosis in up to 10% of these.

HO can manifest itself in the course of the disease with pain, fever, swelling, erythema, and decreased joint mobility. In this early inflammatory phase, the condition may mimic cellulitis, thrombophlebitis, osteo-myelitis, or tumor (99).

Indomethacin is currently used as a prophylactic agent for total hip arthroplasty. Its action is two-fold: firstly, it exerts a direct effect through inhibition of the differentiation of mesenchymal cells into osteogenic cells; secondly, it has an indirect effect through inhibition of post-traumatic bone remodelling by suppression of the prostaglandin-mediated response (99).

Radiation therapy, like indomethacin, has a generally accepted prophylactic effect after total hip arthroplasty or resection of HO, but literature data on its efficacy in patients with brain and spinal cord injuries are still non-existent.

The rationale of bisphosphonate use is based on three effects: inhibition of calcium phosphate precipitation, slowing of

hydroxyapatite crystal aggregation and inhibition of the transformation of calcium phosphate to hydroxyapatite.

After cessation of treatment the matrix undergoes uninhibited mineralization, known as the “rebound-effect”. Consequently, it is essential to start treatment as soon as possible and continue it for a sufficiently long period of time, i.e. at least 6 months (99,101).

Once HO has developed to the point that it interferes significantly with the functional capacity of the patient, the only treatment option remaining is surgery, which most commonly is required at the hip (102). It is necessary to ensure that HO has reached maturity before resection, because removal of immature HO leads to recurrence rates of nearly 100%. Haemorrhage may be a significant problem at the time of surgery, with an average blood loss of 2100 mL reported (100).

A genetic form of HO is Fibrodysplasia Ossificans Progressiva (FOP), a rare and disabling disorder with a worldwide prevalence of approximately one in two million individuals. There is no ethnic, racial, gender, or geographic predisposition (103).

Two clinical features define classic FOP: malformations of the great toes and progressive heterotopic endochondral ossification (HO) in characteristic anatomic patterns. Individuals with FOP appear normal at birth except for malformations of the great toes that are present in all classically affected individuals and they can frequently show some minor abnormalities in the skeleton. During the first decade of life, most children with FOP develop episodic, painful inflammatory soft tissue swellings (or flare-ups). While some flare-ups regress

spontaneously, most transform soft connective tissues including aponeuroses, fascia, ligaments, tendons, and skeletal muscles into mature heterotopic bone. Ribbons, sheets, and plates of heterotopic bone replace skeletal muscles and connective tissues through a process of endochondral ossification that leads to an armament-like encasement of bone and permanent immobility. Minor trauma such as intramuscular immunizations, mandibular blocks for dental work, muscle fatigue, blunt muscle trauma from bumps, bruises, falls, or influenza-like viral illnesses can trigger painful new flare-ups of FOP leading to progressive heterotopic ossification. Some flare-ups also develop spontaneously without inflammatory triggers (104).

HO in FOP progresses in characteristic anatomic and temporal patterns that mimic the patterns of normal embryonic skeletal formation. Typically occurring first in the dorsal, axial, cranial, and proximal regions of the body and later seen in the ventral, appendicular, caudal, and distal regions (105). Several skeletal muscles including the diaphragm, tongue, and extra-ocular muscles are spared from FOP. Cardiac muscle and smooth muscle are not involved.

HO in FOP is episodic, but disability is cumulative. Most patients with FOP are confined to a wheelchair by the third decade of life, and require lifelong assistance in performing activities of daily living. Severe weight loss may result following ankylosis of the jaw. Pneumonia or right-sided heart failure may complicate rigid fixation of the chest wall. The median age of survival is approximately 40 years,

and death often results from complications of thoracic insufficiency syndrome (105) .

Currently, the main treatment for FOP is trauma prevention. Anti-inflammatory drugs are used with some doubts about their efficacy for the rebound effects. Surgical removal of heterotopic bone is not recommended since it would provoke explosive and painful new bone growth (105).

1.3.2 Histopathology of HO lesions

Whatever the cause, heterotopic bone formation appears to follow an endochondral process similar to the normal bone development, in which a cartilage intermediate serves as a scaffold for mature bone tissue. Differently form physiological process, ectopic lesions are enriched with immune cells.

The histopathology of FOP lesions has been well described (106). Early FOP lesions contain an intense mononuclear and perivascular infiltration of macrophages, mast cells, and lymphocytes. The precise roles of these cells in the evolution of FOP flare-ups are unknown, although focal inflammation from any cause is a known trigger of disease activity. Subsequent migration of mononuclear inflammatory cells into affected muscle precedes widespread death of skeletal muscle.

Following a rapid and destructive inflammatory stage, there is an intense fibroproliferative phase associated with robust angiogenesis and neovascularity. Early fibroproliferative lesions are histologically indistinguishable from aggressive juvenile fibromatosis. As lesions mature, fibroproliferative tissue undergoes an avascular condensation into cartilage followed by a revascularization stage with osteogenesis in a characteristic process of HO. Resultant new ossicles of heterotopic bone appear histologically normal with mature lamellar bone and often contain marrow elements (106).

Mast cells have been identified at every histological stage of FOP lesion formation, and are found in much greater abundance compared with normal skeletal muscle and non lesional FOP muscle. In fact, during the intense fibroproliferative stage of the lesion, mast cells are found at a density much higher than in any other inflammatory myopathy (107).

All stages of histological development are present in an active FOP lesion, suggesting that different regions within the lesion mature at different rates. Although heterotopic bone formation in FOP is similar in some respects to bone formation in embryonic skeletal development and postnatal fracture healing, an important difference is the lack of inflammation in primary skeletal formation (104).

1.3.3 Factors involved in HO pathogenesis

1.3.3.1 BMP signalling in HO

The majority of FOP patients carry a missense heterozygous mutation (c.617G>A; R206H) in the glycine-serine residue (GS) activation domain of activin A type I receptor/activin-like kinase 2 (ACVR1/ALK2) (87). Other mutations identified in FOP patients are all located in the GS domain of ALK2 (104). ALK2 is a type I BMP receptor belonging to TGFβ superfamily. Similarly to TGFβ signalling, also BMP ligands require type I and type II receptor association to activate the pathway (108).

In particular, in mammals, there are seven type I receptors, the BMPR-I group (ALK3 and ALK6), the ALK-I group (ALK1 and ALK2) and the TbR-I group (ALK4, ALK5) receptors in mammals, i.e., BMPR-II, ActR-II and ActR- IIB and MISR-II, of which BMPR-II, ActR-II and ActR- IIB can serve as type II receptor for BMPs that are expressed in multiple tissues (108). Both type I and type II receptors are required for signal transduction (109). The type II receptors are constitutively active and are responsible for activating type I receptors. The type I receptor contains a so-called L45 loop that extends from the kinase domain and which is required for interaction and activation of downstream receptor regulated Smads (R-Smads) (108). The intracellular GS domain (glycine and serine-rich domain) of type I receptors located N-terminal to the serine-threonine kinase domain controls the kinase activity of type I receptors. The phosphorylation of serine and threonine residues in the GS domain by type II receptor activates the

kinase activity of the type I receptor and initiates signal transduction mediated by the type I receptor (108). Under normal circumstances, type I receptors can form oligomeric complexes with type II receptors in the absence of ligands. To prevent type I receptor activation independent of ligand stimulation, the negative regulator FKBP12 binds to the intracellular GS domain of type I receptors thereby preventing it from being phosphorylated in the absence of a ligand (110). Upon ligand stimulation, FKBP12 dissociates from the type I receptors, allowing the phosphorylation by type II receptors on serine and threonine residues in the GS domain.

Upon formation and subsequent activation of a BMP ligand-receptor complex, the activated type I receptors phosphorylate receptor regulated Smad proteins (R-Smads) at their two C-terminal serine residues. ALK1, -2, -3, and -6 mediate the phosphorylation of R-Smad1, -5, and -8. The phosphorylated R-Smads can form complexes with the common mediated Smad (Co-Smad), Smad4, and translocate into the nucleus. In the nucleus, this Smad complex binds the DNA and in collaboration with co-activators and repressors and other transcription factors regulates the expression of specific genes (111).

BMP proteins derive their name, Bone Morphogenetic Proteins, from their osteo-inductive capacity when injected in tissue, as demonstrated by Urist in 1971. More than 20 BMPs have been identified and characterized, but not all show osteo-inductive properties. On the basis of phylogenetic analysis and sequence similarities, the osteo-inducing BMPs can be divided into three

subgroups: the BMP2/4 subgroup, the BMP5/6/7/8 subgroup and the BMP9/ 10 subgroup (108). All of the bone-inducing BMPs can induce mesenchymal stem cells to differentiate into osteoblasts *in vitro* (108). BMP proteins are fundamental for skeletal formation and fracture repair but the embryo lethality of knockout mice show that BMP family is involved heart development (112). Some of the BMPs knockout died after birth or show, in addition to skeletal defects, alterations in: kidney, eyes, spermatogenesis and are associated with type II diabetes and iron overload (113).

Different molecular events have been described as consequence of FOP mutation, all resulting in aberrant BMP signalling: i) the mutation seems to decrease the affinity of ALK2 for FKBP12, resulting into leaky activation of the receptor in the absence of ligands (114). ii) Mutated receptor shows increased response to BMP proteins (115) and more recently it has been demonstrated that iii) mutation confers responsiveness to ActivinA (116, 117) behaving as an inhibitor molecule in wild-type cells, it competes with BMPs for binding the receptor without eliciting Smad activation. *In vitro* evidence has shown that ActivinA stimulation induces chondrocytes and osteoblasts differentiation only in FOP mutated cells (118).

The pathogenesis of acquired forms is not well understood, the main inducer of HO in the acquired form seems to be tissue inflammation. Researchers have tried to find a link with fibrodysplasia ossificans progressiva (FOP), but a genetic predisposition has not yet been established. However, evidence from patients sample indicate that

BMP signalling is involved in acquired forms pathogenesis: in the valve where HO was identified, BMP2 and BMP4 were found to be expressed by myofibroblasts and preosteoblasts in areas adjacent to B- and T-lymphocyte infiltrations (119). BMP9 was found to be up-overexpressed within osseous ectopic lesion in a traumatic HO case (120). Moreover, multiple studies showed that BMP2, BMP4, and BMP9-induced HO in skeletal muscle by intramuscular injections (121, 122, 85). It has been postulated that bone morpho- genetic protein is liberated from normal bone in response to venous stasis, inflammation, or diseases of connective tissue attachments to bone, conditions that often accompany immobilization or trauma (124).

BMPs may mediate the induction of acquired HO. Like in FOP, inflammation is involved in the formation of ectopic bone in acquired HO. The pro-inflammatory cytokine TNFα can stimulate the expression of BMP2, an important bone inducer in endothelial cells (125). In addition, TNFα can augment the recruitment and differentiation of muscle-residing stroma cells (mrSCs) to enhance bone formation (126).

Up to now several BMP inhibitors have been developed to interfere with HO development. Since the discovery of dorsomorphin (129), an ALK2, ALK3 and ALK6 inhibitor, different compounds have been synthetize to enhance efficacy and specificity to target ALK2: DMH1 (128), K02288 (129), LDN-193189 (130), LDN-212854 (131), ML347 (132). Also an antisense oligonucleotides (AONs) has been developed to mediated exon skipping of mutated receptor (133). However, none

of this attempts has provided an acceptable therapeutic profile to be translated in a clinical trial.

1.3.3.2 The role of inflammation in HO

Inflammation appears to be a central mediator of HO both in acquired and FOP, many evidences support a link between heterotopic ossification and immune system in FOP: onset of flare-ups are in most of the case preceded by soft tissue trauma: muscle fatigue, viruses, and immunizations (134) Trauma induced by surgical removal of heterotopic bone leads to new bone formation (105). Flare-ups in patients are characterized by swelling, oedema and pain that are accompanied by infiltration of mast cells, lymphocytes and macrophages, similarly to what happened in mouse model of FOP (105,86). Anti-inflammatory and immunosuppressive therapies seem to counteract the development of HO, ameliorate flare-ups symptoms or to prolong the quiescence phase between flare-ups episodes (135).

A connection between BMP signalling and inflammation also exists. Complementary to their effect on stimulating HO, native and recombinant BMPs are potent pro-inflammatory proteins at heterotopic sites (136). Cunningham et al (137) showed that BMP4 was a potent chemoattractant to monocytes *in vitro* and may promote HO through its profound effects on monocyte recruitment and cytokine synthesis. BMP4 can also cause early lymphocytic infiltration

in mouse models similar to that seen in FOP flare-ups. BMP6 induced expression of pro-inflammatory inducible nitric oxide synthase (iNOS) and tumor necrosis factor alpha (TNFα) in macrophages.

In a recent study, Convente and colleagues reported that targeted ablation of macrophages and mast cells in ACVR1R206H+ mice dramatically impaired HO (138)

The discovery of the ALK2 mutated sensitivity to ActivinA permits to establish a new connection between BMP signalling and inflammation, in physiological conditions ActivinA is a competitive inhibitor of BMP proteins since its binding does not trigger Smad activation but it is also an important cytokine in the regulation of inflammatory pathways. In particular, Act A regulates cell growth and maturation of mast cells, a critical innate immune cell involved in all stages of FOP flare-ups. Act A can be induced in many cell types under inflammatory conditions, and can stimulate multiple toll-like receptors (TLRs), a likely component of HO induction in FOP lesions. Act A is highly relevant to the pathogenesis of HO in FOP (134, 116,117).

Act A expression is induced in skeletal muscle after cardiotoxin-induced injury and overexpression of Act A causes significant damage to skeletal muscle. Additionally, Act A neutralization improves repair and regeneration and restores normal muscle function in cardiotoxin-induced skeletal muscle injury. Importantly, Act A inhibition after cardiotoxin-induced skeletal muscle injury is associated with histological improvements and alterations in inflammatory biomarkers (134)

While it is known that ActivinA enhanced chondrogenesis in mutated osteoprogenitors cells, the effect of the mutation in immune cells behaviour is yet to be investigated.

Acquired HO forms arise after severe tissue trauma, the development of HO was found to be correlated with presence and severity of traumatic brain injury, amputation, and injury severity (100). Patients with traumatic HO exhibit an exaggerated inflammatory response with unique pattern of cytokines expression compared to patients with similar injuries but who do not develop HO (140).

Regarding acquired forms, also neuroinflammation seems to be involved in the pathogenesis of HO following cord spinal injury. Upon nerve damage, substance P is released by mast cells and leading to BMP-mediated HO. In addition to inflammatory stimulus, other factors have been taking in consideration in favouring an osteo-inductive environment like hypoxia and neuroinflammation (141).

1.3.4 Study of the cellular origin of HO osteoprogenitors

A better comprehension of the cells involved in the pathogenesis of HO could bring about important findings valuable to develop a cure for HO. Identifying progenitors cells that give rise to ectopic bone can lead to the discovery on new therapeutic targets. Currently, the nature of osteoprogenitors cells is still a debated discussion.

Many studies have focused their attention on identifying progenitors cells that give rise to ectopic bone. Lineage tracing techniques, by enabling reporter gene expression in specific type of cells through inducible Cre-recombinase, used in mouse models of HO shed some light on this issue. Several mice models of HO have been developed to mimicry the different cues leading to HO. Basically mice models of HO have been achieved by i) injecting BMP proteins in tissue, ii) introducing hyperactive BMP signalling mutations , iii) inducing severe tissue trauma.

As demonstrated first by Urist in 1965 (136) injections of BMP proteins trigger an endochondral program. It is known that BMP2, BMP4, BMP9 can induce HO (121, 122, 85). Osteo-inductive BMPs effects can require or be potentiated by concomitant presence of cardiotoxin. Delivery of BMPs proteins has been achieved also by injecting cells infected with adenoviruses, retroviral viruses, overexpressing BMP-genes (mostly BMP 2 or 4) are used to induce HO (141). Before the discovery of FOP mutation, several attempts at up-regulating BMP expression under the control of different promotors have been made, surprisingly most of the transgenic mice failed to induce HO, mainly for embryo or perinatal lethality, while in some cases led to no visible alterations or affected specific organs (142). Only BMP4 overexpression under the control of neuron specific enolase promoter (Nse-BMP4) develops a phenotype that closely recapitulates the FOP phenotype and that also displays the histological hallmarks of typical acquired HO (142).

The identification of FOP mutation enabled the generation of ALK206H knock-in mouse that recapitulates all phenotypic features of FOP patients but germline transmission of the mutation causes lethality revealing the limits of this mouse model, partially overcome by the use of chimeric mice (86). Conditional knock-in has provided another strategy to bypass germline transmission and to maintain clinical features of FOP: development of ectopic bone in injured sites as well as spontaneous ossifications following the typical pattern (117).

Models to study acquired heterotopic ossification includes Achilles tenotomy, immobilization and manipulation of joints, spinal cord injury, dorsal scald burn. All the above mentioned models lead to heterotopic ossification following an endochondral model (141) .

Regarding the study of the osteoprogenitors nature, first lineage tracing experiments performed in mice overexpressing BMP4 ruled out lymphocytes, macrophages, somite derived cells as ectopic bone progenitors cells (143).

Positive results from lineage tracing experiments have been achieved by Tie2 activated Cre-recombinase, Tie2 is a marker expressed by endothelial, hematopoietic and mesenchymal cells. Other experiments support the hypothesis of tissue resident mesenchymal cells as osteoprogenitors (144). The evidence of endothelial markers in the ossified region in the samples derived from patients affected by FOP (84) and acquired HO (83) suggest that EndMT can give rise to osteogenic mesenchymal cells. The work of Medici (84) illustrates how the introduction of FOP mutation in endothelial cells confers

multipotency: ALK2R206H EC cells express stem cell markers and acquire sensitivity to BMP stimulus enabling osteogenic differentiation.

Generation of lineage tracing mice in which both the induction of mutation and the reporter gene occur only in FAP cells, shows how fibroadipogenic precursors directly differentiate in chondrocytes and osteoblasts of ectopic lesions (145).

Due to the differences in the animal model used the question of cellular origin of osteoprogenitors is not fully addressed and evidence reported up to know suggest that more than one population is able to differentiate in chondrocytes and osteoblasts.

1.4 Scope of the thesis

The aims of this project are:

1) Identify new BMP inhibitors to counteract HO
2) Study the role of Endothelial to mesenchymal transition and macrophages in heterotopic ossification
3) Explore the involvement of Adar proteins in TGFβ signalling.

Chapter 1 is an extensive review on the current knowledge on the role of endothelial cells in tissue regeneration in coordination with immune cells, and the pathological transition from endothelial to mesenchymal phenotype as a pathogenetic mechanism of heterotopic ossification, a disease in which muscle tissue turns into bone. The last part of this chapter introduces general aspects of HO and discusses the sources of osteoprogenitors cells.

The work presented in Chapter 2 focusses on the pharmacologically targeting of ACVR1, (BMP type I receptor), found mutated in Fibrodysplasia Ossificans Progressiva (FOP), a genetic form of HO. A BMP signalling inhibition screening strategy led us to the identification of a drug able to counteract the development of HO in mice.

In Chapter 3 I show the participation of endothelial cells to initial phase of HO and the protective role of macrophages in restricting the identity of endothelial progenitors and limiting the extent of ectopic bone.

Chapter 4 gathers preliminary results about the role of RNA editing enzymes in endothelial identity and interactions with TGFb pathway.

Chapter 5 collects the implications of the findings described in chapter 2, 3 and 4. “Future perspectives” paragraph discusses about the therapy for HO, paying special attention to FOP and unclear roles of ECs and macrophages in this pathology.

1.5 References

1. Galley, H.F. & Webster, N.R. (2004). Physiology of the endothelium. British Journal of Anaesthesia, 93, 105-113.

2. Michiels, C. Endothelial Cell Functions. (2003). J Cell Physiol. 196(3), 430-43.

3. Rafii, S., Butler, J.M., & Ding, B.-s. (2016). Angiocrine functions of organ-specific endothelial cells. 529, 316-325.

4. Carmeliet, P. & Conway, E.M. (2001). Molecular mechanisms of blood vessel growth. 49, 507-521.

5. Eming, S.A., Martin, P., & Tomic-canic, M. (2014). STATE OF THE ART REVIEW Wound repair and regeneration : Mechanisms , signaling , and translation. (2014). Sci Transl Med, 3;6(265)6.

6. Vitorino, P. & Meyer, T. (2008). Modular control of endothelial sheet migration. Genes Dev, 22, 3268-3281.

7. Hellström, M., Phng, L.K., & Gerhardt, H. (2007). VEGF and Notch signaling: the yin and yang of angiogenic sprouting. Cell Adh Migr, 1, 133-136.

8. Lobov, I.B., Renard, R.A., Papadopoulos, N., Gale, N.W., Thurston, G., Yancopoulos, G.D., & Wiegand, S.J. (2007). Delta-like ligand 4 (Dll4) is induced by VEGF as a negative regulator of angiogenic sprouting. Proc Natl Acad Sci U S A, 104, 3219-3224.

9. Gerhardt, H., Golding, M., Fruttiger, M., Ruhrberg, C., Lundkvist, A., Abramsson, A., Jeltsch, M., Mitchell, C., Alitalo, K., Shima, D., & Betsholtz, C. (2003). VEGF guides angiogenic sprouting utilizing endothelial tip cell filopodia. J Cell Biol, 161, 1163-1177.

10. Iijima, M. & Devreotes, P. (2002). Tumor suppressor PTEN mediates sensing of chemoattractant gradients. Cell, 109, 599-610.

11. Srinivasan, S., Wang, F., Glavas, S., Ott, A., Hofmann, F., Aktories, K., Kalman, D., & Bourne, H.R. (2003). Rac and Cdc42 play distinct roles in regulating PI(3,4,5)P3 and polarity during neutrophil chemotaxis. J Cell Biol, 160, 375-385.

12. Lauffenburger, D.A. & Horwitz, A.F. (1996). Cell migration: a physically integrated molecular process. Cell, 84, 359-369.

13. Wolf, K., Mazo, I., Leung, H., Engelke, K., von Andrian, U.H., Deryugina, E.I., Strongin, A.Y., Bröcker, E.B., & Friedl, P. (2003). Compensation mechanism in tumor cell migration: mesenchymal-amoeboid transition after blocking of pericellular proteolysis. J Cell Biol, 160, 267-277.

14. Stapor, P.C., Sweat, R.S., Dashti, D.C., Betancourt, A.M., & Murfee, W.L. (2014a). Pericyte dynamics during angiogenesis: new insights from new identities. J Vasc Res, 51, 163-174

15. Stellos, K., Gatsiou, A., Stamatelopoulos, K., Perisic Matic, L., John, D., Lunella, F.F., Jaé, N., Rossbach, O., Amrhein, C., Sigala, F., Boon, R.A., Fürtig, B., Manavski, Y., You, X., Uchida, S., Keller, T.,

Boeckel, J.N., Franco-Cereceda, A., Maegdefessel, L., Chen, W., Schwalbe, H., Bindereif, A., Eriksson, P., Hedin, U., Zeiher, A.M., & Dimmeler, S. (2016). Adenosine-to-inosine RNA editing controls cathepsin S expression in atherosclerosis by enabling HuR-mediated post-transcriptional regulation. Nat Med, 22, 1140-1150.

16. Shi, G.P., Sukhova, G.K., Kuzuya, M., Ye, Q., Du, J., Zhang, Y., Pan, J.H., Lu, M.L., Cheng, X.W., Iguchi, A., Perrey, S., Lee, A.M., Chapman, H.A., & Libby, P. (2003). Deficiency of the cysteine protease cathepsin S impairs microvessel growth. Circ Res, 92, 493-500.

17. Riese, R.J., Mitchell, R.N., Villadangos, J.A., Shi, G.P., Palmer, J.T., Karp, E.R., De Sanctis, G.T., Ploegh, H.L., & Chapman, H.A. (1998). Cathepsin S activity regulates antigen presentation and immunity. J Clin Invest, 101, 2351-2363.

18. van der Kwast, R.V.C.T., van Ingen, E., Parma, L., Peters, H.A.B., Quax, P.H.A., & Nossent, A.Y. (2018). Adenosine-to-Inosine Editing of MicroRNA-487b Alters Target Gene Selection After Ischemia and Promotes Neovascularization. Circ Res, 122, 444-456.

19. Eming, S.A., Martin, P., & Tomic-canic, M. (2014). STATE OF THE ART REVIEW Wound repair and regeneration : Mechanisms , signaling , and translation.

20. Sica, A. & Mantovani, A. (2012). Macrophage plasticity and polarization: *in vivo* veritas. J Clin Invest, 122, 787-795.

21. Martinez, F.O., Sica, A., Mantovani, A., & Locati, M. (2008). Macrophage activation and polarization. Front Biosci, 13, 453-461.

22. Nucera, S., Biziato, D., & Palma, M.D.E. (2011). The interplay between macrophages and angiogenesis in development , tissue injury and regeneration. 495-503.

23. Fantin, A., Vieira, J.M., Gestri, G., Denti, L., Schwarz, Q., Prykhozhij, S., Peri, F., Wilson, S.W., & Ruhrberg, C. (2010). Tissue macrophages act as cellular chaperones for vascular anastomosis downstream of VEGF-mediated endothelial tip cell induction. Blood, 116, 829-840.

24. Rymo, S.F., Gerhardt, H., Wolfhagen Sand, F., Lang, R., Uv, A., & Betsholtz, C. (2011). A two-way communication between microglial cells and angiogenic sprouts regulates angiogenesis in aortic ring cultures. PLoS One, 6, e15846.

25. Ishida, S., Yamashiro, K., Usui, T., Kaji, Y., Ogura, Y., Hida, T., Honda, Y., Oguchi, Y., & Adamis, A.P. (2003). Leukocytes mediate retinal vascular remodeling during development and vaso-obliteration in disease. Nat Med, 9, 781-788.

26. De Palma, M., Venneri, M.A., Galli, R., Sergi Sergi, L., Politi, L.S., Sampaolesi, M., & Naldini, L. (2005). Tie2 identifies a hematopoietic lineage of proangiogenic monocytes required for tumor vessel formation and a mesenchymal population of pericyte progenitors. Cancer Cell, 8, 211-226.

27. Lucas, T., Waisman, A., Ranjan, R., Roes, J., Krieg, T., Müller, W., Roers, A., & Eming, S.A. (2010). Differential roles of macrophages in diverse phases of skin repair. J Immunol, 184, 3964-3977.

28. Newman, A.C., Nakatsu, M.N., Chou, W., Gershon, P.D., & Hughes, C.C. (2011). The requirement for fibroblasts in angiogenesis: fibroblast-derived matrix proteins are essential for endothelial cell lumen formation. Mol Biol Cell, 22, 3791-3800

29. Stapor, P.C., Sweat, R.S., Dashti, D.C., Betancourt, A.M., & Murfee, W.L. (2014a). Pericyte dynamics during angiogenesis: new insights from new identities. J Vasc Res, 51, 163-174.

30. Folkman, J. & D'Amore, P.A. (1996). Blood vessel formation: what is its molecular basis? Cell, 87, 1153-1155.

31. Kusumbe, A.P., Ramasamy, S.K., & Adams, R.H. (2014). Coupling of angiogenesis and osteogenesis by a specific vessel subtype in bone. Nature, 507, 323-328.

32. Nolan, D.J., Ginsberg, M., Israely, E., Palikuqi, B., Poulos, M.G., James, D., Ding, B.S., Schachterle, W., Liu, Y., Rosenwaks, Z., Butler, J.M., Xiang, J., Rafii, A., Shido, K., Rabbany, S.Y., Elemento, O., & Rafii, S. (2013). Molecular signatures of tissue-specific microvascular endothelial cell heterogeneity in organ maintenance and regeneration. Dev Cell, 26, 204-219.

33. Matsumoto, K., Yoshitomi, H., Rossant, J., & Zaret, K.S. (2001). Liver organogenesis promoted by endothelial cells prior to vascular function. Science, 294, 559-563.

34. LeCouter, J., Moritz, D.R., Li, B., Phillips, G.L., Liang, X.H., Gerber, H.P., Hillan, K.J., & Ferrara, N. (2003). Angiogenesis-independent endothelial protection of liver: role of VEGFR-1. Science, 299, 890-893.

35. Wang, L., Wang, X., Xie, G., Hill, C.K., & DeLeve, L.D. (2012). Liver sinusoidal endothelial cell progenitor cells promote liver regeneration in rats. J Clin Invest, 122, 1567-1573.

36. Carlson, B.M. (1973). The regeneration of skeletal muscle. A review. Am J Anat, 137, 119-149.

37. Cossu, G. & Sampaolesi, M. (2007). New therapies for Duchenne muscular dystrophy: challenges, prospects and clinical trials. Trends Mol Med, 13, 520-526.

38. Relaix, F., Montarras, D., Zaffran, S., Gayraud-Morel, B., Rocancourt, D., Tajbakhsh, S., Mansouri, A., Cumano, A., & Buckingham, M. (2006). Pax3 and Pax7 have distinct and overlapping functions in adult muscle progenitor cells. J Cell Biol, 172, 91-102.

39. Tatsumi, R., Anderson, J.E., Nevoret, C.J., Halevy, O., & Allen, R.E. (1998). HGF/SF is present in normal adult skeletal muscle and is capable of activating satellite cells. Dev Biol, 194, 114-128.

40. Wozniak, A.C. & Anderson, J.E. (2007). Nitric oxide-dependence of satellite stem cell activation and quiescence on normal skeletal muscle fibers. Dev Dyn, 236, 240-250.

41. Troy, A., Cadwallader, A.B., Fedorov, Y., Tyner, K., Tanaka, K.K., & Olwin, B.B. (2012). Coordination of satellite cell activation and self-renewal by Par-complex-dependent asymmetric activation of p38α/β MAPK. Cell Stem Cell, 11, 541-553.

42. Zammit, P.S., Golding, J.P., Nagata, Y., Hudon, V., Partridge, T.A., & Beauchamp, J.R. (2004). Muscle satellite cells adopt divergent fates: a mechanism for self-renewal? J Cell Biol, 166, 347-357.

43. Tidball, J.G. & Villalta, S.A. (2010). Regulatory interactions between muscle and the immune system during muscle regeneration. Am J Physiol Regul Integr Comp Physiol, 298, R1173-1187.

44. Lu, H., Huang, D., Ransohoff, R.M., & Zhou, L. (2011). Acute skeletal muscle injury: CCL2 expression by both monocytes and injured muscle is required for repair. FASEB J, 25, 3344-3355.

45. Tonkin, J., Temmerman, L., Sampson, R.D., Gallego-Colon, E., Barberi, L., Bilbao, D., Schneider, M.D., Musarò, A., & Rosenthal, N. (2015). Monocyte/Macrophage-derived IGF-1 Orchestrates Murine Skeletal Muscle Regeneration and Modulates Autocrine Polarization. Mol Ther, 23, 1189-1200.

46. Tidball, J.G. (2017). Regulation of muscle growth and regeneration by the immune system. Nat Rev Immunol, 17, 165-178.

47. Tidball, J.G. & Wehling-Henricks, M. (2007). Macrophages promote muscle membrane repair and muscle fibre growth and regeneration during modified muscle loading in mice *in vivo*. J Physiol, 578, 327-336.

48. Christov, C., Chrétien, F., Abou-Khalil, R., Bassez, G., Vallet, G., Authier, F.J., Bassaglia, Y., Shinin, V., Tajbakhsh, S., Chazaud, B., & Gherardi, R.K. (2007a). Muscle satellite cells and endothelial cells: close neighbors and privileged partners. Mol Biol Cell, 18, 1397-1409.

49. Scholz D, Thomas S, Sass S, Podzuweit T. Angiogenesis and myogenesis as two facets of inflam- matory post-ischemic tissue regeneration. Mol Cell Biochem 2003; 246:57-67.

50. Bryan, B.A., Walshe, T.E., Mitchell, D.C., Havumaki, J.S., Saint-Geniez, M., Maharaj, A.S., Maldonado, A.E., & D'Amore, P.A. (2008). Coordinated vascular endothelial growth factor expression and signaling during skeletal myogenic differentiation. Mol Biol Cell, 19, 994-1006.

51. Walgenbach, K.J., Gratas, C., Shestak, K.C., & Becker, D. (1995). Ischaemia-induced expression of bFGF in normal skeletal muscle: a potential paracrine mechanism for mediating angiogenesis in ischaemic skeletal muscle. Nat Med, 1, 453-459.

52. Doukas, J., Blease, K., Craig, D., Ma, C., Chandler, L.A., Sosnowski, B.A., & Pierce, G.F. (2002). Delivery of FGF genes to wound repair cells enhances arteriogenesis and myogenesis in skeletal muscle. Mol Ther, 5, 517-527.

53. Abou-khalil, R., Mounier, R., & Chazaud, B. (2010). The “ ménage à trois ” of satellite cells , periendothelial cells and endothelial cells Regulation of myogenic stem cell behavior by vessel cells. 4101.

54. Dejana, E., Tournier-Lasserve, E., & Weinstein, B.M. (2009). The control of vascular integrity by endothelial cell junctions: molecular basis and pathological implications. Dev Cell, 16, 209-221.

55. Giannotta, M., Trani, M., & Dejana, E. (2013b). VE-cadherin and endothelial adherens junctions: active guardians of vascular integrity. Dev Cell, 26, 441-454.

56. Murakami, M., Nguyen, L.T., Hatanaka, K., Schachterle, W., Chen, P.Y., Zhuang, Z.W., Black, B.L., & Simons, M. (2011). FGF-dependent regulation of VEGF receptor 2 expression in mice. J Clin Invest, 121, 2668-2678.

57. Hatanaka, K., Lanahan, A.A., Murakami, M., & Simons, M. (2012). Fibroblast growth factor signaling potentiates VE-cadherin stability at adherens junctions by regulating SHP2. PLoS One, 7, e37600.

58. Chen, P.Y., Qin, L., Barnes, C., Charisse, K., Yi, T., Zhang, X., Ali, R., Medina, P.P., Yu, J., Slack, F.J., Anderson, D.G., Kotelianski, V., Wang, F., Tellides, G., & Simons, M. (2012). FGF regulates TGFβ signaling and endothelial-to-mesenchymal transition via control of let-7 miRNA expression. Cell Rep, 2, 1684-1696.

59. Ichise, T., Yoshida, N., & Ichise, H. (2014). FGF2-induced Ras-MAPK signalling maintains lymphatic endothelial cell identity by upregulating endothelial-cell-specific gene expression and suppressing TGFβ signalling through Smad2. J Cell Sci, 127, 845-857.

60. Goumans, M.J., van Zonneveld, A.J., & ten Dijke, P. (2008). Transforming growth factor beta-induced endothelial-to-mesenchymal transition: a switch to cardiac fibrosis? Trends Cardiovasc Med, 18, 293-298.

61. Zeisberg, E.M., Tarnavski, O., Zeisberg, M., Dorfman, A.L., McMullen, J.R., Gustafsson, E., Chandraker, A., Yuan, X., Pu, W.T., Roberts, A.B., Neilson, E.G., Sayegh, M.H., Izumo, S., & Kalluri, R. (2007). Endothelial-to-mesenchymal transition contributes to cardiac fibrosis. Nat Med, 13, 952-961.

62. Li, J. & Bertram, J.F. (2010). Review: Endothelial-myofibroblast transition, a new player in diabetic renal fibrosis. Nephrology (Carlton), 15, 507-512.

63. Piera-Velazquez, S., Li, Z., & Jimenez, S.A. (2011). Role of endothelial-mesenchymal transition (EndoMT) in the pathogenesis of fibrotic disorders. Am J Pathol, 179, 1074-1080.

64. LeBleu, V.S., Taduri, G., O'Connell, J., Teng, Y., Cooke, V.G., Woda, C., Sugimoto, H., & Kalluri, R. (2013). Origin and function of myofibroblasts in kidney fibrosis. Nat Med, 19, 1047-1053.

65. eisberg, M. & Kalluri, R. (2013). Cellular mechanisms of tissue fibrosis. 1. Common and organ-specific mechanisms associated with tissue fibrosis. Am J Physiol Cell Physiol, 304, C216-225.

66. Rieder, F., Kessler, S.P., West, G.A., Bhilocha, S., de la Motte, C., Sadler, T.M., Gopalan, B., Stylianou, E., & Fiocchi, C. (2011). Inflammation-induced endothelial-to-mesenchymal transition: a novel mechanism of intestinal fibrosis. Am J Pathol, 179, 2660-2673.

67. Yoshimatsu, Y. & Watabe, T. (2011). Roles of TGFβ signals in endothelial-mesenchymal transition during cardiac fibrosis. Int J Inflam, 2011, 724080.

68. Welch-Reardon, K.M., Wu, N., & Hughes, C.C. (2015). A role for partial endothelial-mesenchymal transitions in angiogenesis? Arterioscler Thromb Vasc Biol, 35, 303-308.

69. Zordan, P., Rigamonti, E., Freudenberg, K., Conti, V., Azzoni, E., Rovere-Querini, P., & Brunelli, S. (2014). Macrophages commit postnatal endothelium-derived progenitors to angiogenesis and restrict endothelial to mesenchymal transition during muscle regeneration. Cell Death Dis, 5, e1031.

70. Massagué, J. (1998). TGFβ signal transduction. Annu Rev Biochem, 67, 753-791.

71. Lebrin, F., Deckers, M., Bertolino, P., & Ten Dijke, P. (2005). TGFβ receptor function in the endothelium. Cardiovasc Res, 65, 599-608.

72. Ota, T., Fujii, M., Sugizaki, T., Ishii, M., Miyazawa, K., Aburatani, H., & Miyazono, K. (2002). Targets of transcriptional regulation by two distinct type I receptors for transforming growth factor-beta in human umbilical vein endothelial cells. J Cell Physiol, 193, 299-318.

73. Stefansson, S. & Lawrence, D.A. (1996). The serpin PAI-1 inhibits cell migration by blocking integrin alpha V beta 3 binding to vitronectin. Nature, 383, 441-443.

74. Goumans, M.J., Valdimarsdottir, G., Itoh, S., Lebrin, F., Larsson, J., Mummery, C., Karlsson, S., & ten Dijke, P. (2003). Activin receptor-like kinase (ALK)1 is an antagonistic mediator of lateral TGFβ/ALK5 signaling. Mol Cell, 12, 817-828.

75. Medici, D., Potenta, S., & Kalluri, R. (2011). Transforming growth factor-β2 promotes Snail-mediated endothelial-mesenchymal transition through convergence of Smad-dependent and Smad-independent signalling. Biochem J, 437, 515-520.

76. van Meeteren, L.A. & ten Dijke, P. (2012). Regulation of endothelial cell plasticity by TGFβ. Cell Tissue Res, 347, 177-186.

77. Lopez, D., Niu, G., Huber, P., & Carter, W.B. (2009). Tumor-induced upregulation of Twist, Snail, and Slug represses the activity of the human VE-cadherin promoter. Arch Biochem Biophys, 482, 77-82.

78. Aisagbonhi, O., Rai, M., Ryzhov, S., Atria, N., Feoktistov, I., & Hatzopoulos, A.K. (2011). Experimental myocardial infarction triggers

canonical Wnt signaling and endothelial-to-mesenchymal transition. Dis Model Mech, 4, 469-483.

79. Cho, J.G., Lee, A., Chang, W., Lee, M.S., & Kim, J. (2018). Endothelial to Mesenchymal Transition Represents a Key Link in the Interaction between Inflammation and Endothelial Dysfunction. Front Immunol, 9, 294.

80. Deanfield, J.E., Halcox, J.P., & Rabelink, T.J. (2007). Endothelial function and dysfunction: testing and clinical relevance. Circulation, 115, 1285-1295.

81. Pérez, L., Muñoz-Durango, N., Riedel, C.A., Echeverría, C., Kalergis, A.M., Cabello-Verrugio, C., & Simon, F. (2017). Endothelial-to-mesenchymal transition: Cytokine-mediated pathways that determine endothelial fibrosis under inflammatory conditions. Cytokine Growth Factor Rev, 33, 41-54.

82. Medici, D. (2016). Endothelial-Mesenchymal Transition in Regenerative Medicine. Stem Cells Int, 2016, 6962801.

83. Sun, Y., Cai, J., Yu, S., Chen, S., Li, F., & Fan, C. (2016). MiR-630 Inhibits Endothelial-Mesenchymal Transition by Targeting Slug in Traumatic Heterotopic Ossification. Sci Rep, 6, 22729.

84. Medici, D., Shore, E.M., Lounev, V.Y., Kaplan, F.S., Kalluri, R., & Olsen, B.R. (2010). Conversion of vascular endothelial cells into multipotent stem-like cells. Nat Med, 16, 1400-1406.

85. Lounev, V.Y., Ramachandran, R., Wosczyna, M.N., Yamamoto, M., Maidment, A.D., Shore, E.M., Glaser, D.L., Goldhamer, D.J., & Kaplan, F.S. (2009). Identification of progenitor cells that contribute to heterotopic skeletogenesis. J Bone Joint Surg Am, 91, 652-663.

86. Chakkalakal, S.A., Zhang, D., Culbert, A.L., Convente, M.R., Caron, R.J., Wright, A.C., Maidment, A.D., Kaplan, F.S., & Shore, E.M. (2012). An Acvr1 R206H knock-in mouse has fibrodysplasia ossificans progressiva. J Bone Miner Res, 27, 1746-1756.

87. Shore, E.M., Xu, M., Feldman, G.J., Fenstermacher, D.A., Cho, T.J., Choi, I.H., Connor, J.M., Delai, P., Glaser, D.L., LeMerrer, M., Morhart, R., Rogers, J.G., Smith, R., Triffitt, J.T., Urtizberea, J.A., Zasloff, M., Brown, M.A., & Kaplan, F.S. (2006). A recurrent mutation in the BMP type I receptor ACVR1 causes inherited and sporadic fibrodysplasia ossificans progressiva. Nat Genet, 38, 525-527.

88. Cai, J., Orlova, V.V., Cai, X., Eekhoff, E.M.W., Zhang, K., Pei, D., Pan, G., Mummery, C.L., & Ten Dijke, P. (2015). Induced Pluripotent Stem Cells to Model Human Fibrodysplasia Ossificans Progressiva. Stem Cell Reports, 5, 963-970.

89. Yao, Y., Jumabay, M., Ly, A., Radparvar, M., Cubberly, M.R., & Boström, K.I. (2013). A role for the endothelium in vascular calcification. Circ Res, 113, 495-504.

90. Hjortnaes, J., Shapero, K., Goettsch, C., Hutcheson, J.D., Keegan, J., Kluin, J., Mayer, J.E., Bischoff, J., & Aikawa, E. (2015).

Valvular interstitial cells suppress calcification of valvular endothelial cells. Atherosclerosis, 242, 251-260.

91. Dudley, A.C., Khan, Z.A., Shih, S.C., Kang, S.Y., Zwaans, B.M., Bischoff, J., & Klagsbrun, M. (2008). Calcification of multipotent prostate tumor endothelium. Cancer Cell, 14, 201-211.

92. Yung, L.M., Sánchez-Duffhues, G., Ten Dijke, P., & Yu, P.B. (2015). Bone morphogenetic protein 6 and oxidized low-density lipoprotein synergistically recruit osteogenic differentiation in endothelial cells. Cardiovasc Res, 108, 278-287.

93. Tang, R., Gao, M., Wu, M., Liu, H., Zhang, X., & Liu, B. (2012). High glucose mediates endothelial-to-chondrocyte transition in human aortic endothelial cells. Cardiovasc Diabetol, 11, 113.

94. Tran, K.V., Gealekman, O., Frontini, A., Zingaretti, M.C., Morroni, M., Giordano, A., Smorlesi, A., Perugini, J., De Matteis, R., Sbarbati, A., Corvera, S., & Cinti, S. (2012). The vascular endothelium of the adipose tissue gives rise to both white and brown fat cells. Cell Metab, 15, 222-229.

95. Huang, L., Nakayama, H., Klagsbrun, M., Mulliken, J.B., & Bischoff, J. (2015). Glucose transporter 1-positive endothelial cells in infantile hemangioma exhibit features of facultative stem cells. Stem Cells, 33, 133-145.

96. Moonen, J.R., Krenning, G., Brinker, M.G., Koerts, J.A., van Luyn, M.J., & Harmsen, M.C. (2010). Endothelial progenitor cells give

rise to pro-angiogenic smooth muscle-like progeny. Cardiovasc Res, 86, 506-515.

97. Huang, P., Schulz, T.J., Beauvais, A., Tseng, Y.H., & Gussoni, E. (2014). Intramuscular adipogenesis is inhibited by myo-endothelial progenitors with functioning Bmpr1a signalling. Nat Commun, 5, 4063.

98. Fioret, B.A., Heimfeld, J.D., Paik, D.T., & Hatzopoulos, A.K. (2014). Endothelial cells contribute to generation of adult ventricular myocytes during cardiac homeostasis. Cell Rep, 8, 229-241.

99. Shehab, D., Elgazzar, A.H., & Collier, B.D. (2002). Heterotopic ossification. J Nucl Med, 43, 346-353.

100. Vanden Bossche, L. & Vanderstraeten, G. (2005). Heterotopic ossification: a review. J Rehabil Med, 37, 129-136.

101. van Kuijk, A.A., Geurts, A.C., & van Kuppevelt, H.J. (2002). Neurogenic heterotopic ossification in spinal cord injury. Spinal Cord, 40, 313-326.

102. Horne, L.T. & Blue, B.A. (1999). Intraarticular heterotopic ossification in the knee following intramedullary nailing of the fractured femur using a retrograde method. J Orthop Trauma, 13, 385-388.

103. Morales-Piga, A. & Kaplan, F.S. (2010). Osteochondral diseases and fibrodysplasia ossificans progressiva. Adv Exp Med Biol, 686, 335-348.

104. Pignolo, R.J., Shore, E.M., & Kaplan, F.S. (2013). Fibrodysplasia ossificans progressiva: diagnosis, management, and therapeutic horizons. Pediatr Endocrinol Rev, 10 Suppl 2, 437-448.

105. Pignolo, R.J., Bedford-Gay, C., Liljesthröm, M., Durbin-Johnson, B.P., Shore, E.M., Rocke, D.M., & Kaplan, F.S. (2016). The Natural History of Flare-Ups in Fibrodysplasia Ossificans Progressiva (FOP): A Comprehensive Global Assessment. J Bone Miner Res, 31, 650-656.

106. Kaplan, F.S., Tabas, J.A., Gannon, F.H., Finkel, G., Hahn, G.V., & Zasloff, M.A. (1993). The histopathology of fibrodysplasia ossificans progressiva. An endochondral process. J Bone Joint Surg Am, 75, 220-230.

107. Gannon, F.H., Glaser, D., Caron, R., Thompson, L.D., Shore, E.M., & Kaplan, F.S. (2001). Mast cell involvement in fibrodysplasia ossificans progressiva. Hum Pathol, 32, 842-848.

108. Miyazono, K., Kamiya, Y., & Morikawa, M. (2010). Bone morphogenetic protein receptors and signal transduction. J Biochem, 147, 35-51.

109. Wrana, J.L., Attisano, L., Wieser, R., Ventura, F., & Massagué, J. (1994). Mechanism of activation of the TGFβ receptor. Nature, 370, 341-347.

110. Wang, T., Li, B.Y., Danielson, P.D., Shah, P.C., Rockwell, S., Lechleider, R.J., Martin, J., Manganaro, T., & Donahoe, P.K. (1996). The

immunophilin FKBP12 functions as a common inhibitor of the TGFβ family type I receptors. Cell, 86, 435-444.

111. Miyazono, K., Maeda, S., & Imamura, T. (2005). BMP receptor signaling: transcriptional targets, regulation of signals, and signaling cross-talk. Cytokine Growth Factor Rev, 16, 251-263.

112. Yuasa, S., Fukuda, K.,.(2008). Multiple roles for BMP signaling in cardiac development. Cardiovascular stem cells.

113. Shi, S., de Gorter, D.J., Hoogaars, W.M., 't Hoen, P.A., & ten Dijke, P. (2013). Overactive bone morphogenetic protein signaling in heterotopic ossification and Duchenne muscular dystrophy. Cell Mol Life Sci, 70, 407-423.

114. Shen, Q., Little, S.C., Xu, M., Haupt, J., Ast, C., Katagiri, T., Mundlos, S., Seemann, P., Kaplan, F.S., Mullins, M.C., & Shore, E.M. (2009). The fibrodysplasia ossificans progressiva R206H ACVR1 mutation activates BMP-independent chondrogenesis and zebrafish embryo ventralization. J Clin Invest, 119, 3462-3472.

115. Kaplan, F.S., Pignolo, R.J., & Shore, E.M. (2009). The FOP metamorphogene encodes a novel type I receptor that dysregulates BMP signaling. Cytokine Growth Factor Rev, 20, 399-407.

116. Hino, K., Ikeya, M., Horigome, K., Matsumoto, Y., Ebise, H., Nishio, M., Sekiguchi, K., Shibata, M., Nagata, S., Matsuda, S., & Toguchida, J. (2015). Neofunction of ACVR1 in fibrodysplasia ossificans progressiva. Proc Natl Acad Sci U S A, 112, 15438-15443.

117. Hatsell, S.J., Idone, V., Wolken, D.M., Huang, L., Kim, H.J., Wang, L., Wen, X., Nannuru, K.C., Jimenez, J., Xie, L., Das, N., Makhoul, G., Chernomorsky, R., D'Ambrosio, D., Corpina, R.A., Schoenherr, C.J., Feeley, K., Yu, P.B., Yancopoulos, G.D., Murphy, A.J., & Economides, A.N. (2015). ACVR1R206H receptor mutation causes fibrodysplasia ossificans progressiva by imparting responsiveness to activin A. Sci Transl Med, 7, 303ra137.

118. Wang, H., Shore, E.M., Pignolo, R.J., & Kaplan, F.S. (2018). Activin A amplifies dysregulated BMP signaling and induces chondro-osseous differentiation of primary connective tissue progenitor cells in patients with fibrodysplasia ossificans progressiva (FOP). Bone, 109, 218-224.

119. Mohler, E.R., Gannon, F., Reynolds, C., Zimmerman, R., Keane, M.G., & Kaplan, F.S. (2001). Bone formation and inflammation in cardiac valves. Circulation, 103, 1522-1528.

120. Grenier, G., Leblanc, E., Faucheux, N., Lauzier, D., Kloen, P., & Hamdy, R.C. (2013). BMP-9 expression in human traumatic heterotopic ossification: a case report. Skelet Muscle, 3, 29.

121. Leblanc, E., Trensz, F., Haroun, S., Drouin, G., Bergeron, E., Penton, C.M., Montanaro, F., Roux, S., Faucheux, N., & Grenier, G. (2011). BMP-9-induced muscle heterotopic ossification requires changes to the skeletal muscle microenvironment. J Bone Miner Res, 26, 1166-1177.

122. Glaser, D.L., Economides, A.N., Wang, L., Liu, X., Kimble, R.D., Fandl, J.P., Wilson, J.M., Stahl, N., Kaplan, F.S., & Shore, E.M. (2003). *In vivo* somatic cell gene transfer of an engineered Noggin mutein prevents BMP4-induced heterotopic ossification. J Bone Joint Surg Am, 85-A, 2332-2342.

123. Scott, M.A., Levi, B., Askarinam, A., Nguyen, A., Rackohn, T., Ting, K., Soo, C., & James, A.W. (2012). Brief review of models of ectopic bone formation. Stem Cells Dev, 21, 655-667.

124. Urist, M.R., Nakagawa, M., Nakata, N., & Nogami, H. (1978). Experimental myositis ossificans: cartilage and bone formation in muscle in response to a diffusible bone matrix-derived morphogen. Arch Pathol Lab Med, 102, 312-316.

125. Csiszar, A., Smith, K.E., Koller, A., Kaley, G., Edwards, J.G., & Ungvari, Z. (2005). Regulation of bone morphogenetic protein-2 expression in endothelial cells: role of nuclear factor-kappaB activation by tumor necrosis factor-alpha, H2O2, and high intravascular pressure. Circulation, 111, 2364-2372.

126. Glass, G.E., Chan, J.K., Freidin, A., Feldmann, M., Horwood, N.J., & Nanchahal, J. (2011). TNFα promotes fracture repair by augmenting the recruitment and differentiation of muscle-derived stromal cells. Proc Natl Acad Sci U S A, 108, 1585-1590.

127. Yu, P.B., Hong, C.C., Sachidanandan, C., Babitt, J.L., Deng, D.Y., Hoyng, S.A., Lin, H.Y., Bloch, K.D., & Peterson, R.T. (2008).

Dorsomorphin inhibits BMP signals required for embryogenesis and iron metabolism. Nat Chem Biol, 4, 33-41.

128. Neely, M.D., Litt, M.J., Tidball, A.M., Li, G.G., Aboud, A.A., Hopkins, C.R., Chamberlin, R., Hong, C.C., Ess, K.C., & Bowman, A.B. (2012). DMH1, a highly selective small molecule BMP inhibitor promotes neurogenesis of hiPSCs: comparison of PAX6 and SOX1 expression during neural induction. ACS Chem Neurosci, 3, 482-491.

129. Sanvitale, C.E., Kerr, G., Chaikuad, A., Ramel, M.C., Mohedas, A.H., Reichert, S., Wang, Y., Triffitt, J.T., Cuny, G.D., Yu, P.B., Hill, C.S., & Bullock, A.N. (2013). A new class of small molecule inhibitor of BMP signaling. PLoS One, 8, e62721.

130. Yu, P.B., Deng, D.Y., Lai, C.S., Hong, C.C., Cuny, G.D., Bouxsein, M.L., Hong, D.W., McManus, P.M., Katagiri, T., Sachidanandan, C., Kamiya, N., Fukuda, T., Mishina, Y., Peterson, R.T., & Bloch, K.D. (2008). BMP type I receptor inhibition reduces heterotopic [corrected] ossification. Nat Med, 14, 1363-1369.

131. Mohedas, A.H., Xing, X., Armstrong, K.A., Bullock, A.N., Cuny, G.D., & Yu, P.B. (2013). Development of an ALK2-biased BMP type I receptor kinase inhibitor. ACS Chem Biol, 8, 1291-1302

132. Kim, M., Choi, O., Pyo, S., Choi, S.U., & Park, C.H. (2017). Identification of novel ALK2 inhibitors and their effect on cancer cells. Biochem Biophys Res Commun, 492, 121-127.

133. Shi, S., Cai, J., de Gorter, D.J., Sanchez-Duffhues, G., Kemaladewi, D.U., Hoogaars, W.M., Aartsma-Rus, A., 't Hoen, P.A., & ten Dijke, P. (2013). Antisense-oligonucleotide mediated exon skipping in activin-receptor-like kinase 2: inhibiting the receptor that is overactive in fibrodysplasia ossificans progressiva. PLoS One, 8, e69096.

134. Kaplan, F.S., Pignolo, R.J., & Shore, E.M. (2016). Granting immunity to FOP and catching heterotopic ossification in the Act. Semin Cell Dev Biol, 49, 30-36.

135. Kaplan, F.S. (2011). THE MEDICAL MANAGEMENT OF FIBRODYSPLASIA OSSIFICANS PROGRESSIVA: CURRENT TREATMENT CONSIDERATIONS. Clin Proc Intl Clin Consort FOP, 4,1-100

136. Urist, M.R. (1965). Bone: formation by autoinduction. Science, 150, 893-899.

137. Cunningham, N.S., Paralkar, V., & Reddi, A.H. (1992). Osteogenin and recombinant bone morphogenetic protein 2B are chemotactic for human monocytes and stimulate transforming growth factor beta 1 mRNA expression. Proc Natl Acad Sci U S A, 89, 11740-11744.

138. Convente, M.R., Chakkalakal, S.A., Yang, E., Caron, R.J., Zhang, D., Kambayashi, T., Kaplan, F.S., & Shore, E.M. (2018). Depletion of Mast Cells and Macrophages Impairs Heterotopic Ossification in an Acvr1. J Bone Miner Res, 33, 269-282.

139. Evans, K.N., Forsberg, J.A., Potter, B.K., Hawksworth, J.S., Brown, T.S., Andersen, R., Dunne, J.R., Tadaki, D., & Elster, E.A. (2012). Inflammatory cytokine and chemokine expression is associated with heterotopic ossification in high-energy penetrating war injuries. J Orthop Trauma, 26, e204-213.

140. Kan, L., Lounev, V.Y., Pignolo, R.J., Duan, L., Liu, Y., Stock, S.R., McGuire, T.L., Lu, B., Gerard, N.P., Shore, E.M., Kaplan, F.S., & Kessler, J.A. (2011). Substance P signaling mediates BMP-dependent heterotopic ossification. J Cell Biochem, 112, 2759-2772.

141. Anthonissen, J., Ossendorf, C., Ritz, U., Hofmann, A., & Rommens, P.M. (2014). Animal models for acquired heterotopic ossification. Acta Orthop Belg, 80, 2-10.

142. Kan, L. & Kessler, J.A. (2011). Animal models of typical heterotopic ossification. J Biomed Biotechnol, 2011, 309287.

143. Kan, L., Liu, Y., McGuire, T.L., Berger, D.M., Awatramani, R.B., Dymecki, S.M., & Kessler, J.A. (2009b). Dysregulation of local stem/progenitor cells as a common cellular mechanism for heterotopic ossification. Stem Cells, 27, 150-156.

144. Wosczyna, M.N., Biswas, A.A., Cogswell, C.A., & Goldhamer, D.J. (2012). Multipotent progenitors resident in the skeletal muscle interstitium exhibit robust BMP-dependent osteogenic activity and mediate heterotopic ossification. J Bone Miner Res, 27, 1004-1017.

145. Lees-Shepard, J.B., Yamamoto, M., Biswas, A.A., Stoessel, S.J., Nicholas, S.E., Cogswell, C.A., Devarakonda, P.M., Schneider, M.J., Cummins, S.M., Legendre, N.P., Yamamoto, S., Kaartinen, V., Hunter, J.W., & Goldhamer, D.J. (2018a). Activin-dependent signaling in fibro/adipogenic progenitors causes fibrodysplasia ossificans progressiva. Nat Commun, 9, 471.

CHAPTER 2

High-throughput screening for modulators of ACVR1 transcription: discovery of potential therapeutics for fibrodysplasia ossificans progressiva.

Cappato S, Tonachini L, Giacopelli F, Tirone M, Galietta LJ, Sormani M, Giovenzana A, Spinelli AE, Canciani B, Brunelli S, Ravazzolo R, Bocciardi R.

Dis Model Mech. 2016.

© 2016. Published by The Company of Biologists Ltd | Disease Models & Mechanisms (2016) 9, 685-696 doi:10.1242/dmm.023929

RESEARCH ARTICLE

High-throughput screening for modulators of *ACVR1* transcription: discovery of potential therapeutics for fibrodysplasia ossificans progressiva

Serena Cappato[1], Laura Tonachini[1], Francesca Giacopelli[1], Mario Tirone[2,3], Luis J. V. Galietta[4], Martina Sormani[3], Anna Giovenzana[3], Antonello E. Spinelli[5], Barbara Canciani[6], Silvia Brunelli[3], Roberto Ravazzolo[1,4] and Renata Bocciardi[1,4,*]

ABSTRACT

The *ACVR1* gene encodes a type I receptor of bone morphogenetic proteins (BMPs). Activating mutations in *ACVR1* are responsible for fibrodysplasia ossificans progressiva (FOP), a rare disease characterized by congenital toe malformation and progressive heterotopic endochondral ossification leading to severe and cumulative disability. Until now, no therapy has been available to prevent soft-tissue swelling (flare-ups) that trigger the ossification process. With the aim of finding a new therapeutic strategy for FOP, we developed a high-throughput screening (HTS) assay to identify inhibitors of *ACVR1* gene expression among drugs already approved for the therapy of other diseases. The screening, based on an *ACVR1* promoter assay, was followed by an *in vitro* and *in vivo* test to validate and characterize candidate molecules. Among compounds that modulate the *ACVR1* promoter activity, we selected the one showing the highest inhibitory effect, dipyridamole, a drug that is currently used as a platelet anti-aggregant. The inhibitory effect was detectable on *ACVR1* gene expression, on the whole Smad-dependent BMP signaling pathway, and on chondrogenic and osteogenic differentiation processes by *in vitro* cellular assays. Moreover, dipyridamole reduced the process of heterotopic bone formation *in vivo*. Our drug repositioning strategy has led to the identification of dipyridamole as a possible therapeutic tool for the treatment of FOP. Furthermore, our study has also defined a pipeline of assays that will be useful for the evaluation of other pharmacological inhibitors of heterotopic ossification.

KEY WORDS: *ACVR1*, Transcriptional regulation, BMP signaling pathway, FOP, Dipyridamole, High-throughput screening, Drug repositioning

[1]Department of Neurosciences, Rehabilitation, Ophthalmology, Genetics, Maternal and Child Health and CEBR, Università degli Studi di Genova, Genova 16132, Italy. [2]Division of Immunology, Transplantation and Infectious Diseases, San Raffaele Scientific Institute, Milano 20132, Italy. [3]School of Medicine and Surgery, University of Milano-Bicocca, Monza 20900, Italy. [4]Medical Genetics Unit, IRCCS Istituto Giannina Gaslini, Genova 16147, Italy. [5]Medical Physics Department and Centre for Experimental Imaging, San Raffaele Scientific Institute, Milano 20132, Italy. [6]Dipartimento di Medicina Sperimentale, Università di Genova & IRCCS AOU San Martino-IST, Istituto Nazionale per la Ricerca sul Cancro, 16132 Genova, Italy.

*Author for correspondence (bocciardi@unige.it)

R.B., 0000-0001-8415-3802

Received 12 November 2015; Accepted 22 April 2016

INTRODUCTION

Fibrodysplasia ossificans progressiva (FOP; OMIM 135100) is a rare genetic disease with a prevalence of about one per 2-million people. The inheritance is autosomal dominant, although most cases are due to sporadic new mutations (Shore et al., 2005). Individuals with FOP are characterized by a peculiar congenital toe malformation and, usually starting within the first decade of life, by a progressive heterotopic ossification (HO) that takes place following some types of injury (such as trauma, medical surgery, intramuscular immunization, infections) or spontaneously. Inflammatory soft-tissue swellings, commonly called flare-ups, progressively transform skeletal muscles, tendons, ligaments, fascia and aponeuroses into a second skeleton of heterotopic bone (Kaplan et al., 2008).

The FOP gene (*ACVR1*) encodes a type I receptor of bone morphogenetic proteins (BMPs), ACVR1 (also known as ALK-2). The most recurrent *ACVR1* mutation is in the glycine-serine (GS) domain (c.617G>A, p.R206H) (Shore et al., 2006). Additional mutations have been identified in the GS and in the kinase domain of the protein in 3% of all known individuals with FOP (for a review, see Kaplan et al., 2009; Bocciardi et al., 2009). The consequence of *ACVR1* mutations is an alteration of inter-intramolecular interaction of the mutant receptor that causes a deregulation of the downstream BMP signaling (Shore et al., 2006; Bocciardi et al., 2009; van Dinther et al., 2010; Song et al., 2010; Groppe et al., 2011; Chaikuad et al., 2012).

At present, no established medical treatment is available for FOP. Early diagnosis prevents unnecessary interventions, such as biopsies or surgical operations that can exacerbate the progression of the disease, and high-dose glucocorticoids are used in the management of inflammatory flare-ups (Kaplan et al., 2013).

In recent years, much effort has been devoted to designing new therapeutic approaches to FOP treatment and to identify new, potentially useful, drugs (Kaplan et al., 2013; Sanvitale et al., 2013; Yu et al., 2008a; Kitoh et al., 2013). A promising alternative to the discovery of new drugs is the drug repositioning strategy, in which a drug already developed for a specific disease can be used to treat a different condition. Drug repositioning reduces costs and accelerates the drug development process. Moreover, this approach might contribute to clarify the mechanism of action of a given compound by establishing a relationship between the molecular basis of the disease and the ability of the compound to intervene at a certain step of the disease process (Shameer et al., 2015).

A possible strategy to find drugs for the treatment of a genetic disease could rely on a sensitive, specific and fast cell-based assay. In this way, a large number of small molecules can be screened [high-throughput screening (HTS)] to find agents that correct the

basic defect. The recent identification and characterization of the promoter region of *ACVR1* (Giacopelli et al., 2013) inspired us to develop an HTS assay by generating cells stably expressing the luciferase reporter gene controlled by a 2.9-kb region of the gene promoter. We expected that this type of assay would allow the identification of molecules that, by inhibiting the *ACVR1* promoter, would also negatively regulate the downstream signaling that is upregulated and hyper-responsive to BMPs because of the mutation in the receptor.

In this work, we describe the screening of a library of 1280 US Food and Drug Administration (FDA)-approved compounds, in order to identify modulators of *ACVR1* gene expression. Characterization of hit molecules included a series of second-level assays to evaluate the effect of compounds on chondrogenic and osteogenic differentiation models *in vitro* and *in vivo*.

We found that dipyridamole, commonly used as an antithrombotic and vasodilator drug, has an inhibitory effect on *ACVR1* expression, as well as on the whole BMP signaling pathway, and is able to affect chondrogenesis and osteogenesis, both in cellular assays and in a BMP-induced HO mouse model.

RESULTS

Screening of the Prestwick Chemical Library

Our primary screening was designed to find drugs that downregulate BMP signaling by targeting the expression of the *ACVR1* gene at the transcriptional level. Accordingly, we developed a quantitative assay based on expression of a reporter gene under the control of the *ACVR1* promoter. To this end, we generated clones of the ATDC5 cell line (mouse chondrogenic cell line derived from teratocarcinoma) stably expressing the luciferase coding sequence under the control of the 2.9-kb promoter of the gene, previously characterized by our group (Giacopelli et al., 2013). We obtained several clones that were expanded and selected for the level and stability of reporter gene expression over time. The availability of different clones, with putative different integration sites of the reporter construct in the genome of ATDC5 cells, allowed us to verify that the effect measured for a given compound was not related to a 'position effect' operated by the genomic region surrounding the reporter construct itself.

The generated cell system and the compound analysis procedure were tested by screening a small library of 43 molecules with chromatin-modifier properties. This allowed us to validate the protocol for the primary screening and provided us with a positive control because we identified resveratrol as a transcriptional activator of *ACVR1* gene expression (Fig. S1).

We used these cells to screen the Prestwick Chemical Library, which includes 1280 FDA-approved compounds, with the idea that 'repositioning' of an already approved drug could have the great advantage to overcome several steps of the drug discovery process. The screening detailed in Table 1 (see also Fig. S2) was performed in duplicate: compounds were added to cells seeded in 96-well plates for 24 h at the concentrations of 20 and 2 µM, respectively. We included in each plate DMSO, the vehicle in which compounds are dissolved, and resveratrol (20 µM) as a transcriptional activator of the *ACVR1* promoter and positive control. When we started this work, no transcriptional inhibitors of the *ACVR1* expression were known. However, during the screening of the second plate of the Prestwick Chemical Library, we detected dipyridamole as an inhibitor of *ACVR1* expression. Therefore, this compound was subsequently included in all the remaining plates as an additional control. To monitor the performance of the screening, we used the Z′-factor statistical parameter (Zhang et al., 1999). The calculated

Table 1. HTS assay protocol

Step	Parameter	Description
1	Cell plating (Pr2.9-Luc ATDC5)	3×10^5 cells/well
2	Controls	10 µM resveratrol, positive control; 1% DMSO, neutral control; 20 µM dipyridamole, negative control*
3	Prestwick Chemical Library	1200 compounds diluted to 20 and 2 µM
4	Incubation	24 h at 37°C and 5% CO_2
5	Viability assay	Addition of 20 µl CellTiter-Fluor reagent to living cells
6	Viability assay (incubation)	1 h at 37°C and 5% CO_2
7	Viability assay (detection)	Detection of the fluorescent signal (GLOMAX Automated Plate Reader $380\text{-}400_{Ex}/505_{Em}$ nm)
8	Reporter gene assay	Addition of the ONE-Glo reagent (100 µl), cell lysis
9	Assay readout	Detection of the luminescence signal (GLOMAX Automated Plate Reader)
10	Evaluation of HTS performance	Calculation of the Z'-factor statistical parameter according to Zhang et al. (1999)
11	Data analysis	Evaluation of cell viability (Vi) and effect of compounds (E) on the reporter gene activity. Selection of compounds for further characterization

Step	Notes
1	96-well format culture plates
2,3	80 compounds per plate (columns 2 to 11); columns 1 and 12 were used for positive, negative and neutral controls (8 wells for DMSO, 4 wells for each control)
5-7	12-tip dispense of the CellTiter-Fluor reagent; automated fluorescence detection
8-9	These steps are fully automated; the ONE-Glo reagent is added *in situ* by injection followed by luminescence detection
10	$0\geq Z'\leq 1$, with $Z'\geq 0.5$ for a good HTS (Zhang et al., 1999) $Z'_{(+Resv)}=0.63\pm0.1$ and $Z'_{(-Dipy)}=0.65\pm0.1$
11	Evaluation of cell viability, $Vi=(fluoC_x/\text{average } fluo_{DMSO})\times100$ Normalization, $N_x=LumC_x/fluoC_x$ and $N_{DMSO}=LumC_x/fluoC_x$ Effect of compounds, $E=(N_x/\text{average}N_{DMSO})\times100$

*Identified in the second experimental plate and introduced as negative control from plate 5 to 15.

Z′-factor was 0.63±0.1 and 0.65±0.1 when considering resveratrol and dipyridamole, respectively. These values are considered optimal for an HTS assay (Zhang et al., 1999). During the primary screening, we also evaluated the toxicity of all tested compounds by an *in situ* fluorescence-based assay (Table 1 and see Materials and Methods for details). We therefore normalized the activity of the luciferase reporter gene driven by the *ACVR1* promoter with a fluorescence signal proportional to the number of viable cells at the end of the treatment. This allowed us to select molecules not affecting cell viability, inducing a reduction in the luciferase activity of at least 0.4- or an upregulation of at least 2.4-fold compared to cells treated with DMSO (Table S1).

Validation assays of dipyridamole

According to our inclusion criteria, the primary screening provided a list of compounds putatively working as activators (4 hits) or inhibitors (18 hits) of *ACVR1* transcriptional activity (listed in Table S1). Among these latter molecules, we found that dipyridamole (abbreviated henceforth as Dipy), was the compound that, during the retesting of primary hits, generated the

Disease Models & Mechanisms (2016) 9, 685-696 doi:10.1242/dmm.023929

most reproducible and significant results. Therefore, Dipy was selected for further experimental confirmations.

Dipy showed a dose-dependent suppression of the luciferase activity driven by the *ACVR1* promoter, with the strongest effect at 50 µM (Fig. 1A). The inhibition was detectable after 6 h of treatment for the highest dose, further increasing at 24 h (Fig. 1B).

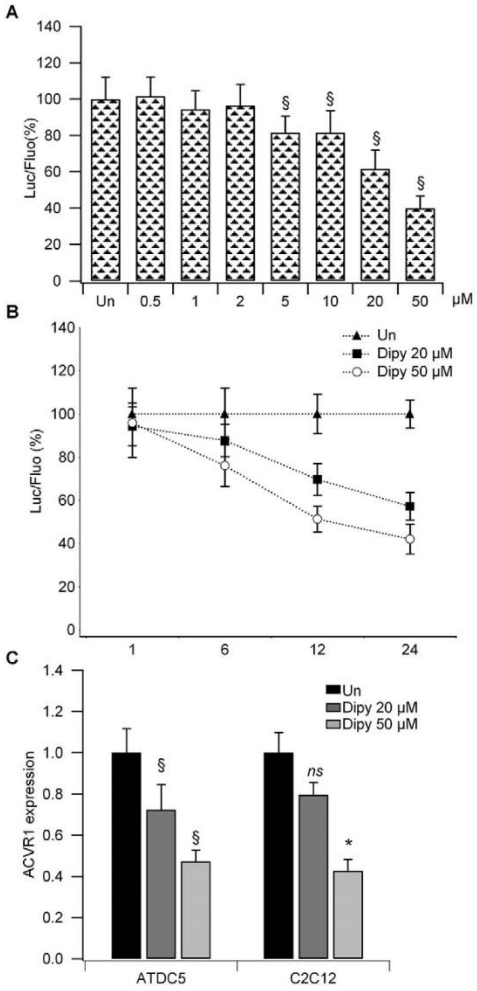

Fig. 1. Cellular assays of Dipy treatment. (A) Dose-response curve of Dipy on the luciferase reporter gene controlled by the promoter region of *ACVR1* in ATDC5 cells (Pr2.9-Luc). The ratio of luciferase (Luc)/fluorescence (Fluo) was normalized to that obtained with DMSO [untreated (Un); value 100]. Bar graph represents the mean and s.d. of three independent experiments. $^{\S}P<0.001$. (B) Time course of Dipy treatment in ATDC5 Pr2.9-Luc clones. The ratio of luciferase/fluorescence was normalized to that obtained with DMSO (Un; value 100) for each time point. (C) Effect of Dipy on the expression of *ACVR1* mRNA in native ATDC5 and C2C12 cells. Values were normalized on *GAPDH* and *β2M* and compared to expression level measured in cells treated with DMSO (Un). Bar graphs represent the mean and s.d. of at least three experiments, $^{*}P<0.01$, $^{\S}P<0.001$, ns, non-significant.

Normalization of the luciferase activity and monitoring of cell viability were obtained as described for the primary screening.

In accordance with the inhibitory effect of Dipy on the promoter of the *ACVR1* gene, we found that Dipy was able to downregulate the expression of *ACVR1* mRNA, as assessed by reverse-transcription quantitative PCR (RT-qPCR), both in native ATDC5 and C2C12 (mouse myoblast cell line) cells (Fig. 1C). After 24 h of treatment, we observed a gene-expression reduction of nearly 20% at 20 µM and 60% at 50 µM.

The effect of Dipy on the expression of genes encoding other type I and II receptors of the BMP family was also tested (Fig. S3). The highest degree of mRNA reduction was exerted on *ACVR1* (*Alk2*) but was also observed with *Alk3* and *BMPRII*. *Alk5*, involved in the growth differentiation factor (GDF)–transforming growth factor β (TGF-β) signaling cascade, and *Alk4*, *ActRIIa* and *ActRIIb* showed a low level of expression that was not affected by Dipy. Other type I receptors, such as *Alk1*, *Alk6* and *Alk7*, were not expressed in ATDC5 cells.

Effect of dipyridamole on the Smad-dependent BMP pathway

In order to test the effect of Dipy on the activation state of the Smad-dependent BMP signaling pathway, we generated ATDC5 clones stably expressing the luciferase reporter gene under the control of a minimal promoter carrying a BMP-responsive element (BRE-Luc) isolated from *Id1*, a well-known BMP target gene (Monteiro et al., 2008). Cells were treated with Dipy in the presence of BMP2 for 6 h. As reported in Fig. 2A, Dipy weakened the amplitude of the activation induced by BMP2 in a dose-dependent manner. Consistently, we found a downregulation in the mRNA expression of native *Id1*, *Id2* and *Id3* target genes, as assessed by RT-qPCR in ATDC5 cells (Fig. 2B), and a significant reduction in the phosphorylation state of the Smad1/5 proteins both in ATDC5 and C2C12 cells (Fig. 2C,D and Table S2 for immunoblot densitometric analysis).

Effect of dipyridamole on chondrogenic differentiation

The heterotopic bone that forms in individuals with FOP derives from an endochondral ossification process. ATDC5 cells are able to differentiate into mature chondrocytes when grown in three-dimensional (3D) cultures in differentiating medium (Tare et al., 2005).

ATDC5 cells were induced to develop 3D pellets in the presence of differentiating medium (DM), with and without Dipy (50 µM). After 3 weeks of culture, pellets were embedded in paraffin, and histological sections stained with Alcian Blue to verify the deposition of glycosaminoglycans typical of the cartilage extracellular matrix. As shown in Fig. 3A (left panels), compared to what was observed in proliferative medium (PM), pellets grown in DM are characterized by the presence of cells with peculiar morphology, with typical lacunae embedded in the extracellular matrix. By contrast, pellets grown in the presence of Dipy, both in PM and DM, showed the presence of small and undifferentiated cells (Fig. 3A, right panels).

The result was confirmed in ATDC5 cells cultured in alginate spheres. In the presence of inductive medium, we observed changes in cell morphology correlating with the differentiation state (Fig. 3B, upper panels). By contrast, treatment with Dipy induced a significant reduction of extracellular-matrix deposition as assessed by Alcian Blue staining of sections (Fig. 3B, left panels) and reduced expression of matrix proteins Sox9 and collagen II (Col II) as assessed by immunohistochemical analysis with specific antibodies (Fig. 3B, central and right panels, respectively).

Disease Models & Mechanisms (2016) 9, 685-696 doi:10.1242/dmm.023929

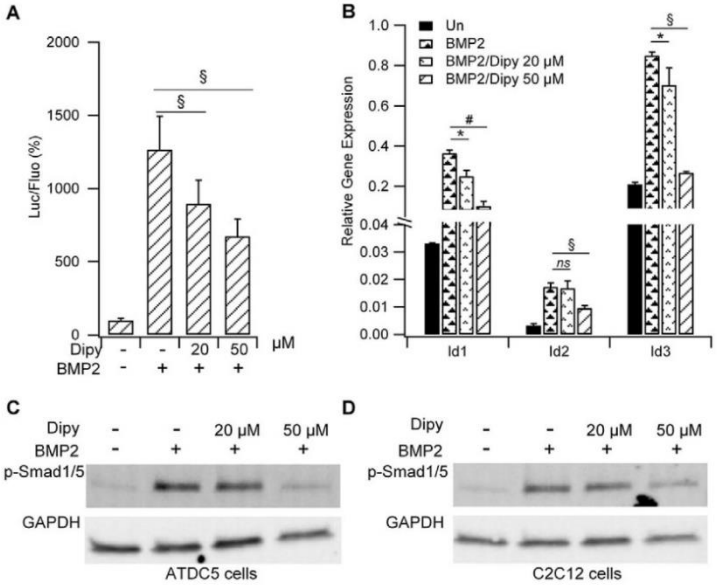

Fig. 2. Effect of Dipy on the BMP-mediated signaling pathway. (A) Luciferase activity measured in ATDC5 BRE-Luc cells treated with the indicated doses of Dipy and activated with [50 ng/ml] BMP2. The ratio of luciferase (Luc)/fluorescence (Fluo) was normalized to that obtained with DMSO (value 100). Bar graph represents the mean and s.d. of three independent experiments. $^{\S}P<0.001$. (B) Effect of Dipy on the expression level of *Id1*, *Id2* and *Id3* BMP target genes in native ATDC5 cells. Values were normalized on the *β2M* reference gene (relative quantification by the ΔC_t method: ratio reference/target=$2^{\Delta Ct}$). Bars represent the mean and s.d. of three independent experiments. ns, non-significant; $^{*}P<0.05$, $^{\#}P<0.01$, $^{\S}P<0.001$. (C,D) Effect of Dipy on the activation of the Smad-dependent pathway. ATDC5 (C) and C2C12 (D) cells were treated with Dipy and activated with [200 ng/ml] BMP2 for 1 h.

In accordance, RT-qPCR analysis on mRNA extracted from cells cultured in alginate spheres showed that the expression level of *ACVR1* and markers of cartilage differentiation [*Runx2*, *Sox9*, *Col II* and collagen X (*Col X*)] was downregulated upon Dipy treatment compared to untreated cells (Fig. 4).

Effect of dipyridamole on osteogenic differentiation

We also investigated the effect of Dipy on the osteoblastic transformation of C2C12 cells upon BMP2 induction (Katagiri et al., 1994). As shown in Fig. 5A and B, Dipy caused a dose-dependent reduction in alkaline phosphatase activity without significantly affecting cell viability (Fig. S4). The effect was accompanied by a downregulation of the mRNA of markers typical of the osteoblastic differentiation – Runx2, osterix and osteocalcin – which was statistically significant at the highest dose (Fig. 5C). During the differentiation process, in the presence of Dipy, we confirmed the reduction in the expression of *ACVR1* mRNA.

Effect of dipyridamole on heterotopic ossification in a BMP-induced mouse model

We examined the effect of Dipy on a BMP-induced model of HO *in vivo*. C57BL/6 2-month-old mice were injected with BMP2 intramuscularly in the quadriceps and treated with vehicle or 10 mg/kg (body weight) Dipy, administered daily by intra-peritoneal (IP) injection as described in Wang et al. (2013), according to two different experimental protocols as schematically represented in Fig. S5. Serum concentration of Dipy in mice was assessed according to Oshrine et al. (2005), and results were comparable to what was described in the same work (not shown).

Ossicle formation and HO volume were evaluated by µCT scan after 10 (n=6 for each group, Fig. S5 protocol A) and 21 (n=11 for each group, Fig. S5 protocol A) days of treatment. After 10 days of treatment, we observed highly variable volumes of HO (mineralized volume, mm^3) in control mice and no significant difference in HO volume was observed in treated mice compared to controls (Fig. 6A,B). By contrast, after 21 days of treatment, µCT scans showed a significant reduction of HO volume in mice treated with Dipy compared to controls (Fig. 6C,D). Histological analysis revealed that HO lesions (Fig. 7A) in treated mice were reduced, possibly due to a delay in maturation. In particular, Toluidine Blue staining indicated a reduced deposition of cartilage matrix, also at 10 days of treatment (Fig. S6), whereas Alizarin Red staining at 21 days and quantification of the area of calcium deposition showed a decrease in lesions of Dipy-treated mice (Fig. 7B,C), in agreement with the µCT scan results.

Smad1/5 phosphorylation in the injured tissue was assessed at the two different time points, 10 and 21 days, by immunofluorescence with a specific anti-phospho-Smad1/5 (p-Smad1/5) antibody.

We observed that, at 10 days after injury, the number of cells showing Smad phosphorylation was higher than at 21 days. This is consistent with the ongoing osteogenic differentiation of the HO lesions at the early time point, when the extent of mature heterotopic ossification was still comparable in untreated and treated mice, as described above. This is also indicated by the shape and intensity of p-Smad staining per cell. Interestingly, the effect of Dipy at this stage was already detectable as a statistically significant reduction in the expression of p-Smad1/5 (Fig. S7). This decrease was still present as a trend at 21 days of treatment (Fig. S7B), when the overall number of p-Smad1/5-positive cells was reduced in the lesions of both control and treated mice.

When Dipy was administered to the mice starting from 10 days after the ossification trigger by BMP2 (Fig. S5, protocol B), the µCT-scan analysis of ectopic lesions (Fig. S8A) showed a trend of reduction (P=0.074) of the HO volume increase between 10 and 21 days (Fig. S8B,C). Histological analysis revealed that, at day 21, calcium deposition was also significantly reduced as assessed by Alizarin Red staining (Fig. S9A) and corresponding quantification (Fig. S9B).

Disease Models & Mechanisms (2016) 9, 685-696 doi:10.1242/dmm.023929

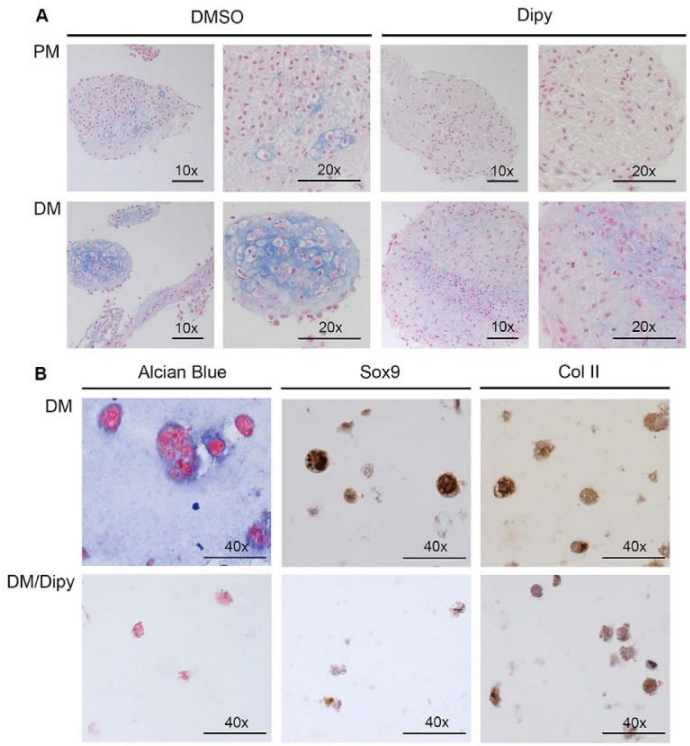

Fig. 3. Histological analysis of ATDC5 chondrogenic differentiation. (A) Alcian Blue staining of sections from ATDC5 cell 3D cultures grown in proliferative medium (PM, upper panels) and in differentiation medium (DM, lower panels), in the presence of 50 µM Dipy or DMSO. Scale bars: 100 µm (10×) and 50 µm (20×). (B) Histological and immunohistochemical analysis of ATDC5 cells cultured as alginate spheres grown in DM in the presence of DMSO or 50 µM Dipy (upper and lower panels, respectively). Scale bars: 25 µm.

DISCUSSION

To date, no therapy is available to prevent or control HO in FOP patients. Therefore, intense work is being carried out to find potential therapeutic intervention essentially based on inhibition of BMP signaling using different approaches (Kaplan et al., 2013).

The rationale basis of a therapeutic approach for FOP is that small molecules might function as inhibitors, thus correcting the hyper-functioning BMP signaling pathway(s), either by inhibiting directly the receptor function or the transcriptional or post-transcriptional expression of the encoding gene, which will in turn result in the quantitative reduction of the receptor protein.

Following the identification of dorsomorphin as an inhibitor of BMP type I receptors, through HTS in zebrafish (Yu et al., 2008b), other inhibitors have been described (Yu et al., 2008a; Cuny et al., 2008; Hao et al., 2010). Previously published work demonstrated that treatment of bone-marrow-derived mesenchymal stem cells (MSCs) with RAR-γ agonists negatively regulates BMP signaling. This is due to the reduction of the intracellular concentration of p-Smads by a post-translational mechanism of degradation, supporting the idea that quantitative reduction of components of this pathway might cause a reduction of signaling function (Sanvitale et al., 2013; Shimono et al., 2011; Sheng et al., 2010).

In the current work, we introduced an HTS approach aimed at identifying potential therapeutic candidates acting by modulation of the *ACVR1* gene expression. The primary screening was made possible by the generation of a cell system consisting of murine ATDC5 cells stably expressing the luciferase gene controlled by the 2.9-kb promoter region of *ACVR1* that was previously identified and functionally characterized by our group (Giacopelli et al., 2013). Our method was able to pinpoint molecules with both positive and negative effects. However, in the context of FOP pathogenesis, in which activating mutations of *ACVR1* cause an inappropriate BMP-mediated signaling, our interest was focused on molecules able to reduce the expression level of the gene.

In addition to the primary screening, our approach included assays to confirm the effect of candidate molecules on the different steps of the BMP pathway, on chondrogenic and osteogenic differentiation processes and on HO *in vivo*. The experimental procedure described in this workflow can also be exploited to test compounds able to affect BMP signaling, even when discovered by other cell-based HTS assays or by *in silico* virtual screening approaches.

An advantageous approach to search for innovative treatments for rare disease in a relative short time is to perform an HTS approach with a drug repositioning purpose (Muthyala, 2011; Li and Jones, 2012; Sardana et al., 2011; Yamamoto et al., 2013). To this aim, we screened a library of 1280 FDA-approved compounds. We identified a list of interesting molecules with positive or negative effect and decided to focus on the candidate with the most significant effect as a transcriptional inhibitor, dipyridamole.

Validation assays confirmed a specific negative effect of Dipy on the *ACVR1* gene expression and demonstrated that such an effect resulted in the attenuation of the entire BMP-specific signaling pathway. This was demonstrated by the reduction of BMP2-induced activation tested by the luciferase reporter gene under the control of BMP-responsive element (BRE-Luc). Consistently, this effect was

Disease Models & Mechanisms (2016) 9, 685-696 doi:10.1242/dmm.023929

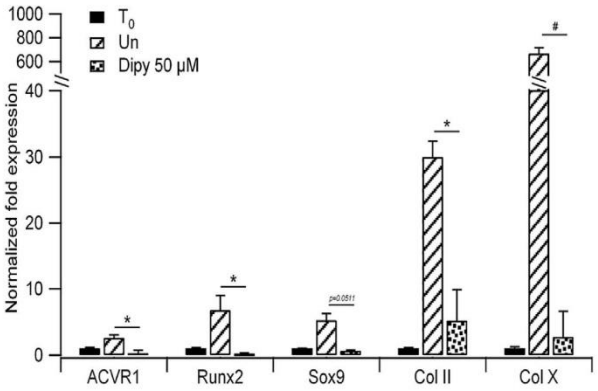

Fig. 4. Effect of Dipy on the expression of chondrogenic markers. RT-qPCR on RNA extracted from ATDC5 cells cultured as alginate spheres for 14 days in differentiation medium. Bars show mean and s.d. of three independent experiments. Expression levels were normalized on *GAPDH* and *18S* and compared to that of cells at T_0 (cells harvested at the beginning of the differentiation protocol). Un, untreated cells. ns, non-significant; **P*<0.05, §*P*<0.001.

confirmed as reduced expression of the Smad-signaling target genes *Id1*, *Id2* and *Id3*, and as reduced phosphorylation of Smad1/5 mediators.

Although the highest effect of Dipy treatment was found to impact *ACVR1* (*Alk2*) expression, we found that Dipy could also affect the expression of other BMP receptors that can synergistically contribute to the downregulation of the overall BMP signaling, such as, among type I receptors, Alk3 or, among type II, BMPRII, which cooperates with ACVR1 as a type I partner in the receptor complex. It is of interest to note that Dipy did not affect the expression of specific receptors, such as *Alk5*, which is involved in cascade mediated by TGF-β type I, or *Alk4*, *ActRIIa* and *ActIIb*, which intervene in GDF-BMP signaling. This finding suggests that the downregulating effect of Dipy is mainly, but not exclusively, exerted on Alk2 (ACVR1), possibly because of common regulatory mechanisms for the expression of molecules belonging to the same family and participating in common pathways.

Because HO in FOP derives from an endochondral ossification process (Kaplan et al., 1993; Medici and Olsen, 2012; Shore, 2012), we set up assays to evaluate both chondrogenesis and osteogenesis. To simulate differentiation *in vitro*, we took advantage of the ability of ATDC5 cells to differentiate towards mature chondrocytes in 3D cultures, with cell morphological changes and deposition of glycosaminoglycans typical of the cartilage extracellular matrix. Using this assay, we observed that Dipy could inhibit chondrogenic differentiation.

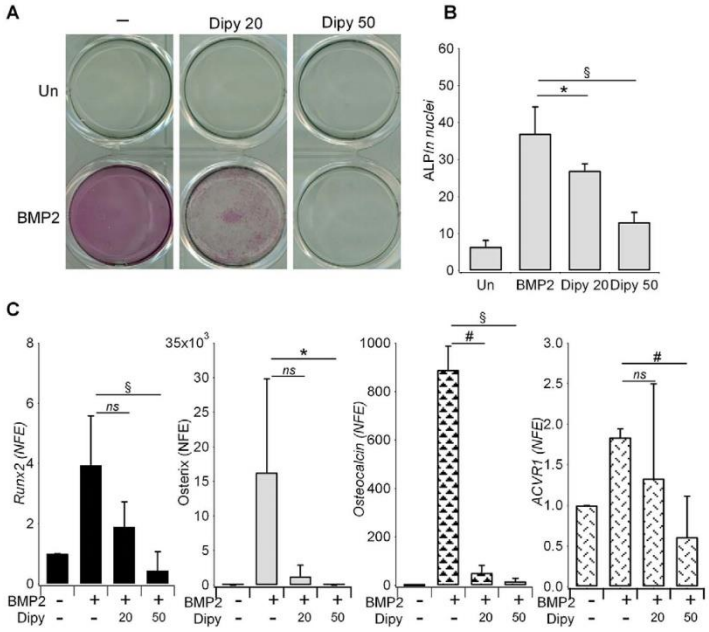

Fig. 5. Effect of Dipy on osteoblastic differentiation of C2C12 cells. (A) Specific staining for alkaline phosphatase activity in C2C12 native cells cultured for 6 days in the presence of [200 ng/ml] BMP2, ±Dipy as indicated (20 or 50 µM). Un, untreated. (B) ALP activity measured in C2C12 cells treated as in A, normalized against the number of nuclei (cells) obtained by automated count after Hoechst staining in each well (see Materials and Methods and Fig. S3). (C) Gene expression level of osteogenic marker genes in C2C12 untreated or treated with Dipy (20 or 50 µM). Bar graphs represent mean and s.d. of three independent experiments. mRNA levels were normalized on *GAPDH* and *18S* and compared to that measured in untreated cells (value 1). NFE, normalized fold expression; ns, non-significant; **P*<0.05, #*P*<0.01, §*P*<0.001.

Disease Models & Mechanisms (2016) 9, 685-696 doi:10.1242/dmm.023929

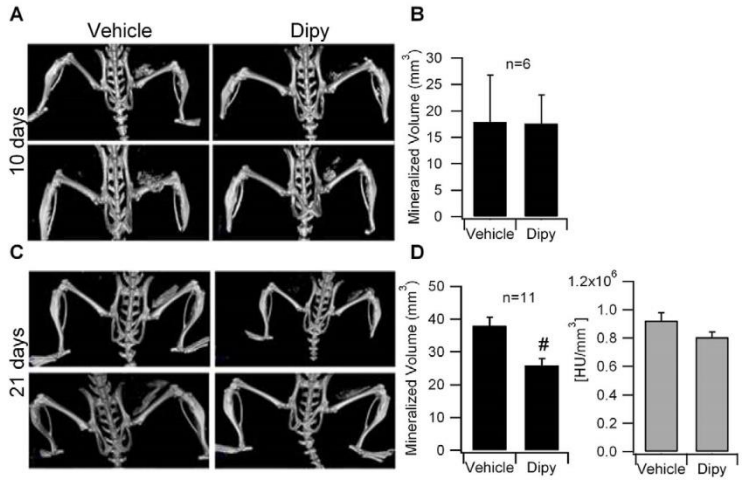

Fig. 6. Effect of Dipy on HO *in vivo*. (A) Micro-computerized tomography (μCT) scans of C57BL/6 mice treated with vehicle or Dipy (10 mg/kg body weight) for 10 days. (B) Quantification of the mineralized ossicle volume. *n*=6 mice/condition. (C) μCT scans of C57BL/6 mice after 21 days of treatment with vehicle or Dipy (10 mg/kg body weight). (D) Quantification of the mineralized ossicle volume (left panel) and lesion bone density (HU/mm^3, right panel). *n*=11 mice/condition. Bars represent mean and s.e.m. $^{\#}P<0.01$. HU, Hounsfield unit.

C2C12 cells were used to evaluate osteogenic differentiation, which was inhibited by Dipy as indicated by the reduction in the alkaline phosphatase (ALP) activity and expression of different markers (Runx2, osterix and osteocalcin).

The effect of Dipy was also verified *in vivo* in a BMP-induced mouse model of HO (Medici et al., 2010). During the induction of the ectopic ossification process, triggered by the implantation of a BMP2-embedded Matrigel coupled to cardiotoxin (CTX) injection, muscle fibers degenerate and the site of injury is infiltrated by different populations of inflammatory cells that contribute to the orchestration of the subsequent repair/differentiation process (Zordan et al., 2014; Rigamonti et al., 2014). During the first week after injury, progenitor cells of different origin are then recruited to the site of the lesion (Bentzinger et al., 2013) and committed towards the endochondral ossification process by the local presence of BMP2. At 10 days, HO lesions are not completely differentiated, and recruitment and activation of cells is ongoing: this was consistent with our finding that, at this stage, the overall number of cells able to respond by activating a specific BMP2/Smad-dependent signaling was higher than what was observed at 21 days after BMP2 induction.

At the earliest time point, the effect of treatment with Dipy became evident as a statistically significant decrease in the number of cells expressing an activated BMP/Smad pathway inside the HO lesions that finally resulted in the reduction of the volume of mineralized heterotopic ossicles, of decreased deposition of extracellular matrix and of a reduced area of calcified nodules that we observed after 21 days of treatment.

Most interestingly, Dipy effect was evident also when mice were treated after the establishment of heterotopic ossification, and resulted in a reduced calcium deposition within the ectopic bone and a decreased mineralization. However, concerning the choice of an *in vivo* prevention strategy versus a treatment on established/ongoing lesions, it is important to consider that the course of FOP is episodic with quiescent phases, lasting even for years, and acute phases that can be triggered by several types of recognizable stimuli (trauma, vaccinations, infection, iatrogenic harms etc.), but that can also occur apparently spontaneously or, more likely, without a recognizable trigger. In this context, a treatment for FOP is ideally a drug that can be administered chronically or for long periods of time in order to prevent the occurrence of even unpredictable flare-ups, thus counteracting their consequences.

Dipy is a commercially available drug that was introduced on the market more than 50 years ago as a coronary vasodilator (Kadatz, 1959). At present, it is widely used as an antithrombotic and vasodilator agent both as monotherapy and in combination with aspirin to prevent secondary stroke or transient ischemic attack (Gresele et al., 2011; Balakumar et al., 2014; de Vos-Koppelaar et al., 2014). At the pharmacological level, Dipy acts by different mechanisms. By inhibiting the activity of phosphodiesterases 5 and 3 (PDE5 and PDE3), it increases the intracellular level of cyclic adenosine monophosphate (cAMP), which is a potent inhibitor of platelet activation, and of cyclic guanine monophosphate (cGMP), which has a vasodilator effect on smooth muscle, thus potentiating the platelet inhibitory actions of prostacyclin (PGI2) (Gresele et al., 2011; de Vos-Koppelaar et al., 2014; Kim and Liao, 2008; Yip and Benavente, 2011). Moreover, Dipy inhibits the re-uptake of adenosine by blocking the equilibrative nucleoside transporters (ENTs), thus increasing plasma levels of this nucleoside, which also plays a role in inhibiting platelet aggregation (Kim and Liao, 2008; Visser et al., 2005; Dresse et al., 1982; German et al., 1989), regulation of vascular tone, vasodilation, immunity and inflammation (Kim and Liao, 2008).

It should be noted that the effect of Dipy in our *in vitro* assay of C2C12 cells was not in accordance with other *in vitro* experiments performed to correlate adenosine level to osteoblast differentiation (Costa et al., 2011; He et al., 2013). This discrepancy might be due to differences in the cellular model and experimental conditions. Moreover, very recently, Mediero and colleagues (2015) reported that local daily injection of Dipy administered with a collagen sponge was able to induce bone regeneration and proposed this treatment as an alternative to recombinant human BMP2 (rhBMP2). At difference with the above report, in the BMP-induced *in vivo* model that we used, HO was locally triggered in quadriceps muscles, whereas treatment with Dipy was systemic, by daily IP injection. Moreover, it has been shown that, in humans, blood cells tend to accumulate the drug (Serebruany et al., 2009), and Dipy is able to inhibit at the mRNA level the production of TNF-α and

Disease Models & Mechanisms (2016) 9, 685-696 doi:10.1242/dmm.023929

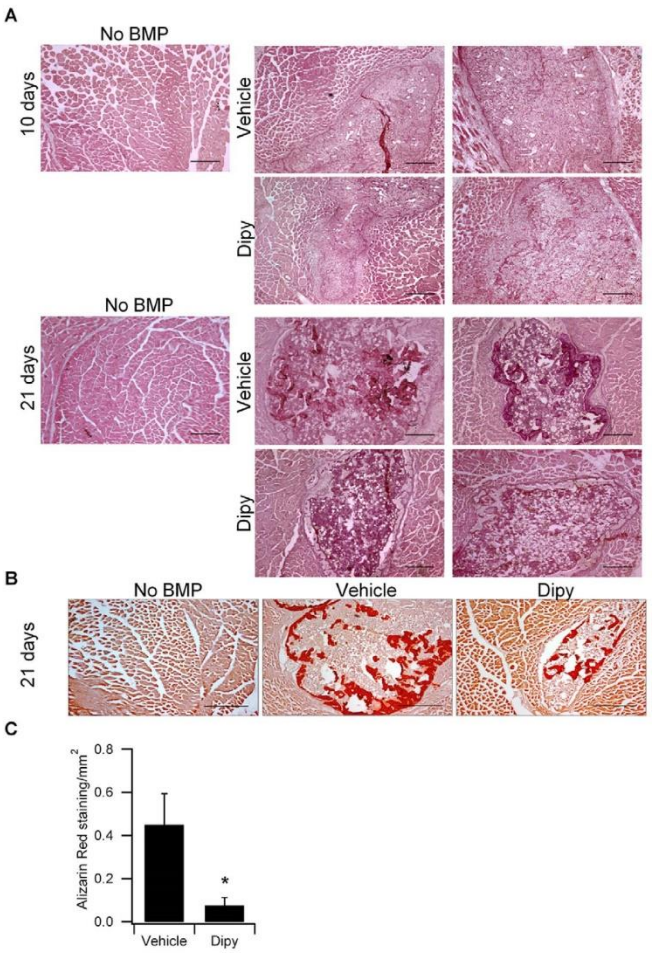

Fig. 7. Chronic Dipy treatment decreases BMP2-induced HO lesions and calcium deposition. (A) Hematoxylin and eosin (H&E) staining showing lesions in muscle injected with BMP-2 and cardiotoxin in mice treated with vector or Dipy for 10 or 21 days. No lesions appear in muscle damaged without BMP. Scale bars: 1 mm. (B) Alizarin Red S staining showing calcium deposition in tissue sections of muscle injected with BMP2 and cardiotoxin in mice treated with the vehicle or Dipy for 21 days. Scale bars: 500 μm. (C) Graph representing the relative quantification of the Alizarin-Red-S-positive area. Data represent mean±s.e.m. $*P \leq 0.05$ ($n=3$, Dipy versus control).

MMP-9 of peripheral blood mononuclear cells (PBMCs) and derived macrophages (Massaro et al., 2013). Because several types of immune cells are recruited at the site of HO lesions, this might contribute to the overall effect observed in our HO model.

Several observations suggest a role of an immune-mediated response in FOP pathogenesis, in particular a possible relevant contribution to the episodic neo-formation of ectopic bone. In humans, FOP flare-ups can be triggered or exacerbated by trauma, immunizations, medical procedures and infections, all of which are conditions in which the immune response is solicited/stimulated (for a review, see Kaplan et al., 2016). Both in humans and in animal models, histological examination of early pre-osseous lesions has clearly demonstrated that several types of immune cells, such as lymphocytes, monocytes/macrophages and mast cells, are readily recruited to these sites (Kaplan et al., 1993; Chakkalakal et al., 2012). In addition, it has been demonstrated that *in vivo* targeted ablation of macrophages or of macrophages and mast cells concomitantly leads to a significant reduction in the ectopic bone formation in FOP mouse models (Kan et al., 2009; Convente et al., 2015).

The deregulated BMP signaling in cells harboring the mutated *ACVR1* gene might contribute to the amplification of inflammatory pathways (Convente et al., 2015); moreover, it has been recently demonstrated that the presence of FOP mutations specifically confers to the mutated receptor the ability to respond to activin A (Hatsell et al., 2015; Hino et al., 2015). Activin A is a ligand member of the TGF-β superfamily that is rapidly released during inflammation and considered a crucial mediator of inflammation and immunity. Its activity is stimulated by inflammatory cytokines, Toll-like receptor ligands and oxidative stress, and it is involved in regulating growth and maturation of mast cells, monocyte/macrophage differentiation, and interaction between natural killer (NK) and dendritic cells (Funaba et al., 2003; Ogawa and Funaba, 2011; Aleman-Muench and Soldevila, 2012; Seeger et al., 2014).

Given the known pleiotropic effect of Dipy, with anti-inflammatory, anti-oxidant and anti-proliferative properties, and

Disease Models & Mechanisms (2016) 9, 685-696 doi:10.1242/dmm.023929

the complexity of the action of a drug *in vivo*, related to its absorption, metabolism and distribution, we cannot exclude that the observed decrease of ectopic ossification in our *in vivo* model might depend on the involvement of different pathways. However, we showed that Dipy is also able to affect specifically the Smad-dependent pathway in HO lesions of treated mice.

Summarizing, the overall effect of Dipy on the process of HO *in vivo* might be mediated by different mechanisms of action, such as the metabolic effect of extracellular adenosine, regulatory properties on differentiation and activation of immune cells, and anti-inflammatory action.

In conclusion, our study implicates this molecule as a candidate drug for the treatment of FOP, considering the great advantage that Dipy is already widely used in the therapy of cardiovascular disorders, and that safety and adverse effect profiles have already been evaluated and established.

MATERIALS AND METHODS

Chemicals and reagents

The Prestwick Chemical Library was purchased from Prestwick Chemical (Illkirch-Graffenstaden, France) and supplied in a special academic format with the 1280 FDA-approved compounds at 10 mM concentration in DMSO, in 16 96-well format plates, each containing 80 compounds.

Resveratrol (CAS no. 501-36-0, Enzo Life Sciences, Farmingdale, NY, USA) and dipyridamole (CAS no. 58-32-2, Sigma, Buchs, SG, Switzerland) were dissolved in DMSO and prepared as 1 M and 200 mM stock solutions, respectively.

Recombinant human BMP2 [rhBMP2; Chinese hamster ovary (CHO)-derived, R&D Systems, Minneapolis, MN, USA] was prepared as a 100 µg/ml stock solution in 4 mM HCl containing 0.1% bovine serum albumin (BSA; Sigma-Aldrich, Buchs, SG, Switzerland).

Antibodies for western blot analyses were: anti-p-Smad1/5 (13820S, Cell Signaling, Danvers, MA, USA), anti-GAPDH (MAB3749, Millipore, Billerica, MA, USA), and horseradish peroxidase (HRP)-conjugated anti-rabbit and anti-mouse secondary antibodies (Dako, Glostrup, Denmark). For immunohistochemical analyses, the following antibodies were used: rabbit anti-bovine polyclonal antibody anti-collagen type II (AB746P, Millipore, Billerica, MA, USA), rabbit polyclonal antibody anti-Sox9 (AB5535, Millipore, Billerica, MA, USA), and anti-rabbit (K4002) and anti-mouse (K4000) EnVision System-HRP Labelled Polymer (Dako, Glostrup, Denmark).

Expression plasmid preparation

The isolation of the genomic region, corresponding to the *ACVR1* promoter, was previously described by our group (Giacopelli et al., 2013). The whole 2.9-kb genomic fragment was subcloned in the pGL4.17 vector (Promega Corporation, Madison, WI, USA) upstream of the luciferase coding sequence as a reporter gene; this expression plasmid carries the Neomycin-resistance gene for selection of stable transfectants. The obtained reporter construct is reported as Pr2.9-Luc throughout the present work. A second reporter gene construct was also prepared by isolating a minimal promoter containing the BMP-responsive element (BRE) of the *Id1* gene from the pGL3-$(BRE)_2$Luc plasmid (kindly provided by Dr Peter ten Djike, Leiden University Medical Center, Leiden, The Netherlands) (Monteiro et al., 2008). BRE was transferred in to the pGL4.17 vector upstream of the luciferase reporter gene (referred to as BRE-Luc) plasmid, carrying the Neomycin-resistance gene that allowed the generation of stable transfectants as described below.

Cell culture

ATDC5 cells (mouse chondrogenic cell line derived from teratocarcinoma) were obtained from the Cell Bank of the Riken BioResource Center upon material transfer agreement (MTA); C2C12 myoblasts were purchased from the ATCC Cell Biology Collection (LGC standards, Bury, Lancashire, UK). ATDC5 cells were routinely cultured in complete medium consisting of 1:1 mixture of Dulbecco's modified Eagle's medium and Ham's F-12 medium (DMEM/F12), containing 5% fetal bovine serum (FBS, Gibco, Thermo Fisher Scientifics, Waltham, MA, USA). C2C12 cells were cultured in DMEM containing 10% FBS. Both culture media were supplemented with 2 mM glutamine, 100 U/ml penicillin, 0.1 mg/ml streptomycin (EuroClone® S.p.a., Pero, MI, Italy), and cells were maintained at 37°C in a humidified atmosphere with 5% CO_2. Where indicated, in depletion media, FBS was replaced by 0.1% BSA (Sigma-Aldrich, Buchs, SG, Switzerland).

Transfection and generation of the cellular system

For stable transfection, ATDC5 cells were plated in 100-mm dishes at a density of $2\times10^4/cm^2$. The next day, cells were transfected with 30 µg of the Pr2.9-Luc and of the BRE-Luc constructs, using the Lipofectamine 2000 reagent protocol (Invitrogen, Thermo Fisher Scientifics, Waltham, MA, USA). After 24 h and for 2 weeks, transfected cells were maintained in complete medium containing 400 µg/ml of Neomycin/G418 (Sigma-Aldrich, Buchs, SG, Switzerland) as selective agent. Thereafter, Neomycin-resistant clones were picked up and expanded. For each clone, 1×10^5 cells were collected after every cell-culture passage and lysed to evaluate the Luciferase activity with the ONE-Glo™ Luciferase Reporter Assay (Promega Corporation, Madison, WI, USA) according to the manufacturer's instruction. Clones showing stable expression of the reporter gene over the time course were considered suitable for our purposes and used to set up the culture and treatment protocols in 96-well format plates.

Screening of the Prestwick Chemical Library in ATDC5 cells

A selected clone of ATDC5 Pr2.9-Luc was seeded into 96-well plates in depletion medium (3×10^5 cells/well). After overnight culture, cells were treated with compounds at the final concentration of 20 µM and 2 µM. We tested 80 molecules in each plate; cells in columns 1 and 12 were treated with 1% DMSO as neutral control, resveratrol (10 µM) as positive control and dipyridamole (20 µM) as negative control (8 wells for DMSO, four wells for each control).

After 24 h, we measured the effect of the compounds on both cell viability and Luciferase activity by using the ONE-Glo™+Tox Luciferase Reporter and Cell Viability Assay (Promega Corporation, Madison, WI, USA) as suggested by the manufacturer. In brief, 20 µl of the CellTiter-Fluor Reagent were added *in situ* to living cells; after 1 h at 37°C, a fluorescent signal proportional to the number of viable cells in the culture well was measured by Glomax Multi Detection System (Promega Corporation, Madison, WI, USA). 100 µl of the second ONE-Glo Reagent were then added directly to each well to allow cell lysis and detection of the luciferase signal (Glomax Multi Detection System, Promega Corporation, Madison, WI, USA).

Fluorescence (fluo) and luminescence (*ACVR1* promoter activity; Lum) raw data were handled with the Instinct Software (Promega Corporation, Madison, WI, USA) and analyzed as an Excel spreadsheet. Cell viability (Vi) was first evaluated by comparing the fluo signal obtained in cells treated with compounds ($fluoC_x$) versus that of cells exposed to the vehicle [$Vi=(fluoC_x/\text{average } fluo_{DMSO})\times100$, with $0\geq Vi\geq100$]. In parallel, the effect of compounds (E) on *ACVR1* transcriptional activity was evaluated as follows: first, by normalizing luminescence signal over the fluorescence signal for each test well ($N_x=LumC_x/fluoC_x$) and for the neutral control ($N_{DMSO}=Lum_{DMSO}/fluo_{DMSO}$), then by comparing the normalized values of compounds with that of the vehicle [$E=(N_x/\text{average}N_{DMSO})\times100$].

RNA extraction and quantitative RT-PCR (RT-qPCR)

For expression studies, treated and untreated cells (ATDC5 and C2C12) were harvested and total RNA was isolated by using the RNeasy Mini Kit (Qiagen, Valencia, CA, USA), according to the provided protocol.

RNA was quantified with a Nanodrop Spectrophotometer (Thermo Scientific, Thermo Fisher Scientifics, Waltham, MA, USA), and first-strand cDNA was synthesized by the Advantage RT-for-PCR Kit (Becton) from 200 ng of total RNA.

Expression of endogenous *ACVR1* gene and of selected markers was evaluated through RT-qPCR using specific TaqMan Gene Expression Assay (Life Technologies, Thermo Fisher Scientifics, Waltham, MA, USA) (see Table S3 for specification). Samples were measured in triplicate and the results were normalized on reference genes *18S*, *GAPDH* and β2-microglobulin (*β2M*), depending on the cell line. qPCR was run on the IQ5

Disease Models & Mechanisms (2016) 9, 685-696 doi:10.1242/dmm.023929

instrument from Bio-Rad and data analysis was performed using the provided Bio-Rad iQ5 software for Gene Expression Study.

Western blot

For detection of p-Smad, 1.2×10^6 cells were plated in 100-mm dishes in 1:1 complete/depletion medium for ATDC5 cells, and in depletion medium for C2C12 (DMEM containing 1% FBS). The next day, serum-starved cells were treated with Dipy for 24 h and, where indicated, with BMP2 (R&D Systems, Minneapolis, MN, USA) 200 ng/ml for 1 h. Cells were then washed once with PBS and lysed in 1× RIPA buffer (50 mM Tris HCl pH 7.5, 150 mM NaCl, 1% Nonidet P-40, 1% sodium deoxycholic, 0.1% SDS) containing phosphatase and protease inhibitors (PhosSTOP cocktail and Complete tablets, Roche, Basel, Switzerland). Protein concentration was determined by the Pierce™ BCA Protein Assay Kit (Thermo Scientific, Thermo Fisher Scientifics, Waltham, MA, USA) according to the manufacturer's protocol and 15 µg of total lysates run onto precasted 4-15% Mini Protean®TGX-gels (Bio-Rad, Hercules, CA, USA). Proteins were transferred onto PVDF membrane (Millipore, Billerica, MA, USA) and probed with the indicated primary antibody at 4°C overnight. After incubation with HRP-conjugated secondary antibodies, protein bands were revealed by chemiluminescence with the ECL kit (Pierce, Thermo Fisher Scientifics, Waltham, MA, USA) and detected with the ChemiDoc instrument (Bio-Rad, Hercules, CA, USA). Densitometric analysis of western blot signals was performed by using the ImageJ software.

Culture in 3D pellets

ATDC5 cells were trypsinized from monolayer cultures and 1 ml of cell suspension with 5×10^5 cells in DMEM was added to 15 ml polycarbonate sterile tubes according to Tare et al. (2005). The cell suspension was centrifuged at 400 *g* for 10 min at 4°C to obtain pellets that were cultured both in standard complete medium and in chondrogenic medium containing 10 ng/ml TGF-β3 (Calbiochem, Millipore, Billerica, MA, USA), 10^{-8} M dexamethasone (Sigma-Aldrich, Buchs, SG, Switzerland), 100 mM ascorbate-2-phosphate (Sigma-Aldrich, Buchs, SG, Switzerland), 1× insulin-trasferrin-selenium (ITS) solution (Life Technologies, Thermo Fisher Scientifics, Waltham, MA, USA). Pellets were cultured for 21 days in a humidified incubator at 37°C and 5% CO_2. Pellets were swirled within to allow medium access to all sides and prevent adhesion to the inner walls of the tube. Once compact pellets were formed, both proliferative and differentiating media were replaced every 3 days and thereafter over the culture period. Three pellets from each group were harvested and processed for histological analysis.

Culture in alginate spheres

ATDC5 cells were cultured in alginate spheres according to Culbert et al. (2014). Briefly, cell suspensions at 6.7×10^6 cells/ml in 1.2% alginate acid sodium salt (Sigma-Aldrich, Buchs, SG, Switzerland) solution were extruded through 16-gauge needles as ~30 µl drops in 30 ml of 102 mM $CaCl_2$ (Sigma-Aldrich, Buchs, SG, Switzerland) in order to allow sphere formation. After drop solidification, cells/alginate spheres were washed with PBS and cultured in chondrogenic medium, replenishing every 3 days. A number of alginate spheres for each condition were formalin-fixed and processed for histological stainings and immunohistochemical assays. In parallel, spheres were also incubated with 55 mM sodium citrate (Sigma, Buchs, SG, Switzerland) to recover cells for total RNA extraction and expression analysis of markers specific for chondrogenesis such as *Runx2*, *Sox9*, *Col II*, *Col X*, aggrecan and also *ACVR1* by RT-qPCR with TaqMan Assays probes (Life Technologies, Thermo Fisher Scientifics, Waltham, MA, USA) (see Table S3 for specification).

Histological analysis

Cell aggregates were fixed with 4% formaldehyde (Santa Cruz Biotechnology, Dallas, TX, USA) in PBS for 10-15 min, and embedded in paraffin according to standard protocols. Paraffin sections (5 µm) were obtained by microtome, dewaxed and rehydrated with decreasing ethanol solutions. For histological analysis, sections were stained with Alcian Blue 8GX (Sigma-Aldrich, Buchs, SG, Switzerland) following established procedures and viewed in transmitted and polarized light microscopy.

Immunohistochemistry

Dewaxed and rehydrated sections were incubated with 3% hydrogen peroxide in methanol for 30 min to inhibit endogenous peroxidase activity, rinsed in PBS/0.2% Triton X-100, then were subjected to digestion with 1 mg/ml hyaluronidase in PBS, pH 6.0 for 15 min at 37°C prior to use. Sections were exposed to normal goat serum (Dako, Glostrup, Denmark) 1 h before incubation with the primary antibodies (24 h, 4°C). Slides were then washed with PBS (four times for 5 min each) and incubated with the HRP-conjugated secondary antibodies for 1 h at room temperature (RT). The peroxidase reaction was developed using 3,3′-diaminobenzidine tetrahydrochloride (DAB) as chromogens. After rinsing in distilled water, sections were dehydrated in increasing ethanol solutions, cleared in xylene and mounted.

C2C12 cell culture and osteogenic differentiation

In order to induce C2C12 differentiation towards the osteoblastic lineage (Katagiri et al., 1994), 1.2×10^4 cells were seeded in 6-well plates and cultured in complete medium supplemented with 5% FBS (low-mitogen medium). The day after, cells were treated with 300 ng/ml BMP2 (R&D Systems, Minneapolis, MN, USA) for 6 days. Where indicated, Dipy (50 µM) was also added to both standard and differentiating media.

Cells were processed to evaluate the alkaline phosphatase (ALP) enzymatic activity by the Alkaline Phosphatase (Sigma Diagnostics, Buchs, SG, Switzerland) kit following the manufacturer's instructions and total RNA was extracted to evaluate the expression of *Runx2*, osterix and osteocalcin by RT-qPCR with TaqMan Assays probes. In order to quantify the ALP activity in C2C12 cells induced by BMP2 treatment, 5×10^3 cells were plated in CellCarrier-96-well™ microplates (Perkin Elmer, Waltham, MA, USA) and cultured in the presence of BMP2±Dipy as described. After 6 days, Hoechst 33342 Nuclear Stain (ENZ-51031-HOE33342, Enzo Life Sciences) was added to the culture medium at a 1:1000 dilution and incubated for 20 min. Cells were then visualized with the NIKON Ti Eclipse microscope; 16 640×490-µm fields for each well and condition were acquired and analyzed by the NIS-Elements AR software to obtain an automated count of the present nuclei. The number of nuclei has been used to normalize the ALP activity measured as follows. After analysis, cells were washed with PBS and incubated with 200 µl of the Alkaline Phosphatase Yellow liquid substrate system (nNPP) (Sigma, Buchs, SG, Switzerland). Reaction was stopped with 60 µl 3 M NaOH and ALP activity measured at 405 nm by Mithras LB940 plate reader (Berthold Technologies).

Heterotopic ossification *in vivo*

0.05 µg/µl of BMP2 (Peprotech, Rocky Hill, NJ, USA) in 200 µl growth-factor-reduced Matrigel (BD Biosciences) were injected intramuscularly in the quadriceps of C57BL/6 2-month-old mice (11 mice/group). The contralateral muscle was used as internal control and injected with Matrigel only. Both quadriceps were injected with 50 µl cardiotoxin 5 µM (CTX from *Naja mossambica mossambica*, Sigma-Aldrich, Buchs, SG, Switzerland) to increase muscle damage. Animals were anesthetized by inhalation of 2-bromo-2-chloro-1,1,1-trifluoroethane, ≥99% (CAS no. 151-67-7, Sigma-Aldrich, Buchs, SG, Switzerland) before the injection. 10 mg/kg (body weight) dipyridamole was administered daily IP to the treated animals (n=11, for Protocol A; n=5 for Protocol B, see Fig. S5) in a solution composed of 10% ethanol, 5% 2-pyrolidone, 12-15% propylene glycol, 10% Cremophor ELP, saline to 100% (Wang et al., 2013). Control mice (n=11, for Protocol A; n=5 for Protocol B, see Fig. S5) received the injection solution without drug. Mice were housed at the San Raffaele Institute SPF animal facility and were kept in pathogen-free conditions. All procedures were in accordance with Italian law and were performed under internal regulations for animal care and handling.

In vivo CT imaging of heterotopic ossification

At day 10 and 21 after BMP injection, *in vivo* micro-computerized tomography (µCT) scans were carried out to assess progression of ossification and any effect on the normal skeletal structure. *In vivo* µCT imaging was performed using the IVIS SpectrumCT Pre-clinical *in vivo* imaging system (Perkin-Elmer, Waltham, MA, USA). CT images were acquired without any contrast medium with the following parameters: x-ray

tube voltage=50 kV, tube current=1 mA, x-ray focal spot size=50 µm. The CT images calibrated in Hounsfield unit (HU) were reconstructed with a voxel size of 75 μm^3. Threshold-based image segmentation were performed to obtain a 3D reconstruction and quantification of the ossification.

The total mineralized volume V=N×voxel size (mm^3) was quantified using MIPAV (medical imaging processing analysis and visualization) and MATLAB software, where N is the number of voxels corresponding to bone derived from the image segmentation procedure. The bone density quantification was calculated by using the following formula: $\sum Ni=1\ HUi/V$.

Morphological and histochemical analysis of the heterotopic ossification

At 21 days after BMP injection, muscles were collected and processed for further morphological and histological analyses. BMP/Matrigel-injected and Matrigel-injected quadriceps from treated and control mice were frozen in liquid-nitrogen-cooled isopentane, to allow preparation of 10-µm-thick sections.

Muscle sections were stained with hematoxylin and eosin (H&E) (Sigma-Aldrich, Buchs, SG, Switzerland) or Toluidine Blue (Bio-Optica, Milano, Italy) or Alizarin Red (Sigma-Aldrich, Buchs, SG, Switzerland) according to the manufacturers' instructions. Images were acquired using a Nikon Eclipse E600 microscope (Nikon, Tokyo, Japan). To quantify heterotopic ossification, images of Alizarin-Red-stained sections were subsequently analyzed using the batch mode of the ImageJ vs1.49 macro. The color thresholding algorithm used by this macro is based on an algorithm written by G. Landini (version v1.8) available at http://www.mecourse.com/landinig/software/software.html.

Immunofluorescence on muscle sections

For immunofluorescence, 8-µm sections from OCT-embedded muscles were fixed with 4% PFA in PBS. They were permeabilized with a 0.2% Triton X-100, 1% BSA solution in PBS for 30 min at RT and then blocked in 10% serum, 1% BSA solution in PBS for 30 min before incubation with the primary antibody p-Smad1/5 (1:800; Cell Signaling, Danvers, MA, USA), after a demasking step in sodium citrate 10 mM pH 6 for 10 min between fixation and blocking steps (2 h). Alexa-Fluor-546-conjugated antibody (1:500; Invitrogen, Thermo Fisher Scientifics, Waltham, MA, USA) was used as second-step reagents. Specimens were counterstained with DAPI (Sigma, Buchs, SG, Switzerland) and analyzed using a Zeiss LSM710 confocal microscope. Images showing double fluorescence were first acquired separately using appropriate filters, then the different layers were merged using Adobe Photoshop CS4.

Statistical analysis

All luciferase reporter gene assays were performed in triplicate and repeated independently at least twice (2-5 times). Z′ factor was evaluated by using the formula $[Z'=1-3\times(\sigma_s+\sigma_c)/|\mu_s-\mu_c|]$, where σ_s and σ_c are the s.d. of positive or negative sample and of the solvent (control) and μ_s and μ_c represent the average. Experiments to evaluate gene expression by RT-qPCR were performed in triplicate from at least two independent RNA extractions. Both the non-parametric Mann–Whitney test (Social Science Statistics) and the unpaired two-tailed Student's *t*-test (GraphPad *t*-test Calculator; http://graphpad.com/quickcalcs/ttest1.cfm) were applied to verify statistical significance of the observed variations. Significant differences were given as $^{*}P<0.05$, $^{\#}P<0.01$ or $^{\S}P<0.001$.

Acknowledgements

We thank the FOP Italia Association, FOP patients and their families for funding and for their special support to our research. We also acknowledge the Preclinical Imaging Facility of the San Raffaele Centre for Experimental Imaging. The excellent technical support of Paolo Scudieri and Anita Muraglia is gratefully acknowledged.

Competing interests

The authors declare no competing or financial interests.

Author contributions

S.C. conceived, designed, performed and analyzed the experiments, and prepared the manuscript; L.T. and B.C. performed differentiation assays and 3D cultures; F.G. performed and analyzed RT-qPCR experiments; M.T., M.S. and A.G. performed *in vivo* experiments; L.J.V.G. provided support for HTS protocols and critical reading of the manuscript; A.E.S. performed mouse µCT scan analyses; S.B. supervised *in vivo* experiments and critical discussion of data; R.B. and R.R. conceived and supervised the experiments and manuscript preparation.

Funding

The financial support of Fondazione Telethon (grant no. GGP15196) is gratefully acknowledged. This work was also supported by the contribution of FOP Italia Onlus, and Ministero della Salute (Cinque per mille e Ricerca corrente) (Italian Ministry of Health).

Supplementary information

Supplementary information available online at
http://dmm.biologists.org/lookup/suppl/doi:10.1242/dmm.023929/-/DC1

References

Aleman-Muench, G. R. and Soldevila, G. (2012). When versatility matters: activins/inhibins as key regulators of immunity. *Immunol. Cell Biol.* **90**, 137-148.
Balakumar, P., Nyo, Y. H., Renushia, R., Raaginey, D., Oh, A. N., Varatharajan, R. and Dhanaraj, S. A. (2014). Classical and pleiotropic actions of dipyridamole: not enough light to illuminate the dark tunnel? *Pharmacol. Res.* **87**, 144-150.
Bentzinger, C. F., Wang, Y. X., Dumont, N. A. and Rudnicki, M. A. (2013). Cellular dynamics in the muscle satellite cell niche. *EMBO Rep.* **14**, 1062-1072.
Bocciardi, R., Bordo, D., Di Duca, M., Di Rocco, M. and Ravazzolo, R. (2009). Mutational analysis of the ACVR1 gene in Italian patients affected with fibrodysplasia ossificans progressiva: confirmations and advancements. *Eur. J. Hum. Genet.* **17**, 311-318.
Chaikuad, A., Alfano, I., Kerr, G., Sanvitale, C. E., Boergermann, J. H., Triffitt, J. T., von Delft, F., Knapp, S., Knaus, P. and Bullock, A. N. (2012). Structure of the bone morphogenetic protein receptor ALK2 and implications for fibrodysplasia ossificans progressiva. *J. Biol. Chem.* **287**, 36990-36998.
Chakkalakal, S. A., Zhang, D., Culbert, A. L., Convente, M. R., Caron, R. J., Wright, A. C., Maidment, A. D. A., Kaplan, F. S. and Shore, E. M. (2012). An Acvr1 R206H knock-in mouse has fibrodysplasia ossificans progressiva. *J. Bone Miner. Res.* **27**, 1746-1756.
Convente, M. R., Yang, E., Chakkalakal, S. A., Zhang, D., Caron, R. J., Perrien, D. S., Kambayashi, T., Kaplan, F. S. and Shore, E. M. (2015). Targeted ablation of macrophages and mast cells impairs heterotopic ossification in a mouse model of fibrodysplasia ossificans progressiva. *J. Bone Miner. Res.* **30** (Suppl 1), S484.
Costa, M. A., Barbosa, A., Neto, E., Sá-e-Sousa, A., Freitas, R., Neves, J. M., Magalhães-Cardoso, T., Ferreirinha, F. and Correia-de-Sá, P. (2011). On the role of subtype selective adenosine receptor agonists during proliferation and osteogenic differentiation of human primary bone marrow stromal cells. *J. Cell Physiol.* **226**, 1353-1366.
Culbert, A. L., Chakkalakal, S. A., Theosmy, E. G., Brennan, T. A., Kaplan, F. S. and Shore, E. M. (2014). Alk2 regulates early chondrogenic fate in fibrodysplasia ossificans progressiva heterotopic endochondral ossification. *Stem Cells* **32**, 1289-1300.
Cuny, G. D., Yu, P. B., Laha, J. K., Xing, X., Liu, J.-F., Lai, C. S., Deng, D. Y., Sachidanandan, C., Bloch, K. D. and Peterson, R. T. (2008). Structure-activity relationship study of bone morphogenetic protein (BMP) signaling inhibitors. *Bioorg. Med. Chem. Lett.* **18**, 4388-4392.
de Vos-Koppelaar, N. C. M., Kerkhoff, H., de Vogel, E. M., Zock, E. and Dieleman, H. G. (2014). The effect of a slower than standard dose escalation scheme for dipyridamole on headaches in secondary prevention therapy of strokes: a randomized, open-label trial (DOSE). *Cerebrovasc. Dis.* **37**, 285-289.
Dresse, A., Chevolet, C., Delapierre, D., Masset, H., Weisenberger, H., Bozler, G. and Heinzel, G. (1982). Pharmacokinetics of oral dipyridamole (Persantine) and its effect on platelet adenosine uptake in man. *Eur. J. Clin. Pharmacol.* **23**, 229-234.
Funaba, M., Ikeda, T., Ogawa, K., Murakami, M. and Abe, M. (2003). Role of activin A in murine mast cells: modulation of cell growth, differentiation, and migration. *J. Leukoc. Biol.* **73**, 793-801.
German, D. C., Kredich, N. M. and Bjornsson, T. D. (1989). Oral dipyridamole increases plasma adenosine levels in human beings. *Clin. Pharmacol. Ther.* **45**, 80-84.
Giacopelli, F., Cappato, S., Tonachini, L., Mura, M., Di Lascio, S., Fornasari, D., Ravazzolo, R. and Bocciardi, R. (2013). Identification and characterization of regulatory elements in the promoter of ACVR1, the gene mutated in Fibrodysplasia Ossificans Progressiva. *Orphanet. J. Rare Dis.* **8**, 145.
Gresele, P., Momi, S. and Falcinelli, E. (2011). Anti-platelet therapy: phosphodiesterase inhibitors. *Br. J. Clin. Pharmacol.* **72**, 634-646.
Groppe, J. C., Wu, J., Shore, E. M. and Kaplan, F. S. (2011). In vitro analyses of the dysregulated R206H ALK2 kinase-FKBP12 interaction associated with heterotopic ossification in FOP. *Cells Tissues Organs* **194**, 291-295.
Hao, J., Ho, J. N., Lewis, J. A., Karim, K. A., Daniels, R. N., Gentry, P. R., Hopkins, C. R., Lindsley, C. W. and Hong, C. C. (2010). In vivo structure-activity relationship study of dorsomorphin analogues identifies selective VEGF and BMP inhibitors. *ACS Chem. Biol.* **5**, 245-253.

Hatsell, S. J., Idone, V., Wolken, D. M. A., Huang, L., Kim, H. J., Wang, L., Wen, X., Nannuru, K. C., Jimenez, J., Xie, L. et al. (2015). ACVR1R206H receptor mutation causes fibrodysplasia ossificans progressiva by imparting responsiveness to activin A. *Sci. Transl. Med.* **7**, 303ra137.

He, W., Mazumder, A., Wilder, T. and Cronstein, B. N. (2013). Adenosine regulates bone metabolism via A1, A2A, and A2B receptors in bone marrow cells from normal humans and patients with multiple myeloma. *FASEB J.* **27**, 3446-3454.

Hino, K., Ikeya, M., Horigome, K., Matsumoto, Y., Ebise, H., Nishio, M., Sekiguchi, K., Shibata, M., Nagata, S., Matsuda, S. et al. (2015). Neofunction of ACVR1 in fibrodysplasia ossificans progressiva. *Proc. Natl. Acad. Sci. USA* **112**, 15438-15443.

Kadatz, R. (1959). [Pharmacological properties of a new coronary dilator substance 2, 6-bis(diethanolamino)-4,8-dipiperidino-pyrimido[5,4-d]pyrimidine]. *Arzneimittelforschung* **9**, 39-45.

Kan, L., Liu, Y., McGuire, T. L., Berger, D. M. P., Awatramani, R. B., Dymecki, S. M. and Kessler, J. A. (2009). Dysregulation of local stem/progenitor cells as a common cellular mechanism for heterotopic ossification. *Stem Cells* **27**, 150-156.

Kaplan, F. S., Tabas, J. A., Gannon, F. H., Finkel, G., Hahn, G. V. and Zasloff, M. A. (1993). The histopathology of fibrodysplasia ossificans progressiva. An endochondral process. *J. Bone Joint Surg. Am.* **75**, 220-230.

Kaplan, F. S., Shen, Q., Lounev, V., Seemann, P., Groppe, J., Katagiri, T., Pignolo, R. J. and Shore, E. M. (2008). Skeletal metamorphosis in fibrodysplasia ossificans progressiva (FOP). *J. Bone Miner. Metab.* **26**, 521-530.

Kaplan, F. S., Xu, M., Seemann, P., Connor, J. M., Glaser, D. L., Carroll, L., Delai, P., Fastnacht-Urban, E., Forman, S. J., Gillessen-Kaesbach, G. et al. (2009). Classic and atypical fibrodysplasia ossificans progressiva (FOP) phenotypes are caused by mutations in the bone morphogenetic protein (BMP) type I receptor ACVR1. *Hum. Mutat.* **30**, 379-390.

Kaplan, F. S., Pignolo, R. J. and Shore, E. M. (2013). From mysteries to medicines: drug development for fibrodysplasia ossificans progressiva. *Expert Opin. Orphan. Drugs* **1**, 637-649.

Kaplan, F. S., Pignolo, R. J. and Shore, E. M. (2016). Granting immunity to FOP and catching heterotopic ossification in the Act. *Semin. Cell. Dev. Biol.* **49**, 30-36.

Katagiri, T., Yamaguchi, A., Komaki, M., Abe, E., Takahashi, N., Ikeda, T., Rosen, V., Wozney, J. M., Fujisawa-Sehara, A. and Suda, T. (1994). Bone morphogenetic protein-2 converts the differentiation pathway of C2C12 myoblasts into the osteoblast lineage. *J. Cell. Biol.* **127**, 1755-1766.

Kim, H.-H. and Liao, J. K. (2008). Translational therapeutics of dipyridamole. *Arterioscler. Thromb. Vasc. Biol.* **28**, S39-S42.

Kitoh, H., Achiwa, M., Kaneko, H., Mishima, K., Matsushita, M., Kadono, I., Horowitz, J. D., Sallustio, B. C., Ohno, K. and Ishiguro, N. (2013). Perhexiline maleate in the treatment of fibrodysplasia ossificans progressiva: an open-labeled clinical trial. *Orphanet J. Rare Dis.* **8**, 163.

Li, Y. Y. and Jones, S. J. (2012). Drug repositioning for personalized medicine. *Genome Med.* **4**, 27.

Massaro, M., Scoditti, E., Carluccio, M. A., Pellegrino, M., Calabriso, N., Storelli, C., Martines, G. and De Caterina, R. (2013). Dipyridamole decreases inflammatory metalloproteinase-9 expression and release by human monocytes. *Thromb. Haemost.* **109**, 280-289.

Medici, D. and Olsen, B. R. (2012). The role of endothelial-mesenchymal transition in heterotopic ossification. *J. Bone Miner. Res.* **27**, 1619-1622.

Medici, D., Shore, E. M., Lounev, V. Y., Kaplan, F. S., Kalluri, R. and Olsen, B. R. (2010). Conversion of vascular endothelial cells into multipotent stem-like cells. *Nat. Med.* **16**, 1400-1406.

Mediero, A., Wilder, T., Perez-Aso, M. and Cronstein, B. N. (2015). Direct or indirect stimulation of adenosine A2A receptors enhances bone regeneration as well as bone morphogenetic protein-2. *FASEB J.* **29**, 1577-1590.

Monteiro, R. M., de Sousa Lopes, S. M. C., Bialecka, M., de Boer, S., Zwijsen, A. and Mummery, C. L. (2008). Real time monitoring of BMP Smads transcriptional activity during mouse development. *Genesis* **46**, 335-346.

Muthyala, R. (2011). Orphan/rare drug discovery through drug repositioning. *Drug Discov. Today* **8**, 71-76.

Ogawa, K. and Funaba, M. (2011). Activin in humoral immune responses. *Vitam. Horm.* **85**, 235-253.

Oshrine, B., Malinin, A., Pokov, A., Dragan, A., Hanley, D. and Serebruany, V.; Aggrenox Compliance Task Force. (2005). Criticality of pH for accurate fluorometric measurements of dipyridamole levels in biological fluids. *Methods Find Exp. Clin. Pharmacol.* **27**, 95-100.

Rigamonti, E., Zordan, P., Sciorati, C., Rovere-Querini, P. and Brunelli, S. (2014). Macrophage plasticity in skeletal muscle repair. *Biomed. Res. Int.* **2014**, 560629.

Sanvitale, C. E., Kerr, G., Chaikuad, A., Ramel, M.-C., Mohedas, A. H., Reichert, S., Wang, Y., Triffitt, J. T., Cuny, G. D., Yu, P. B. et al. (2013). A new class of small molecule inhibitor of BMP signaling. *PLoS ONE* **8**, e62721.

Sardana, D., Zhu, C., Zhang, M., Gudivada, R. C., Yang, L. and Jegga, A. G. (2011). Drug repositioning for orphan diseases. *Brief Bioinform.* **12**, 346-356.

Seeger, P., Bosisio, D., Parolini, S., Badolato, R., Gismondi, A., Santoni, A. and Sozzani, S. (2014). Activin A as a mediator of NK-dendritic cell functional interactions. *J. Immunol.* **192**, 1241-1248.

Serebruany, V., Sabaeva, E., Booze, C., Atar, O. D., Eisert, C. and Hanley, D. (2009). Aggrenox Compliance Task Force. Distribution of dipyridamole in blood components among post-stroke patients treated with extended release formulation. *Thromb. Haemost.* **2**, 538-543.

Shameer, K., Readhead, B. and Dudley, J. T. (2015). Computational and experimental advances in drug repositioning for accelerated therapeutic stratification. *Curr. Top. Med. Chem.* **15**, 5-20.

Sheng, N., Xie, Z., Wang, C., Bai, G., Zhang, K., Zhu, Q., Song, J., Guillemot, F., Chen, Y.-G., Lin, A. et al. (2010). Retinoic acid regulates bone morphogenic protein signal duration by promoting the degradation of phosphorylated Smad1. *Proc. Natl. Acad. Sci. USA* **107**, 18886-18891.

Shimono, K., Tung, W.-E., Macolino, C., Chi, A. H.-T., Didizian, J. H., Mundy, C., Chandraratna, R. A., Mishina, Y., Enomoto-Iwamoto, M., Pacifici, M. et al. (2011). Potent inhibition of heterotopic ossification by nuclear retinoic acid receptor-γ agonists. *Nat. Med.* **17**, 454-460.

Shore, E. M. (2012). Fibrodysplasia ossificans progressiva: a human genetic disorder of extraskeletal bone formation, or–how does one tissue become another? *Wiley Interdiscip. Rev. Dev. Biol.* **1**, 153-165.

Shore, E. M., Feldman, G. J., Xu, M. and Kaplan, F. S. (2005). The genetics of fibrodysplasia ossificans progressiva. *Clin. Rev. Bone Miner. Metab.* **3**, 201-204.

Shore, E. M., Xu, M., Feldman, G. J., Fenstermacher, D. A., Cho, T. J., Choi, I. H., Connor, J. M., Delai, P., Glaser, D. L., LeMerrer, M. et al. (2006). A recurrent mutation in the BMP type I receptor ACVR1 causes inherited and sporadic fibrodysplasia ossificans progressiva. *Nat. Genet.* **38**, 525-527.

Song, G.-A., Kim, H.-J., Woo, K.-M., Baek, J.-H., Kim, G.-S., Choi, J.-Y. and Ryoo, H.-M. (2010). Molecular consequences of the ACVR1(R206H) mutation of fibrodysplasia ossificans progressiva. *J. Biol. Chem.* **285**, 22542-22553.

Tare, R. S., Howard, D., Pound, J. C., Roach, H. I. and Oreffo, R. O. C. (2005). Tissue engineering strategies for cartilage generation—micromass and three dimensional cultures using human chondrocytes and a continuous cell line. *Biochem. Biophys. Res. Commun.* **333**, 609-621.

van Dinther, M., Visser, N., de Gorter, D. J., Doorn, J., Goumans, M. J., de Boer, J. and ten Dijke, P. (2010). ALK2 R206H mutation linked to fibrodysplasia ossificans progressiva confers constitutive activity to the BMP type I receptor and sensitizes mesenchymal cells to BMP-induced osteoblast differentiation and bone formation. *J. Bone Miner. Res.* **25**, 1208-1215.

Visser, F., Baldwin, S. A., Isaac, R. E., Young, J. D. and Cass, C. E. (2005). Identification and mutational analysis of amino acid residues involved in dipyridamole interactions with human and Caenorhabditis elegans equilibrative nucleoside transporters. *J. Biol. Chem.* **280**, 11025-11034.

Wang, C., Schwab, L. P., Fan, M., Seagroves, T. N. and Buolamwini, J. K. (2013). Chemoprevention activity of dipyridamole in the MMTV-PyMT transgenic mouse model of breast cancer. *Cancer Prev. Res.* **6**, 437-447.

Yamamoto, R., Matsushita, M., Kitoh, H., Masuda, A., Ito, M., Katagiri, T., Kawai, T., Ishiguro, N. and Ohno, K. (2013). Clinically applicable antianginal agents suppress osteoblastic transformation of myogenic cells and heterotopic ossifications in mice. *J. Bone Miner. Metab.* **31**, 26-33.

Yip, S. and Benavente, O. (2011). Antiplatelet agents for stroke prevention. *Neurotherapeutics* **8**, 475-487.

Yu, P. B., Deng, D. Y., Lai, C. S., Hong, C. C., Cuny, G. D., Bouxsein, M. L., Hong, D. W., McManus, P. M., Katagiri, T., Sachidanandan, C. et al. (2008a). BMP type I receptor inhibition reduces heterotopic ossification. *Nat. Med.* **14**, 1363-1369.

Yu, P. B., Hong, C. C., Sachidanandan, C., Babitt, J. L., Deng, D. Y., Hoyng, S. A., Lin, H. Y., Bloch, K. D. and Peterson, R. T. (2008b). Dorsomorphin inhibits BMP signals required for embryogenesis and iron metabolism. *Nat. Chem. Biol.* **4**, 33-41.

Zhang, J.-H., Chung, T. D. Y. and Oldenburg, K. R. (1999). A Simple Statistical Parameter for Use in Evaluation and Validation of High Throughput Screening Assays. *J. Biomol. Screen* **4**, 67-73.

Zordan, P., Rigamonti, E., Freudenberg, K., Conti, V., Azzoni, E., Rovere-Querini, P. and Brunelli, S. (2014). Macrophages commit postnatal endothelium-derived progenitors to angiogenesis and restrict endothelial to mesenchymal transition during muscle regeneration. *Cell Death Dis.* **5**, e1031.

CHAPTER 3

3. Severe heterotopic ossification in the skeletal muscle is triggered by monocyte depletion and endothelial recruitment to chondro-osteogenesis

Mario Tirone[1,2]*, Anna Giovenzana[1]*, Arianna Vallone[1], Paola Zordan[3]§, Martina Sormani[1], Pier Andrea Nicolosi[1], Raffaela Meneveri[1], Carmen Rosaria Gigliotti[4], Antonello Spinelli[5], Renata Bocciardi[6], Roberto Ravazzolo[6], Ingrid Cifola[7], Silvia Brunelli[1]

Submitted to Disease Models and Mechanisms

Severe heterotopic ossification in the skeletal muscle is triggered by monocyte depletion and endothelial cells recruitment to chondro-osteogenesis

Mario Tirone[1,2*], Anna Giovenzana[1*], Arianna Vallone[1], Paola Zordan[3§], Martina Sormani[1], Pier Andrea Nicolosi[1], Raffaela Meneveri[1], Carmen Rosaria Gigliotti[4], Antonello Spinelli[5], Renata Bocciardi[6], Roberto Ravazzolo[6], Ingrid Cifola[7], Silvia Brunelli[1]

[1]School of Medicine and Surgery, University of Milano-Bicocca, Monza, Italy; [2]Division of Genetics and Cell Biology, San Raffaele Scientific Institute, Milano Italy; [3]Division of Regenerative Medicine, San Raffaele Scientific Institute, Milan, Italy; [4]Medical Physics Department and [5]Centre for Experimental Imaging, San Raffaele Scientific Institute, Milano, Italy; [6]Department of Neurosciences, Rehabilitation, Ophthalmology, Genetics, Maternal and Child Health, Università degli Studi di Genova, Genova 16132, Italy and U.O.C. Genetica Medica, Genova, Italy; [7]Institute for Biomedical Technologies (ITB), National Research Council (CNR), Segrate, Milan, Italy.

Present addresses
[§]Division of Immunology, Transplantation and Infectious Diseases, San Raffaele Scientific Institute, Milano Italy

Running title: Macrophages and ECs-mediated heterotopic ossification

*These authors equally contributed to the work

Corresponding Authors: Silvia Brunelli, silvia.brunelli@unimib.it

ABSTRACT

Altered macrophage infiltration upon tissue damage results in inadequate healing due to inappropriate remodeling and stem cell recruitment and differentiation. We investigated *in vivo* whether cells of endothelial origin phenotypically change after heterotopic ossification induction and whether infiltration of innate immunity cells influences their commitment and alters the ectopic bone formation. Liposome-encapsulated clodronate was used to assess macrophage impact on endothelial cells (ECs) in the skeletal muscle upon acute damage in the ECs specific lineage-tracing Cdh5CreER^{T2}:R26REYFP transgenic mice. Macrophage depletion partially shifts the fate of ECs toward endochondral differentiation. Upon ectopic stimulation of BMP signalling, monocyte depletion leads to a further contribution of ECs to ectopic bone formation, with increased bone volume and density, that is reversed by ACVR1/SMAD pathway inhibitor Dipirydamole. This suggests that macrophages contribute to preserve endothelial fate in trauma-induced heterotopic ossification. Therefore, alterations of the macrophage-endothelial axis may represent a novel target for molecular intervention in heterotopic ossification.

Introduction

The regenerating skeletal muscle niche is a complex environment where distinct cell populations play crucial and non-redundant roles. Progenitors in the muscle comprise the satellite cells, which are quiescent stem cells that, once activated, are the primary myogenic cells responsible for skeletal muscle regeneration (Relaix and Zammit, 2012). Vascular progenitors and interstitial cells, such as fibroadipogenic precursors (FAPs) and $PW1^{+}/Pax7^{-}$ interstitial progenitor cells (PICs), contribute to muscle regeneration in several ways. They induces the formation of the new capillary network to provide nutrients and oxygenation, they directly differentiate to muscle fibers (Dellavalle et al., 2011; Pannerec et al., 2013) and produce growth factors and other soluble signals essential for proper stem cell activation, myogenic differentiation and reconstitution of the contractile apparatus (Abou-Khalil et al., 2009; Christov et al., 2007; Fiore et al., 2016; Joe et al., 2010). Disruption of vessel assembly and jeopardized angiogenesis concur to muscle wasting (Abou-Khalil et al., 2010; Shireman, 2007).

Increasing evidences support the hypothesis that these interactions and processes need to be orchestrated and coordinated by cells of the immune system, in particular macrophages (MPs), that infiltrate the muscle immediately after the initial tissue injury and necrosis and release several cytokines (Arnold et al., 2007; Rigamonti et al., 2014). The two main macrophage populations, i.e. the classically activated inflammatory MPs and the alternatively activated MPs, play a sequential role to set the pace of muscle regeneration upon acute injury(Corna et al., 2010; Mantovani et al., 2012; Rigamonti et al., 2013; Rigamonti et al., 2014). Failure of macrophage recruitment or altered polarization result in impaired tissue regeneration and fibrosis, as described in several chronic pathological conditions (Arnold et al., 2007; Lemos et al., 2015). Furthermore, we have previously demonstrated that a proper macrophage recruitment in muscle after an acute sterile damage is also essential for maintaining a correct angiogenic program and prevent the endothelial contribution to scar formation This seems to occur through a complex biological process, referred to as endothelial to mesenchymal transition (EndoMT). EndoMT involves loss of endothelial cell identity in favour of a multipotent mesenchymal phenotype, which often contributes to exacerbate the severity of many different fibrotic disorders not only in the muscle but also in kidney, liver and heart (Medici, 2016; Pessina et al., 2015; Piera-Velazquez et al., 2016). Many recent studies have suggested that ECs have the potential to differentiate along other mesenchymal derived lineages, including chondrocytes and osteogenic precursors (Tang et al., 2012; Yao et al., 2013; Yung et al., 2015).

Extra-skeletal osteogenesis is a sporadic event with serious clinical consequences. Defined as heterotopic ossification (HO), it describes the development of an endochondral bone in soft tissues due to fracture complication, neurological trauma or genetic defects, such as fibrodysplasia ossificans progressiva (FOP, OMIM 135100) (Kaplan et al., 2008; Potter et al., 2007). FOP arises

from gain-of-function mutations in the bone morphogenetic protein (BMP) type I receptor gene *ACVR1* (alias *ALK2*), resulting in aberrant activation of the BMP signaling pathway and acquired sensitivity to unconventional ligands of the mutated receptor (Hatsell et al., 2015; Shore et al., 2006) (Hino et al., 2015). Lineage tracing studies have suggested that several cell populations may contribute to the ectopic bone formation both in genetic and pharmacological models of FOP, amongst which are ECs (Cai et al., 2015; Dey et al., 2016; Lounev et al., 2009; Medici et al., 2010; Wosczyna et al., 2012). Nonetheless, a definitive endorsement of endothelial cells as source of heterotopic ossification remains controversial, partially due to the lack of strict specificity or efficiency of such lineage tracing tools.

In this study, we rely on a specific *in vivo* endothelial genetic tracing mouse model to unambiguously demonstrate the contribution of EC-derived cells to BMP-dependent ectopic chondro-ossification and to determine that MPs play a non-redundant role in controlling this process.

RESULTS

EC-derived cells in the regenerating skeletal muscle acquire an EndoMT/endochondrogenic gene expression signature upon monocyte/macrophage depletion

To study how the interplay between immune system and ECs may contribute to trauma-induced heterotopic bone formation, we chose a mouse model of severe muscle acute injury, where macrophage infiltration is compromised. In such model, we have shown that EndoMT and fibrosis are induced (Zordan et al., 2014). We generated double transgenic micde Cdh5CreER^{T2}:R26REYFP by crossing Cdh5CreER^{T2} transgenics with R26REYFP reporter mice. This mouse model guarantees very high efficiency and specificity of the original endothelial labeling, thus excluding marking any cell of mesenchymal or hematopoietic lineages (Zordan et al., 2014). In this model, we first targeted MPs by intravenously injecting liposomes containing clodronate (CLL) or PBS as control (Sham) one day before and every other day after acute damage induction by cardiotoxin (CTX) injection, and we freshly sorted EYFP^{+} ECs from muscle of CLL- and Sham-treated mice five days after CTX (Fig.1A, left panel). The monocyte/macrophage depletion efficiency was assessed by measuring the fraction of CD11b^{+} cells in peripheral blood of CLL- and Sham- treated mice by FACS (Fig 1A right panel, Suppl. Fig S1A). This depletion *per se* did not affect the number of EC-derived cells that could be retrieved (Fig 1A, right panel, and Suppl. Figure S1B).

We next characterized the transcriptome profile of genetically labelled isolated cells of endothelial origin (EYFP^{+} ECs), by deep sequencing (RNA-seq) analysis. As a result, we identified 1,399 differentially expressed genes (DEGs) (Suppl. Table 1) in CLL- vs Sham-treated samples. The Gene Ontology enrichment analysis showed, as expected, that these DEGs are mainly involved in

biological processes related to EndoMT and mesenchymal-fibrogenic features (Fig. 1C), as confirmed by qPCR for a panel of lineage-specific markers (Fig 1D). Notably, we also found an enrichment for ossification and bone development processes (Fig.1C) and the gene expression upregulation of Sox9 and Runx2 (Fig. 1D), master genes of endochondral ossification (Hata et al., 2017). This suggests that macrophage depletion enhances the osteogenic potential of ECs.

EC-derived cells contribute to BMP-induced chondrogenesis

To verify whether EC derived cells do really contribute to the process of ectopic chondro-ossification, we induced the formation of cartilage and bone in the muscle of Cdh5CreER^{T2}:R26REYFP or Cdh5CreER^{T2}:tdTomato mice, by intramuscularly injecting rhBMP2, together with CTX, as described in (Cappato et al., 2016) (Fig. 2A). After seven days, we could detect the presence of EYFP^{+} ECs co-expressing the chondrocyte marker Sox9 and pSMAD1-5-8, indicating they have activated the chondrogenic pathway and display high BMP signaling, whic h is suggestive of BMP type I receptor kinase activation by rhBMP2 (Fig. 2B). Interestingly, some EYFP^{+} pSMAD^{+} cells did not express anymore the endothelial marker CD31 (Fig. 2B). On the other hand, after 10 days we could not detect EC-derived cells expressing the osteogenic master gene Osterix (Osx) (Fig. 2C). These results are indicative that in these conditions ECs may contribute to the formation of ectopic cartilage but not of bone.

Macrophages protect from BMP-induced ectopic ossification and conversion of EC-derived cells to chondro-osteoblasts

Infiltrating MPs prevent EndoMT upon acute muscle damage (Zordan et al., 2014) and, as demonstrated above, macrophage depletion *per se* is sufficient to induce the upregulation of the chondrocyte marker Sox9 in EC-derived cells (Fig. 1D). To explore the role of infiltrating MPs during BMP-induced HO, we experimentally depleted phagocytes by intravenously injecting liposomes containing CLL (or PBS as control, Sham) every two days in BMP/CTX-treated Cdh5CreER^{T2}:R26REYFP or Cdh5CreER^{T2}:tdTomato mice (Fig. 3A). Also in this condition, Cd11b^{+} cell counts in peripheral blood were significantly reduced in CLL- versus Sham-treated mice (Supplementary Fig. S2A-B), as well as the number of F4/80^{+} MPs in the muscle (Supplementary Fig. S2C-D), indicating that phagocyte targeting was effective We first focused on the fate of EC-derived cells at early stages of chondro-ossification, by freshly isolating them from the muscle seven days after BMP/CTX treatment (Fig. 3B). dtTomato^{+} EC-derived cells from CLL-treated mice showed an increased expression of Sox9 gene with respect to control samples (Fig. 3C). On the other hand, the dtTomato^{-} fraction in CLL-treated mice showed the upregulation of Bmp4 and Bmp6 gene expression, suggesting that MPs depletion leads to enhanced BMP signaling in the muscle (Fig. 3C).

Immunofluorescence (IF) analysis confirmed that, seven days after BMP/CTX, muscle from CLL mice contains an increased number of EC-derived cells ($EYFP^+$ or $dtTomato^+$) expressing Sox9 protein (Fig. 3D). Only in this condition we also observed that, 10 days after BMP/CTX, some EC-derived cells start to express Osx, indicating that the osteogenic fate has been switched on (Fig. 3E).

In vivo micro-computerized tomography (μCT) scan was carried out on both CLL- and Sham-treated mice to assess the progression of ossification and any other effect on the normal skeletal structure at later stages (10, 21 and 30 days after BMP/CTX treatment) (Fig. 4A). After 10 days, we couldn't detect significant differences in HO (measured as mineralized volume, mm^3) or bone density (HU/mm^3) in control mice (Fig. 4C-D). By contrast, after 21 days of treatment, μCT scans showed a significant increase of HO volume and bone density in CLL vs control mice (Fig. 4C-D). The significant difference in HO volume was maintained also at 30 days after treatment, while bone density further increased in CLL mice but with higher variability (Fig. 4B-D). These results were confirmed by immunohistochemical analysis (IHC) using hematoxylin and eosin (H&E) or Masson staining, which revealed that, at both 21 and 30 days after HO triggering, the area of ectopic bone was greater in CLL- vs Sham-treated mice (Fig. 4E-F). This implies that proper MP infiltration from the beginning of HO triggering is able to limit the extent of the ectopic bone lesions.

At 21 and 30 days, the high bone density of the HO lesions prevented the evaluation of EC-derived cell contribution to the ectopic bone formation by FACS or IHC. Nonetheless, *in vivo* μCT imaging allowed us to show that only in CLL-treated mice there is an increase of fluorescence signal in the area of ectopic ossification at 10 and 21 days after BMP-induction, reflecting an increased recruitment of EC-derived cells upon macrophage depletion (Supplementary Movie 1).

Finally, we wanted to assess whether we could prevent the exacerbated bone formation developed upon macrophage depletion. We have previously shown that dipyridamole has an inhibitory effect on the whole SMAD-dependent BMP signaling pathway and partially inhibits the process of BMP-triggered HO (Cappato et al., 2016). Thus, dipyridamole was administered daily to Sham- or CLL-treated mice (Fig. 5A). We first verified that dipyridamole did not lead to a differential macrophage depletion in CLL mice (Fig. 5B). We therefore compared the extent of HO in Sham-, CLL- and CLL/dipyridamole-treated mice by μCT and IHC (Fig. 5C), and found that after 21 days dipyridamole was able to rescue HO in CLL mice, reducing the mineralized bone volume and bone density to levels comparable to those of Sham mice (Fig. 5D-E).

DISCUSSION

Heterotopic ossification (HO) is a pathological condition where extra-skeletal bone forms in soft tissues due to extreme trauma or genetic defects. Induction of ectopic bone formation, is highly destructive. Therefore, its prevention has become an important focus of research, particularly with

regards to pre- and post-operative preventive care in acquired heterotopic ossification and in fibrodysplasia ossificans progressiva (FOP) patients. Of particular relevance is the research aiming to identify the pathophysiological mechanisms of HO, thus eventually contributing to the development of new and targeted treatment options.

FOP is caused by mutations of the *ACVR1* gene, encoding the ALK2 bone morphogenetic protein (BMP) type 1 receptor, and the consequent dysregulation of the BMP/Activin/TGF-ß family ligand signaling may be a shared property of both genetic and acquired forms of HO. Accordingly, it has therefore been suggested that HO in FOP and in non-genetic conditions might be mediated by common effectors and progenitor cells (Dey et al., 2016).

In the last years, several studies have focused on the cellular origin of ectopic ossification and potential candidates have shown osteogenic potential both *in vitro* and *in vivo* (Agarwal et al., 2016; Dey et al., 2016; Levy et al., 2001; Lounev et al., 2009; Medici et al., 2010; Sun et al., 2016; Wosczyna et al., 2012). More recently, it was shown that the FAPs are the major contributors to HO in a transgenic model of FOP carrying the *ACVR1*^{R206} mutation (Lees-Shepard et al., 2018).

The endothelial involvement in induced and genetic HO is actively debated. By taking advantage of an efficient and extremely endothelial-specific genetic lineage tracing mouse system, we have followed the fate of ECs and their progeny in pathological chondro-osteogenesis leading to ectopic bone formation. EC-derived cells show the potential commit to the chondrogenic lineage upon EndoMT induction in the skeletal muscle. Furthermore, upon BMP2 stimulation, *bona fide* muscle EC derived cells express pSMAD1-5-8, indicating that the BMP pathway has been switched on, as well as the master gene of chondrogenesis Sox9 (Hata et al., 2017), while they downregulate proper endothelial markers, such as CD31.

EndoMT has been suggested to contribute to traumatic HO (Agarwal et al., 2016; Sun et al., 2016) and early lineage tracing studies indicated the Tie2-expressing vascular cells as the leading candidates for the cellular origin of BMP2-mediated heterotopic cartilage and bone (Medici et al., 2010). While Tie2^{+} cells were initially considered to be endothelial cells, it was later demonstrated that Tie2 is not an exclusively endothelial protein (Wosczyna et al., 2012). Indeed, it has been recently shown that the Tie2^{+} cells contributing to ectopic chondro-ossification are FAPs (Lees-Shepard et al., 2018). This same study overruled the contribution of *bona fide* endothelial cells to bone formation on the basis of a different VE-Cadherin dependent lineage tracing murine system (Alva et al., 2006). This particular strain is not inducible and Cre activity starts in endothelial cells from the embryos, resulting in labeling of hematopoietic lineages too. Moreover, labeling efficiency in skeletal muscle, has never been properly evaluated.

Another aspect to be considered when evaluating and comparing the EC-derived cells contribution to induced and genetic HO is the presence of the recurrent *ACVR1*^{R206H} mutation. It is quite predictable that mutation in the *ACVR1* (alias *ALK2*) *locus* would greatly impact the response and fate of all potential osteogenic progenitors. Our results indicate that “wild-type” EC-derived cells in

a “wild-type” environment are able to contribute to the initial phases of endochondral ectopic bone formation.

Cells of both the innate and adaptive immune system have been increasingly implicated in HO through various mechanisms (Kraft et al., 2016). A particular focus has been set on the role of MPS, since they play a crucial function in the innate response to inflammatory stimuli (Mantovani et al., 2005; Shi and Pamer, 2011). A generalization of what is *in vivo* a broad and partially *continuum* set of differentiating populations suggests that activated MPs generate M1 (“classically activated”) and M2 (“alternatively activated”) cells (Mantovani et al., 2005). M1 macrophages are mainly involved in the response against pathogens, while M2 macrophages in the later phases of inflammation, angiogenesis, clearance of dying cells and debris, and tissue regeneration and adaptation (Mantovani et al., 2005; Novak and Koh, 2013). M2 macrophages prompt differentiation of precursors to myofibroblasts, which oversee to the production of the matrix for tissue regeneration. However, MP role might be more complex than anticipated, since M2 cells play also angiogenic and vascular protective roles in inflamed tissues (Mantovani et al., 2005; Novak and Koh, 2013). Indeed, we and other have demonstrated that MPs are necessary to orchestrate proper tissue remodeling and repair upon muscle injury, also by favouring angiogenesis, via the production of several secreted mediators and counteracting EndoMT (Latroche et al., 2017; Zordan et al., 2014).

MPs have a quite established role in physiological osteogenesis in development and fracture repair, both by differentiating into osteoclasts and by directly/indirectly stimulating other progenitors in the osteogenic niche (Kraft et al., 2016; Raggatt et al., 2014) (Simkin et al., 2017). However, their role in ectopic bone formation is still unclear, due to the use of different HO models and conditions, genetic background, different MPs depletion models and protocols, and, consequentially, to the heterogeneity of the immune cell population recruited upon tissue damage and depletion. MPs have been suggested to enhance ossification in a neurological HO model (Genêt et al., 2015; Torossian et al., 2017). On the contrary, in other experimental conditions, partial depletion of differentiated MPs with CLL promoted TGFß1 signaling and sustained an osteogenic environment (Cho et al., 2014). Continuous BMP signaling alteration can also affect MP behaviour: indeed, the sustained expression of the FOP mutant form of ALK2 alters cytokine expression and cell response to injury. Moreover depletion of MPs or mast cells in the R206H mouse model of FOP or in a transgenic mouse where BMP4 is overexpressed under the control of the neuron specific enolase (Nse-BMP4) leads to a decreased ectopic bone formation (Convente et al., 2017) (Kan et al., 2009). Noteworthy, we were able to partially inhibit HO in our model system by administration of the ACVR1/BMP/SMAD inhibitor dipyridamole, suggesting that BMP signaling still plays a key role inducing HO in our monocyte depleted model, where persistent partial MP depletion delays muscle repair, hinders angiogenesis and, by increasing BMP/SMAD signaling, promotes EndoMT and further funnels EC-derived cells, and certainly other progenitors,

toward chondro-osteogenesis and extreme ectopic bone formation.
Further studies will be necessary to get more details in the signaling events at the basis of the crosstalk between the different osteoprogenitor cells and the macrophages and other immune cells remaining in the osteogenic niche after depletion. This would allow the identification of agents that selectively sustain those macrophages that protect from acquired and hereditary HO, as a more valuable strategy with respect to a general anti-inflammatory approach.

Materials & Methods

Animals. Mice were housed in the SPF facility at San Raffaele Scientific Institute (Milan, Italy) and treated with the approval of the Institutional Animal Care and Use Committee (IACUC 489, 663). Cdh5-CreER^{T2} (Wang et al., 2010) and R26R-EYFP (Srinivas et al., 2001) or tdTomato (Madisen et al., 2009) mice were bred to yield heterozygous siblings and genotyped as in (Wang et al., 2010). Cre recombination was induced in Cdh5-CreER^{T2}:R26R-EYFP or Cdh5-CreER^{T2}: tdTomato mice at post-natal days 6-7-8 with three subcutaneous injections of Tamoxifen (250 μg/mouse; Sigma-Aldrich, St. Louis, MO, USA).

Depletion of circulating phagocytes. Mice were injected intravenously (i.v.) with liposomes containing either clodronate (CLL; 1.8 mg/mouse) or PBS (Sham) (http://www.clodronateliposomes.org/ashwindigital.asp?docid=26)**. The treatment was performed** one day before cardiotoxin (CTX) injection and every three days afterward (at 2, 5, 8, 11, 14, 17, 20 days after CTX injection).

Flow cytometry. EYFP^{+} and Tomato^{+} EC-derived cells from Cdh5-CreER^{T2}:R26R-EYFP and Cdh5-CreERT2:tdTomato mice, respectively, were isolated from P11 or adult mice after muscle dissection. Tissues were cut in small pieces and dissociated with 0.15 mg/ml Collagenase IV (Roche, Basel, Switzerland) and 0.25% Trypsin (Gibco, Thermo Fisher Scientific, Waltham, MA, USA) or 0.4 mg/ml Dispase (Gibco). Dissociation reaction was performed at 37°C for 30 min for 2–3 cycles. Resuspended mononucleated cells were filtered with 70 and 40 mM filters. Cells were suspended in either DMEM with 20% FBS, 20mM HEPES, 2mM EDTA or PBS with 2% FBS, 2mM EDTA (for antibody staining). For FACS analyses on circulating cells, blood was retrieved from the mouse tail, washed with red lysis buffer and incubated at 4°C for 30 min in blocking solution (PBS with 2% FBS, 2mM EDTA). Cell sorting was performed using the MoFLoXDP system (Beckman Coulter, Inc., Brea, CA, USA) or FACSAria Fusion system (BD Biosciences, Bedford, MA, USA). FACS analysis was carried out using the BD FacsCANTO system (BD BioscienceUSA). Data were

analyzed by FloJo (TreeStar) and/or FCS Express 6 (De Novo Software, Los Angeles, CA, USA). The antibodies used are listed in Table S1.

Transcriptome sequencing (RNA-seq). Total RNA samples were extracted from freshly sorted $EYFP^+$ EC derived cells of muscle of CLL- and Sham-treated mice using ReliaPrep™ RNA Cell Miniprep System (Promega, Milan, Italy), checked for integrity on 2200 TapeStation instrument (Agilent Technologies, Santa Clara, CA, USA) and stored at -80° until use. Starting from 200 ng total RNA, RNA-seq libraries were prepared using the Illumina TruSeq Stranded mRNA Library Prep Kit (Illumina, San Diego, CA, USA), according to manufacturers' instructions, and sequenced on MiSeq platform (Illumina) in 76-cycle paired-end runs. Three independent replicates were sequenced for each condition (CLL and Sham). Raw sequence data are available in NCBI Short Reads Archive (SRA) under Accession Number PRJNA471032.
After fastq quality control by using FastQC tool, raw reads were mapped to the mouse reference genome (Mus musculus UCSC mm10/GRCm38) using STAR aligner (v.2.3.1s) and gene counts were calculated by HTSeq (v.0.6.1), using the Gencode M12 GTF file as gene model. Differential gene expression analysis was carried out using DESeq2 software (v.1.0.17). A False Discovery Rate (FDR, Benjamini and Hochberg (BH) correction) < 0.05 was used as cut-off to define statistically significant differentially expressed genes (DEGs) in CLL vs Sham samples. ToppGene suite was used to perform gene enrichment analysis for Gene Ontology (GO) categories and pathways (https://toppgene.cchmc.org/enrichment.jsp). A FDR (BH correction) < 0.05 was applied to all the annotation terms to defined statistically significant enrichment.

Quantitative Real-Time PCR. Reverse transcription (RT) was done using the High-Capacity cDNA Reverse Transcription Kit (Applied Biosystems, Foster City, CA, USA). qRT-PCR analysis was carried out using the LightCycler 480 Instrument (Roche) or the 7900HT FAST Real-Time PCR detection system (Applied Biosystems). cDNAs were amplified using the GoTaq qPCR Master Mix and the Hot Start Polymerase (Promega). Primer sequences are listed in Table S3. Ct values greater than 35 were considered as negative. Data points were analyzed in triplicate. Quantification was performed using the relative ddCt method. 28S or cyclophilin A genes were used as internal controls.

***In vivo* heterotopic ossification**. 0.1 μg/μl of rhBMP2 (Peprotech, Rocky Hill, NJ, USA) in 100 μl growth factor-reduced Matrigel (BD Biosciences, 1:100 dilution) were injected intramuscularly in the quadriceps of C57BL/6 2-month-old mice. The contralateral muscle was used as internal control and injected with Matrigel only. Both quadriceps were injected with 5 μl CTX 100 μM (from Naja mossambica mossambica, Sigma-Aldrich, Buchs, SG, Switzerland) to increase muscle

damage. Animals were anesthetized by inhalation of 2-bromo-2-chloro-1,1,1-trifluoroethane, ≥99% (Sigma-Aldrich) before the injection.

***In vivo* μCT imaging of heterotopic ossification**. At day 10 and 21 after BMP injection, *in vivo* micro-computerized tomography (μCT) scans were carried out to assess progression of ossification and any other effect on the normal skeletal structure. *In vivo* μCT imaging was performed using the IVIS SpectrumCT Pre-clinical In Vivo Imaging System (Perkin-Elmer, Waltham, MA, USA). μCT images were acquired without any contrast medium, with the following parameters: x-ray tube voltage=50 kV, tube current=1 mA, x-ray focal spot size=50 μm. The μCT images calibrated in Hounsfield unit (HU) were reconstructed with a voxel size of 75 μm^3. Threshold-based image segmentation was performed to obtain a 3D reconstruction and quantification of the ossification.

The total mineralized volume V=N × voxel size (mm^3) was quantified using MIPAV (Medical Image Processing Analysis and Visualization) and MATLAB software, where N is the number of voxels corresponding to bone derived from the image segmentation procedure. The bone density quantification was calculated using the following formula: $\sum Ni=1$ HUi/V.

The IVIS SpectrumCT was also used to obtain 3D fluorescence images using a transillumination excitation source placed below the animal. More precisely, a set of 2D fluorescence images were acquired at different transillumination points within the region of interest. 3D images were then reconstructed using the Fluorescence Imaging Tomography (FLIT) algorithm, as described in (Kuo 2008), and implemented in the Living Image 4.5 software (Perkin Elmer). Transillumination fluorescence images were acquired using the following setting: excitation filter= 570 nm, emission filter=620 nm, f-stop=2, camera binning=8, exposure= auto, field of view=13 cm.

Dipyridamole treatment. 10 mg/kg (body weight) dipyridamole was intraperitoneally administered daily to the treated animals in a solution composed of 10% ethanol, 5% 2-pyrolidone, 12-15% propylene glycol, 10% Cremophor ELP, saline to 100% as in (Cappato et al., 2016). Control mice received the injection solution without drug.

IHC and IF. Serial muscle sections were stained with H&E (Sigma-Aldrich), according to standard procedures. Muscle sections were stained with H&E or Masson Trichrome (Bio-Optica, Milan, Italy), according to the manufacturers' instructions.

IF on frozen section was carried out as in (Zordan et al., 2014). The antibodies used are listed in Table S2. Images were taken using the following microscopes: Leica TCS SP2 Laser Scanning Confocal or Zeiss LSM 710 Confocal Microscope. Images were processed using Adobe Photoshop CS6 and Adobe Illustrator CS6.

Statistical analysis. Data were analyzed with Microsoft Excel 14.1.0 and GraphPad Prism 6, and were plotted as mean ± standard deviation (SD) or mean ± standard error of mean (SEM). To evaluate statistical significance, unpaired two-tailed Student's *t*- tests were used assuming equal variance. Differences among three different experimental groups were evaluated by ANOVA analysis with Bonferroni as post-hoc tests.

Table 1 Antibodies used for FACS analysis.

Primary Antibodies and Conjugates				
Antibody	**Host**	**Dilution**	**Clone**	**Supplier**
F4/80-APC	Rat	1:100	CI:A3-1	Abd Serotec
CD45-PE	Rat	1:100	30-F11	BD
CD11b-PeCy7	Mouse	1:100	M1/70	BD

Table 2. Antibodies used for IF analysis

Primary Antibodies			
Antibody	**Host**	**Dilution**	**Supplier**
CD31/PECAM1 (MEC13.3)	Rat	1:2	Gift from E.Dejana
GFP	Chicken	1:500	Abcam
p-SMAD1/5/8 (D5B10)	Rabbit	1:800	Cell Signaling
Osterix	Rabbit	1:300	Abcam
Sox9	Rabbit	1:300	Millipore
Secondary Antibodies			
Antibody	**Host**	**Dilution**	**Supplier**
Anti-Rabbit Alexa 488	Donkey	1:500	Molecular Probes
Anti-Rat Alexa 546	Goat	1:500	Molecular Probes
Anti-Rat Alexa 647	Chicken	1:500	Molecular Probes
Anti-Mouse Alexa 546	Goat	1:500	Molecular Probes

Table 3 Primers for qRT-PCR analysis

Gene	**Forward primer**	**Reverse primer**
28S	AAACTCTGGTGGAGGTCCGT	CTTACCAAAAGTGGCCCACTA
Cyclophillin A	CATACGGGTCCTGGCATCTTGTCC	TGGTGATCTTCTTGCTGGTCTTGC
CD31	AGGGGACCAGCTGCACATTAGG	AGGCCGCTTCTCTTGACCACTT
Collagen 1	GGTATGCTTGATCTGTATCTGC	AGTCCAGTTCTTCATTGCATT

Twist1	GGACAAGCTGAGCAAGATTCA	CGGAGAAGGCGTAGCTGAG
Tcf4	TCTGCAACTTCCCCTGACTT	TGTCTTGCAGGTTCTCATCG
Runx2	GACTGTGGTTACCGTCATGGC	ACTTGGTTTTTCATAACAGCGGA
Sox9	TCCAGCAAGAACAAGCCACA	CGAAGGGTCTCTTCTCGCTC
Osterix	ACCAGAAGCGACCACTTGAG	TTGGCTTCTTCTTCCCCGAC
Cadherin 5	GTACAGCATCATGCAGGGCG	ATTCGTATCGGATAGTGGGG
FAP	TCAACTGTGATGGCAAGAGC	GTACCACATCGCCTGGAAAT
Bmp6	ATGGCAGGACTGGATCATTGC	CCATCACAGTAGTTGGCAGCG
Bmp4	TTCCTGGTAACCGAATGCTGA	CCTGAATCTCGGCGACTTTTT

Acknowledgments

Flow cytometry experiments have been carried out in the FRACTAL Cytometry facility (San Raffaele Scientific Institute, Milano, Italy). We thank Gonzalo Sanchez-Duffhues for critical reading of the manuscript.

Grant numbers and sources of support: This work was supported by grants from Università Milano Bicocca (FAR-QC2014 and FAR 2014-2016 to SB), Fondazione Telethon (Grant no. GGP15196, to RR and RB), and Italian Ministry of Health (Progetto Ministero Salute – Giovani Ricercatori, GR-2011-02352026 to IC).

REFERENCES

Abou-Khalil, R., Le Grand, F., Pallafacchina, G., Valable, S., Authier, F.-J., Rudnicki, M. A., Gherardi, R. K., Germain, S., Chrétien, F., Sotiropoulos, A., et al. (2009). Autocrine and paracrine angiopoietin 1/Tie-2 signaling promotes muscle satellite cell self-renewal. *Cell stem cell* **5**, 298-309.

Abou-Khalil, R., Mounier, R. and Chazaud, B. (2010). Regulation of myogenic stem cell behavior by vessel cells: The "ménage à trois"; of satellite cells, periendothelial cells and endothelial cells. *Cell cycle (Georgetown, Tex)* **9**.

Agarwal, S., Loder, S., Cholok, D., Peterson, J., Li, J., Fireman, D., Breuler, C., Hsieh, H. S., Ranganathan, K., Hwang, C., et al. (2016). Local and Circulating Endothelial Cells Undergo Endothelial to Mesenchymal Transition (EndMT) in Response to Musculoskeletal Injury. *Nature Publishing Group* **6**, 1-8.

Alva, J. A., Zovein, A. C., Monvoisin, A., Murphy, T., Salazar, A., Harvey, N. L., Carmeliet, P. and Iruela-Arispe, M. L. (2006). VE-Cadherin-Cre-recombinase transgenic mouse: a tool for lineage analysis and gene deletion in endothelial cells. *Dev Dyn* **235**, 759-767.

Arnold, L., Henry, A., Poron, F., Baba-Amer, Y., van Rooijen, N., Plonquet, A., Gherardi, R. K. and Chazaud, B. (2007). Inflammatory monocytes recruited after skeletal muscle injury switch into antiinflammatory macrophages to support myogenesis. *The Journal of experimental medicine* **204**, 1057-1069.

Cai, J., Orlova, V. V., Cai, X., Eekhoff, E. M. W., Zhang, K., Pei, D., Pan, G., Mummery, C. L. and Ten Dijke, P. (2015). Induced Pluripotent Stem Cells to Model Human Fibrodysplasia Ossificans Progressiva. *Stem Cell Reports* **5**, 963-970.

Cappato, S., Tonachini, L., Giacopelli, F., Tirone, M., Galietta, L. J., Sormani, M., Giovenzana, A., Spinelli, A. E., Canciani, B., Brunelli, S., et al. (2016). High-throughput screening for modulators of ACVR1 transcription: discovery of potential therapeutics for fibrodysplasia ossificans progressiva. *Dis Model Mech* **9**, 685-696.

Cho, S. W., Soki, F. N., Koh, A. J., Eber, M. R., Entezami, P., Park, S. I., van Rooijen, N. and McCauley, L. K. (2014). Osteal macrophages support physiologic skeletal remodeling and anabolic actions of parathyroid hormone in bone. *Proceedings of the National Academy of Sciences* **111**, 1545-1550.

Christov, C., Chretien, F., Abou-Khalil, R., Bassez, G., Vallet, G., Authier, F.-J., Bassaglia, Y., Shinin, V., Tajbakhsh, S., Chazaud, B., et al. (2007). Muscle Satellite Cells and Endothelial Cells: Close Neighbors and Privileged Partners. *Molecular Biology of the Cell* **18**, 1397.

Convente, M. R., Chakkalakal, S. A., Yang, E., Caron, R. J., Zhang, D., Kambayashi, T., Kaplan, F. S. and Shore, E. M. (2017). Depletion of Mast Cells and Macrophages Impairs Heterotopic Ossification in an Acvr1R206H Mouse Model of Fibrodysplasia Ossificans Progressiva. *J Bone Miner Res*.

Corna, G., Campana, L., Pignatti, E., Castiglioni, A., Tagliafico, E., Bosurgi, L., Campanella, A., Brunelli, S., Manfredi, A. A., Apostoli, P., et al. (2010). Polarization dictates iron handling by inflammatory and alternatively activated macrophages. *Haematologica* **95**, 1814-1822.

Dellavalle, A., Maroli, G., Covarello, D., Azzoni, E., Innocenzi, A., Perani, L., Antonini, S., Sambasivan, R., Brunelli, S., Tajbakhsh, S., et al. (2011). Pericytes resident in postnatal skeletal muscle differentiate into muscle fibres and generate satellite cells. *Nature Communications* **2**, 499-411.

Dey, D., Bagarova, J., Hatsell, S. J., Armstrong, K. A., Huang, L., Ermann, J., Vonner, A. J., Shen, Y., Mohedas, A. H., Lee, A., et al. (2016). Two tissue-resident progenitor lineages drive distinct phenotypes of heterotopic ossification. *Sci Transl Med* **8**, 366ra163.

Fiore, D., Judson, R. N., Low, M., Lee, S., Zhang, E., Hopkins, C., Xu, P., Lenzi, A., Rossi, F. M. and Lemos, D. R. (2016). Pharmacological blockage of fibro/adipogenic progenitor expansion and suppression of regenerative fibrogenesis is associated with impaired skeletal muscle regeneration. *Stem Cell Res* **17**, 161-169.

Genêt, F., Kulina, I., Vaquette, C., Torossian, F., Millard, S., Pettit, A. R., Sims, N. A., Anginot, A., Guerton, B., Winkler, I. G., et al. (2015). Neurological heterotopic ossification following spinal cord injury is triggered by macrophage-mediated inflammation in muscle. *J. Pathol.* **236**, 229-240.

Hata, K., Takahata, Y., Murakami, T. and Nishimura, R. (2017). Transcriptional Network Controlling Endochondral Ossification. *J Bone Metab* **24**, 75-78.

Hatsell, S. J., Idone, V., Wolken, D. M. A., Huang, L., Kim, H. J., Wang, L., Wen, X., Nannuru, K. C., Jimenez, J., Xie, L., et al. (2015). ACVR1R206H receptor mutation causes fibrodysplasia ossificans progressiva by imparting responsiveness to activin A. *Sci Transl Med* **7**, 303ra137.

Hino, K., Ikeya, M., Horigome, K., Matsumoto, Y., Ebise, H., Nishio, M., Sekiguchi, K., Shibata, M., Nagata, S., Matsuda, S., et al. (2015). Neofunction of ACVR1 in fibrodysplasia ossificans progressiva. *Proceedings of the National Academy of Sciences* **112**, 15438-15443.

Joe, A. W., Yi, L., Natarajan, A., Le Grand, F., So, L., Wang, J., Rudnicki, M. A. and Rossi, F. M. (2010). Muscle injury activates resident fibro/adipogenic progenitors that facilitate myogenesis. *Nat Cell Biol* **12**, 153-163.

Kan, L., Liu, Y., McGuire, T. L., Berger, D. M. P., Awatramani, R. B., Dymecki, S. M. and Kessler, J. A. (2009). Dysregulation of Local Stem/Progenitor Cells as a Common Cellular Mechanism for Heterotopic Ossification. *Stem Cells* **27**, 150-156.

Kaplan, F. S., Le Merrer, M., Glaser, D. L., Pignolo, R. J., Goldsby, R. E., Kitterman, J. A., Groppe, J. and Shore, E. M. (2008). Fibrodysplasia ossificans progressiva. *Best Pract Res Clin Rheumatol* **22**, 191-205.

Kraft, C. T., Agarwal, S., Ranganathan, K., Wong, V. W., Loder, S., Li, J., Delano, M. J. and Levi, B. (2016). Trauma-induced heterotopic bone formation and the role of the immune system. *Journal of Trauma and Acute Care Surgery* **80**, 156-165.

Latroche, C., Weiss Gayet, M., Muller, L., Gitiaux, C., Leblanc, P., Liot, S., Ben Larbi, S., Abou-Khalil, R., Verger, N., Bardot, P., et al. (2017). Coupling between Myogenesis and Angiogenesis during Skeletal Muscle Regeneration Is Stimulated by Restorative Macrophages. *Stem Cell Reports* **9**, 2018-2033.

Lees-Shepard, J. B., Yamamoto, M., Biswas, A. A., Stoessel, S. J., Nicholas, S.-A. E., Cogswell, C. A., Devarakonda, P. M., Schneider, M. J., Cummins, S. M., Legendre, N. P., et al. (2018). Activin-dependent signaling in fibro/adipogenic progenitors causes fibrodysplasia ossificans progressiva. *Nat Comms*, 1-14.

Lemos, D. R., Babaeijandaghi, F., Low, M., Chang, C. K., Lee, S. T., Fiore, D., Zhang, R. H., Natarajan, A., Nedospasov, S. A. and Rossi, F. M. (2015). Nilotinib reduces muscle fibrosis in chronic muscle injury by promoting TNF-mediated apoptosis of fibro/adipogenic progenitors. *Nat Med* **21**, 786-794.

Levy, M. M., Joyner, C. J., Virdi, A. S., Reed, A., Triffitt, J. T., Simpson, A. H., Kenwright, J., Stein, H. and Francis, M. J. (2001). Osteoprogenitor cells of mature human skeletal muscle tissue: an in vitro study. *Bone* **29**, 317-322.

Lounev, V. Y., Ramachandran, R., Wosczyna, M. N., Yamamoto, M., Maidment, A. D., Shore, E. M., Glaser, D. L., Goldhamer, D. J. and Kaplan, F. S. (2009). Identification of progenitor cells that contribute to heterotopic skeletogenesis. *J Bone Joint Surg Am* **91**, 652-663.

Madisen, L., Zwingman, T. A., Sunkin, S. M., Oh, S. W., Zariwala, H. A., Gu, H., Ng, L. L., Palmiter, R. D., Hawrylycz, M. J., Jones, A. R., et al. (2009). A robust and high-throughput Cre reporting and characterization system for the whole mouse brain. *Nat Neurosci* **13**, 133-140.

Mantovani, A., Biswas, S. K., Galdiero, M. R., Sica, A. and Locati, M. (2012). Macrophage plasticity and polarization in tissue repair and remodelling. *The Journal of Pathology* **229**, 176-185.

Mantovani, A., Sica, A. and Locati, M. (2005). Macrophage polarization comes of age. *Immunity* **23**, 344-346.

Medici, D. (2016). Endothelial-Mesenchymal Transition in Regenerative Medicine. *Stem Cells Int* **2016**, 6962801.

Medici, D., Shore, E. M., Lounev, V. Y., Kaplan, F. S., Kalluri, R. and Olsen, B. R. (2010). Conversion of vascular endothelial cells into multipotent stem-like cells. *Nat Med* **16**, 1400-1406.

Novak, M. L. and Koh, T. J. (2013). Phenotypic transitions of macrophages orchestrate tissue repair. *Am J Pathol* **183**, 1352-1363.

Pannerec, A., Formicola, L., Besson, V., Marazzi, G. and Sassoon, D. A. (2013). Defining skeletal muscle resident progenitors and their cell fate potentials. *Development* **140**, 2879-2891.

Pessina, P., Kharraz, Y., Jardi, M., Fukada, S., Serrano, A. L., Perdiguero, E. and Munoz-Canoves, P. (2015). Fibrogenic Cell Plasticity Blunts Tissue Regeneration and Aggravates Muscular Dystrophy. *Stem Cell Reports* **4**, 1046-1060.

Piera-Velazquez, S., Mendoza, F. A. and Jimenez, S. A. (2016). Endothelial to Mesenchymal Transition (EndoMT) in the Pathogenesis of Human Fibrotic Diseases. *J Clin Med* **5**.

Potter, B. K., Burns, T. C., Lacap, A. P., Granville, R. R. and Gajewski, D. A. (2007). Heterotopic ossification following traumatic and combat-related amputations. Prevalence, risk factors, and preliminary results of excision. *J Bone Joint Surg Am* **89**, 476-486.

Raggatt, L. J., Wullschleger, M. E., Alexander, K. A., Wu, A. C. K., Millard, S. M., Kaur, S., Maugham, M. L., Gregory, L. S., Steck, R. and Pettit, A. R. (2014). Fracture Healing via Periosteal Callus Formation Requires Macrophages for Both Initiation and Progression of Early Endochondral Ossification. *Am J Pathol* **184**, 3192-3204.

Relaix, F. and Zammit, P. S. (2012). Satellite cells are essential for skeletal muscle regeneration: the cell on the edge returns centre stage. *Development* **139**, 2845-2856.

Rigamonti, E., Touvier, T., Clementi, E., Manfredi, A. A., Brunelli, S. and Rovere-Querini, P. (2013). Requirement of inducible nitric oxide synthase for skeletal muscle regeneration after acute damage. *J Immunol* **190**, 1767-1777.

Rigamonti, E., Zordan, P., Sciorati, C., Rovere-Querini, P. and Brunelli, S. (2014). Macrophage plasticity in skeletal muscle repair. *Biomed Res Int* **2014**, 560629.

Shi, C. and Pamer, E. G. (2011). Monocyte recruitment during infection and inflammation. *Nat Rev Immunol* **11**, 762-774.

Shireman, P. K. (2007). The chemokine system in arteriogenesis and hind limb ischemia. *Journal of Vascular Surgery* **45**, A48-A56.

Shore, E. M., Xu, M., Feldman, G. J., Fenstermacher, D. A., Cho, T. J., Choi, I. H., Connor, J. M., Delai, P., Glaser, D. L., LeMerrer, M., et al. (2006). A recurrent mutation in the BMP type I receptor ACVR1 causes inherited and sporadic fibrodysplasia ossificans progressiva. *Nat Genet* **38**, 525-527.

Simkin, J., Sammarco, M. C., Marrero, L., Dawson, L. A., Yan, M., Tucker, C., Cammack, A. and Muneoka, K. (2017). Macrophages are required to coordinate mouse digit tip regeneration. *Development* **144**, 3907-3916.

Sinha, S., Uchibe, K., Usami, Y., Pacifici, M. and Iwamoto, M. (2016). Effectiveness and mode of action of a combination therapy for heterotopic ossification with a retinoid agonist and an anti-inflammatory agent. *Bone*, 1-37.

Srinivas, S., Watanabe, T., Lin, C. S., William, C. M., Tanabe, Y., Jessell, T. M. and Costantini, F. (2001). Cre reporter strains produced by targeted insertion of EYFP and ECFP into the ROSA26 locus. *BMC Dev Biol* **1**, 4.

Sun, Y., Cai, J., Yu, S., Chen, S., Li, F. and Fan, C. (2016). MiR-630 Inhibits Endothelial-Mesenchymal Transition by Targeting Slug in Traumatic Heterotopic Ossification. *Nature Publishing Group*, 1-12.

Tang, R., Gao, M., Wu, M., Liu, H., Zhang, X. and Liu, B. (2012). High glucose mediates endothelial-to-chondrocyte transition in human aortic endothelial cells. *Cardiovasc Diabetol* **11**, 113.

Torossian, F., Guerton, B., Anginot, A., Alexander, K. A., Desterke, C., Soave, S., Tseng, H.-W., Arouche, N., Boutin, L., Kulina, I., et al. (2017). Macrophage-derived oncostatin M contributes to human and mouse neurogenic heterotopic ossifications. *JCI Insight* **2**.

Wang, Y., Nakayama, M., Pitulescu, M. E., Schmidt, T. S., Bochenek, M. L., Sakakibara, A., Adams, S., Davy, A., Deutsch, U., Lüthi, U., et al. (2010). Ephrin-B2 controls VEGF-induced angiogenesis and lymphangiogenesis. *Nature* **465**, 483-486.

Wosczyna, M. N., Biswas, A. A., Cogswell, C. A. and Goldhamer, D. J. (2012). Multipotent progenitors resident in the skeletal muscle interstitium exhibit robust BMP-dependent osteogenic activity and mediate heterotopic ossification. *J Bone Miner Res* **27**, 1004-1017.

Yao, Y., Jumabay, M., Ly, A., Radparvar, M., Cubberly, M. R. and Bostrom, K. I. (2013). A role for the endothelium in vascular calcification. *Circ Res* **113**, 495-504.

Yung, L. M., Sanchez-Duffhues, G., Ten Dijke, P. and Yu, P. B. (2015). Bone morphogenetic protein 6 and oxidized low-density lipoprotein synergistically recruit osteogenic differentiation in endothelial cells. *Cardiovasc Res* **108**, 278-287.

Zordan, P., Rigamonti, E., Freudenberg, K., Conti, V., Azzoni, E., Rovere-Querini, P. and Brunelli, S. (2014). Macrophages commit postnatal endothelium-derived progenitors to angiogenesis and restrict endothelial to mesenchymal transition during muscle regeneration. *Cell Death Dis* **5**, e1031.

FIGURE LEGENDES

Figure 1 Gene expression profiling of EC-derived cells.

A) Experimental scheme of muscle acute injury and macrophage depletion (left panel) and evaluation of the percentage of $EYFP^+$ sorted cells (EC derived cells) and $Cd11b^+$ cells (macrophages) after clodronate (CLL) or control (Sham) treatments (right panel). B) Heatmaps showing genes differentially expressed genes between EC derived cells isolated from muscle of CLL- and Sham-treated Cdh5-$CreER^{T2}$:R26R-EYFP mice. C) Gene Ontology (GO) Biological Process terms enriched in CLL vs control samples. Number of up- and down-regulated differentially expressed genes (DEGs) associated to each term are shown as red and green bars, respectively. All the enrichments shown are statistically significant (blue line indicates significance expressed as -log Pvalue). D) qRT-PCR expression assays for a panel of selected genes. Values are expressed as fold changes relative to Sham mRNA expression, and normalized on the housekeeping (cyclophilln A). Bars represent mean ± SEM. n=3, *p* *≤0.05; **≤0.01; ***≤0.001.

Figure 2. EC-derived cells contribute to the development of ectopic bone.

A) Experimental scheme of BMP2-mediated bone induction. B) IH of muscle section from quadriceps of Cdh5-$CreER^{T2}$:R26R-EYFP mice at seven days after bone induction and stained with Sox9 and EYFP antibodies (top panels) or pSMAD1/5/8, EYFP and CD31 antibodies (bottom panels). Right panels showed merged images, where nuclei are stained with Hoechst (blue). In the top panels, arrows indicate cells that co-express both Sox9 and EYFP. In the bottom panels, arrows show $pSMAD1/5/8^+$ cells of endothelial origin ($EYFP^+$) that have lost CD31 endothelial marker. C) IH of muscle section from quadriceps of Cdh5-$CreER^{T2}$:dtTomato mice at 10 days after bone induction and stained with Osterix (Osx) antibody (left panel). Central panel shows $dtTomato^+$ cells. Right panel shows merged images, where nuclei are stained with Hoechst (blue). Magnification 20X. Scale bar 50 µm.

Figure 3 Macrophage depletion increases EC-derived cells participation to HO.

A) Experimental scheme showing BMP2-mediated bone induction, clodronate (CLL) and Sham liposome treatments, and sacrifice time-points. B) Gating of $tdTomato^+$ sorted cells from Cdh5-$CreER^{T2}$:dtTomato mice quadriceps at seven days after bone induction (left panel). On the right: graph showing the median percentage of $dtTomato^+$ cells among the number of living cells (gated on physical parameters) in Sham and CLL-treated mice. n=4 Bars represent mean ± SEM. C) qRT-PCR expression of Sox9 in $dtTomato^-$ cells (left) and of Bmp4 and Bmp6 in $dtTomato^+$ cells (right), isolated from CLL or Sham Cdh5-$CreER^{T2}$:dtTomato mice quadriceps at seven days after bone induction. are expressed as fold changes relative to Sham mRNA expression, and normalized on the housekeeping (cyclophilln A and/or 28S) (left). n=4. Bars represent mean ± SEM. *p**≤0.05;

**≤0.01. D) Sections of quadriceps of CLL and Sham Cdh5-CreER^{T2}:R26R-EYFP mice at seven days after HO induction. Left panels show images of sections stained with H&E (magnification 10X). Central panels show IH images of muscle sections stained with Sox9 and EYFP antibodies. Right panels showed merged images, where nuclei are stained with Hoechst (blue). Arrows indicate cells that express both markers. Scale bar 50 µM. Graphs on the right represent the median number of Sox9^{+} cells (top) and the median number of Sox9^{+}/EYFP^{+} cells (bottom). n=4. Bars represent mean ± SEM. *p* *≤0.05. E) Sections of quadriceps of CLL and Sham Cdh5-CreER^{T2}:dtTomato mice collected 10 days after HO induction. Left panels show images of sections stained with H&E (magnification 10X). Central panels show IH images of muscle sections stained with Osx antibody or of dtTomato fluorescence. Right panels showed merged images, where nuclei are stained with Hoechst (blue). Arrows indicate cells expressing both Osx and dtTomato markers. Scale bar 50 µM. Graphs (right) represent the median fraction of Osx^{+} cells (top) and the median number of Osx^{+}/dtTomato^{+} cells (bottom). n=3. Bars represent mean ± SEM. *p* *≤0.05

Figure 4 Macrophage depletion increases HO

A) Experimental scheme showing BMP2-mediated bone induction, clodronate (CLL) and Sham liposome treatments, and micro-computerized tomography (µCT) time-points. B) µCT scans of CLL or Sham Cdh5-CreER^{T2}:tdTomato mice at 10, 21 and 30 days after bone induction C) Quantification of the mineralized ossicle volume (mm^3). n=4 mice. Bars represent mean ± SEM. *p* *≤0.05; **≤0.01. D) Quantification of the ectopic bone density (HU/mm^3). n=4 mice. Bars represent mean ± SEM. *p*** <0.01. HU, Hounsfield unit. E-F) H&E and Masson Trichrome stainings of muscle section showing lesions in Sham or CLL Cdh5-CreER^{T2}: tdTomato mice at 21 and 30 days after bone induction.

Figure 5. Dipyridamole decreases HO induced by macrophage depletion.

A) Experimental scheme showing BMP2-mediated bone induction, clodronate (CLL) and Sham liposome treatments, dipyridamole administration and micro-computerized tomography (µCT) time-points. B) Graph representing the percentage of Cd11b^{+} cells after Sham, Sham/dipyridamole (Sham+Dipy), CLL or CLL/dipyridamole (CLL+Dipy) treatment. n=4 mice. Bars represent mean ± SEM. C) µCT scans of Cdh5-CreER^{T2}:tdTomato mice treated with CLL or CLL/dipyridamole (CLL+Dipy) or PBS (Sham) at 21 days after bone induction. Lower panels show representative images of bone lesions in muscle sections after H&E and Masson Trichrome staining. D) Quantification of the mineralized ossicle volume and E) of the ectopic bone lesion density (HU/mm3) (right). n=5 mice. Bars represent mean ± SEM. *p* *≤0.05; **≤0.01 ***≤0.001.

Figure 1

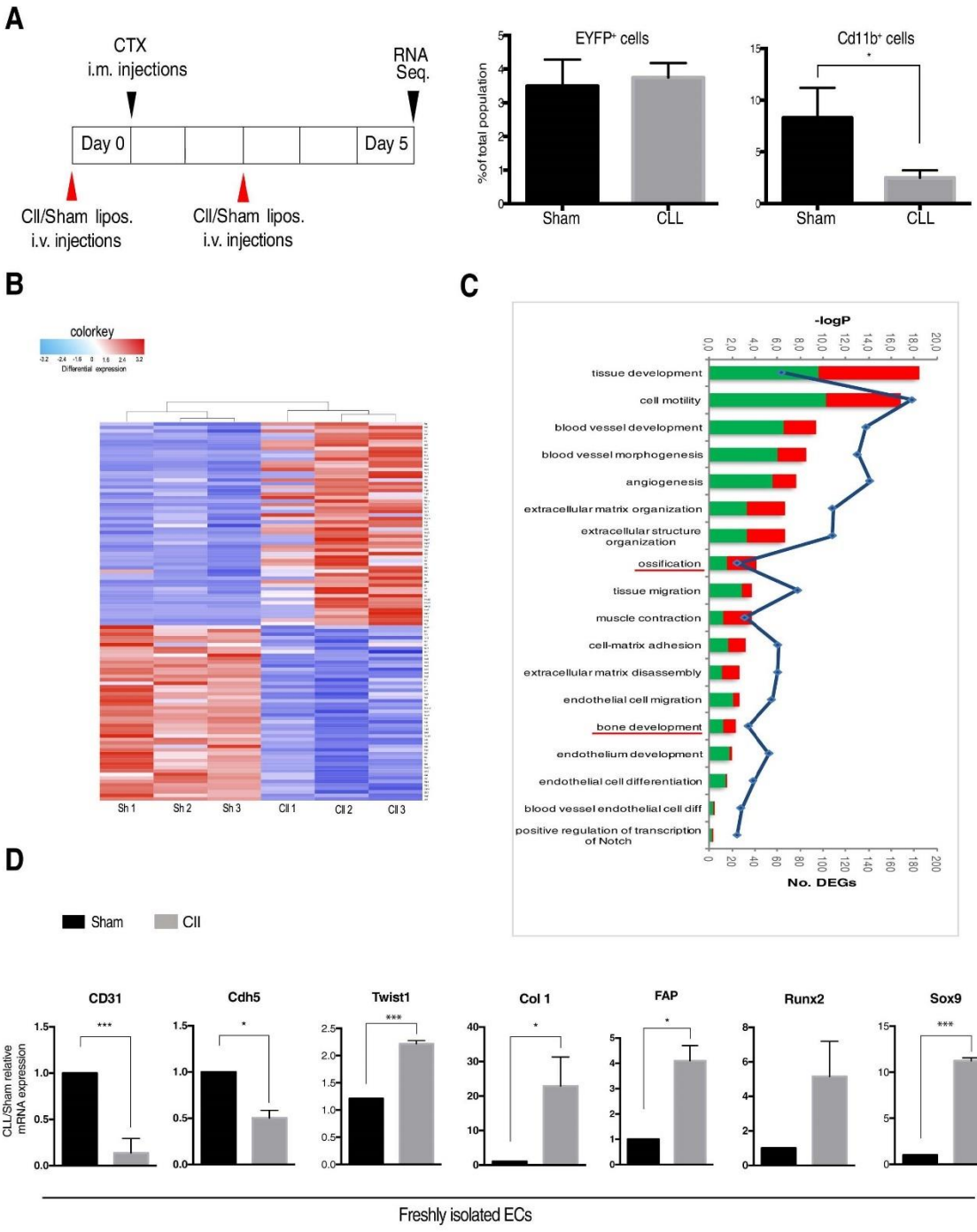
A
CTX
i.m. injections
RNA
Seq.
Day 0
Day 5
CII/Sham lipos.
i.v. injections
CII/Sham lipos.
i.v. injections
EYFP+ cells
%of total population
Sham
CLL
Cd11b+ cells
Sham
CLL
B
colorkey
Differential expression
Sh 1
Sh 2
Sh 3
CII 1
CII 2
CII 3
C
-logP
tissue development
cell motility
blood vessel development
blood vessel morphogenesis
angiogenesis
extracellular matrix organization
extracellular structure organization
ossification
tissue migration
muscle contraction
cell-matrix adhesion
extracellular matrix disassembly
endothelial cell migration
bone development
endothelium development
endothelial cell differentiation
blood vessel endothelial cell diff
positive regulation of transcription of Notch
No. DEGs
D
Sham
CII
CD31
Cdh5
Twist1
Col 1
FAP
Runx2
Sox9
CLL/Sham relative mRNA expression
Freshly isolated ECs

Figure 2

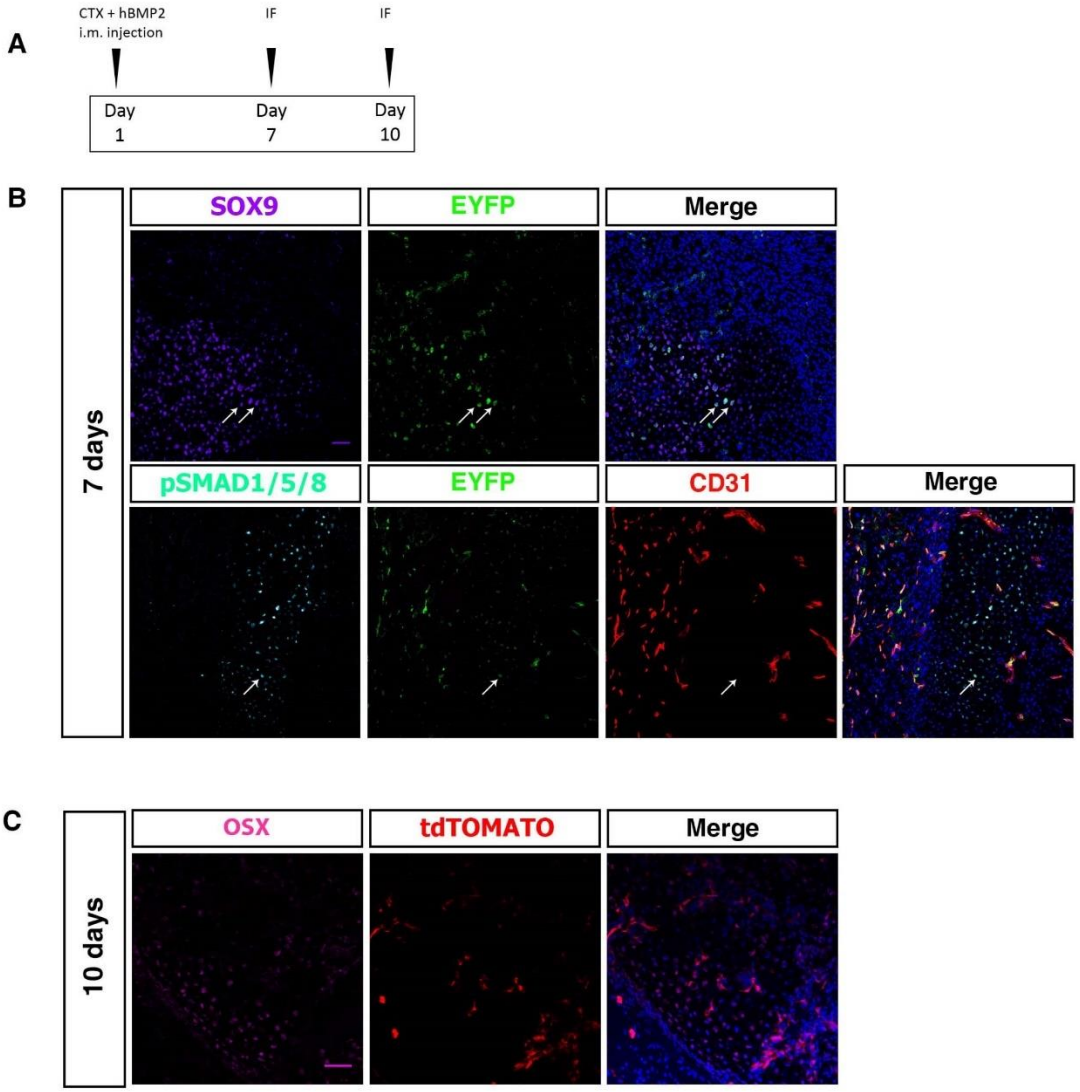
A
CTX + hBMP2
i.m. injection
IF
IF
Day
1
Day
7
Day
10
B
7 days
SOX9
EYFP
Merge
pSMAD1/5/8
EYFP
CD31
Merge
C
10 days
OSX
tdTOMATO
Merge

Figure 3

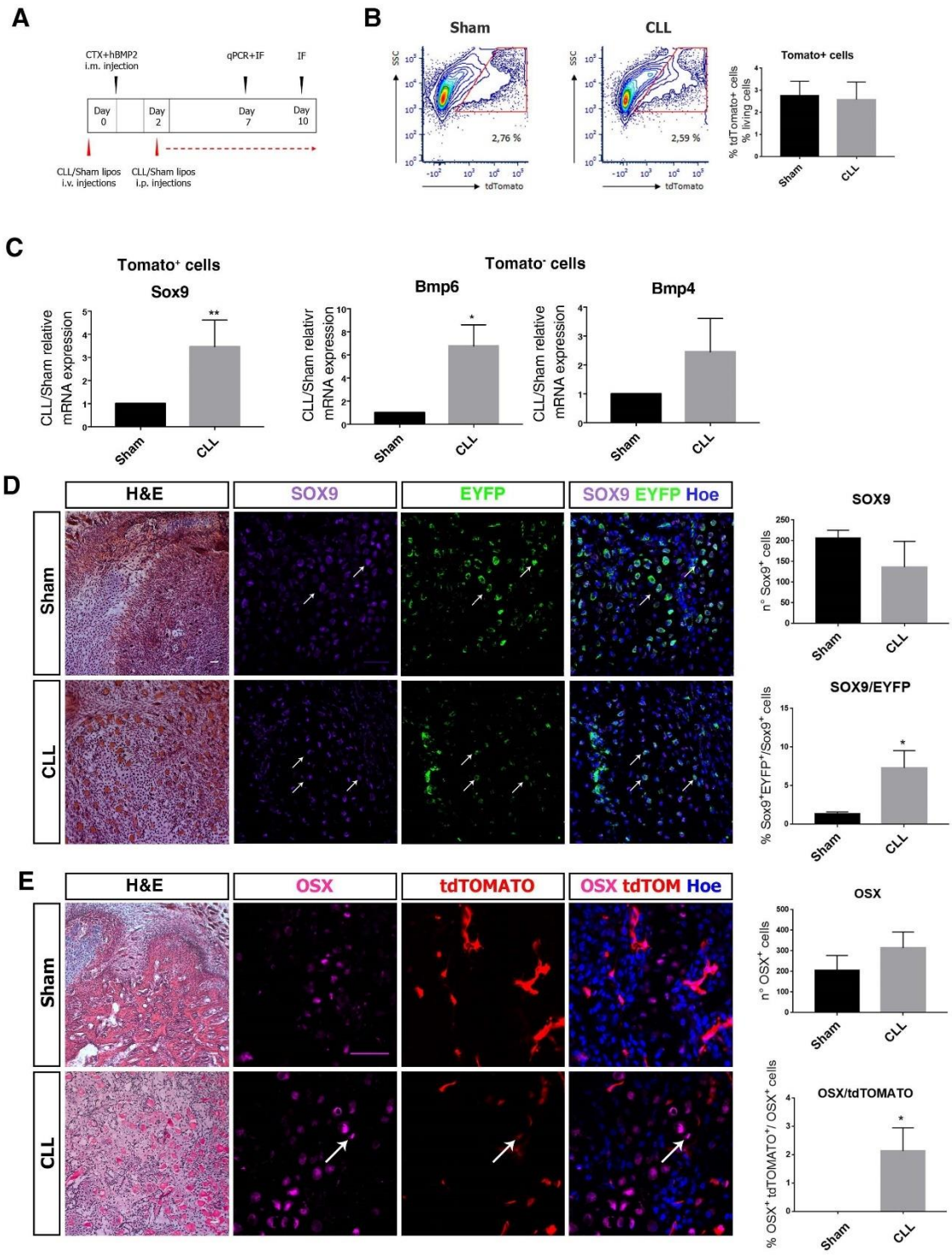
A
CTX+hBMP2
i.m. injection
qPCR+IF
IF
Day 0
Day 2
Day 7
Day 10
CLL/Sham lipos
i.v. injections
CLL/Sham lipos
i.p. injections
B
Sham
CLL
SSC
2,76 %
2,59 %
tdTomato
Tomato+ cells
% tdTomato+ cells / % living cells
Sham
CLL
C
Tomato+ cells
Tomato- cells
Sox9
Bmp6
Bmp4
CLL/Sham relative mRNA expression
CLL/Sham relativr mRNA expression
Sham
CLL
D
H&E
SOX9
EYFP
SOX9 EYFP Hoe
Sham
CLL
SOX9
n° Sox9+ cells
SOX9/EYFP
% Sox9+EYFP+/Sox9+ cells
E
H&E
OSX
tdTOMATO
OSX tdTOM Hoe
Sham
CLL
OSX
n° OSX+ cells
OSX/tdTOMATO
% OSX+ tdTOMATO+/ OSX+ cells

Figure 4

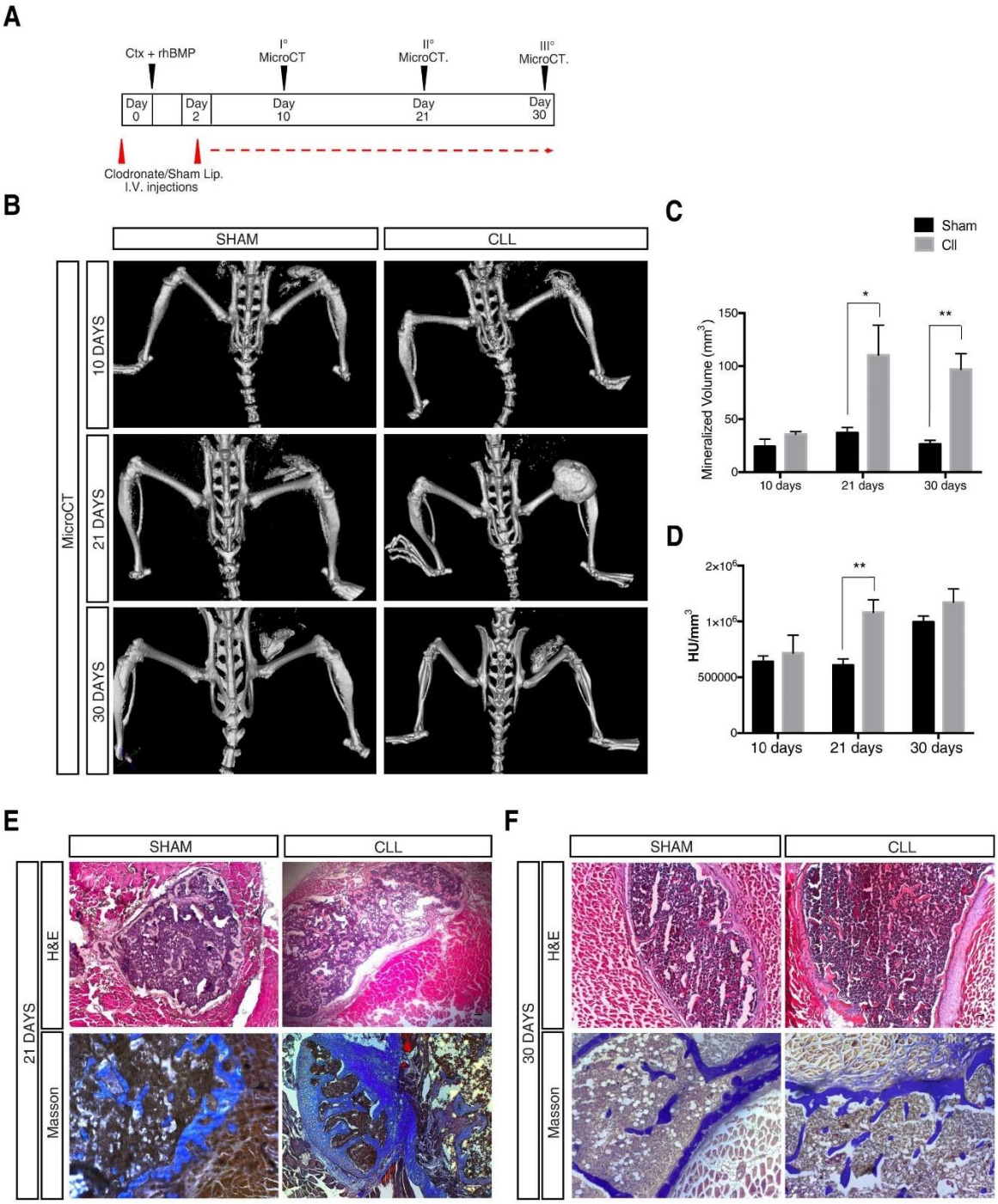
A
Ctx + rhBMP
I° MicroCT
II° MicroCT.
III° MicroCT.
Day 0
Day 2
Day 10
Day 21
Day 30
Clodronate/Sham Lip. I.V. injections
B
SHAM
CLL
MicroCT
10 DAYS
21 DAYS
30 DAYS
C
Sham
Cll
Mineralized Volume (mm3)
150
100
50
0
*
**
10 days
21 days
30 days
D
HU/mm3
2x10^6
1x10^6
500000
0
**
10 days
21 days
30 days
E
SHAM
CLL
21 DAYS
H&E
Masson
F
SHAM
CLL
30 DAYS
H&E
Masson

Figure 5

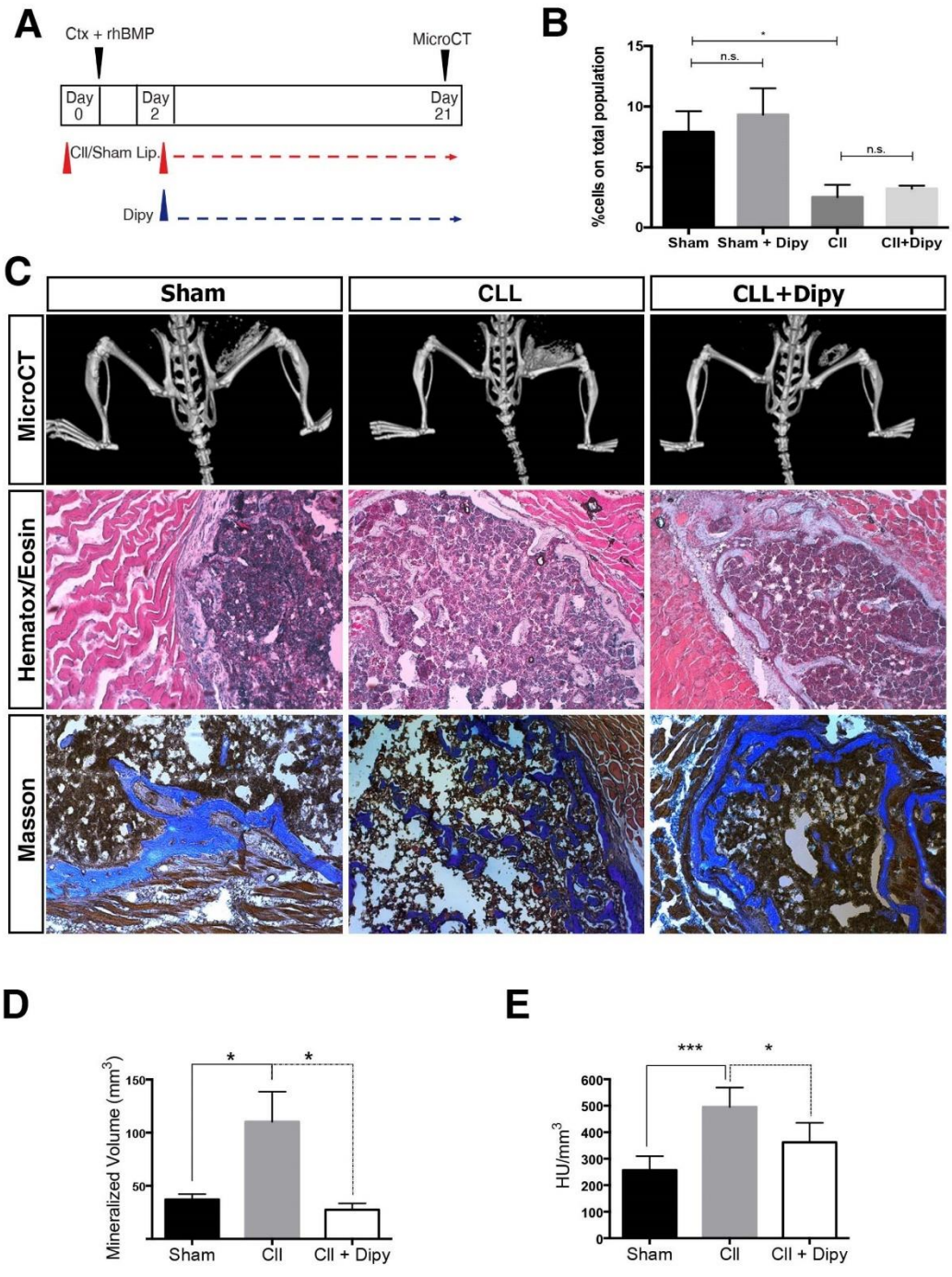
A
Ctx + rhBMP
MicroCT
Day 0
Day 2
Day 21
CII/Sham Lip.
Dipy
B
%cells on total population
n.s.
n.s.
Sham
Sham + Dipy
CII
CII+Dipy
C
Sham
CLL
CLL+Dipy
MicroCT
Hematox/Eosin
Masson
D
Mineralized Volume (mm3)
Sham
CII
CII + Dipy
E
HU/mm3
Sham
CII
CII + Dipy

CHAPTER 4

The role of Adar enzymes in endothelial cells

(Preliminary data)

4.1 Background

Recent works unveiled the role of RNA editing in controlling angiogenesis in endothelial cells. Conversion of adenosine in inosine is a post-transcriptional deamination carried out by Adar1 and Adar2 enzymes. Inosine are read by the translational machinery like G leading eventually to an aminoacidic change. While aminoacidic change is a quite rare event, most of the A to I RNA editing takes place in Alu elements of UTR genes and regulates gene expression. Adars activity can also target microRNA sequence generating a shift in microRNA targetoma (1).

Although Adars are expressed in endothelial cells, most of the research in RNA editing focused the attention on the brain and its role in endothelium is almost an untapped field. The work of Stellos et al (2), describes how Adar1 edits Alu elements in Cathepsin S 3' UTR, resulting in increased Hur binding and consequent mRNA stabilization. When Adar1 is knocked down in HUVEC, cathepsin S mRNA is decreased and it is followed by inhibition of angiogenic sprouting.

It is well known that microRNAs influence complex vascular pathological processes, including atherosclerosis, restenosis, aneurysm formation and neovascularization (3). MicroRNA are

targeted by Adar enzymes during neovascularization as illustrated by the work of Reginald at al, (4) describing the occurrence of RNA editing in miR487b that has a known vasoactive effect and is upregulated during chronic hypertension formation. A-to-I editing alters the seed sequence of miR487b, generating a new targetoma that stimulates angiogenesis.

The transcriptomic analysis described in Chapter 3 indicates that macrophages depletion from regenerating muscle induces EndMT. In addition to up-regulation of mesenchymal genes and down-regulation of endothelial genes, also Adar genes appear to be modulated by macrophage depletion.

These data suggested a potential involvement of Adars in the triggering or progression of EndMT.

On this basis we decided to explore the role of Adar1 and Adar2 in Ea.yh926 cells endothelial cells paying special attention to TGFβ signalling because of is known capacity of inducing EndMT, in addition TGFβ levels are found increased in macrophage depletion conditions after muscle damage (5).

4.2 Materials and methods

Experimental procedures regarding mice and NSG data are described in chapter 3.

Cell culture

EA.hy926 (ATCC® CRL-2922™) were maintained in MDCB131 medium (Gibco, Carlsbad, CA) supplemented with 10% fetal bovine serum (FBS) (Invitrogen, Carlsbad, CA), 10Mm L-Glutamine (Invitrogen), 1mg/ml Hydrocortisone (Sigma-Aldrich, Buchs, SG), penicillin/ streptomycin (Invitrogen) and VEGF 10 ng/µl (Sigma-Aldrich). Cells were grown on 1% gelatin coated plates for gene expression analysis after 24h ligands treatment with 1 ng/µl BMP9 (R&D System, Minneapolis, Minnesota, USA), 5 ng/µl TGFβ3 (OSI Pharmaceuticals, Farmingdale, USA), 10 ng/µl TNF-α (Thermo Fisher Scientific, Waltham, MA, USA), 50 ng/µl ActivinA (Fisher Scientific, Waltham, MA, USA), 10 µM kinase inhibitor SB431542 (Tocris Bioscience, Ellisville, MO, USA).

Quantitative-RT PCR

Total RNA extraction was performed using NucleoSpin RNA II (Machery Nagel, Düren, Germany). 500 ng of RNA were retro-transcribed using RevertAid First Strand cDNA Synthesis Kits (Fisher Scientific, Landsmeer, The Netherlands), and real-time reverse transcription-PCR experiments were performed using SYBR Green (Bio-Rad, Veenendaal, The Netherlands) and a Bio-Rad CFX Connect device.

Lentiviral production.

Lentiviral vectors were produced by transfecting HEK293T cells with helper plasmids: pCMV-VSVG, pMDLg-RRE (gag/pol), pRSV-REV and Adar1 or Adar2 shRNAs (MISSION Sigma-Aldrich). As controls cells were also transfected with pLKO.1 or Scramble plasmids. Cell

supernatants were harvested 48 hours posttransfection and thereafter used for cell infection. At 48 hours after infection, EA.hy926 cells were cultured in medium containing 4 μg/mL puromycin (Sigma-Aldrich) for 1 week to generate stable cell lines expressing pLKO.1 or Scramble construct or short hairpin RNAs (shRNAs) selectively targeting Adar1 or Adar2.

Immunofluorescence

EA.hy926 grown on coverslip were fixed with 4% formaldehyde for 30 minutes at room temperature, washed with glycine for 5 minutes, permeabilized with 0.2% Triton X-100 and blocked in PBS containing 5% BSA for one hour. Next, the cells were incubated o/n at 4°C in blocking solution containing primary antibodies: anti-Adar1 (Abcam, Cambridge, UK), anti-Adar2 (Abcam), anti pSmad2/3 (Cell signaling Technology, Danvers, MA, USA) anti with gentle shaking. Next day, the cells were washed 5 times in washing buffer (PBS containing 0.05% Tween-20 and 1% BSA) and incubated with secondary antibodies (Alexa Fluor, Invitrogen, Breda, the Netherlands) in PBS with 0.5% BSA for 1 one hour. Finally, the cells were washed 5 times in washing buffer and mounted in Prolong Gold containing DAPI (Invitrogen). After careful drying, the preparations were imaged in a Leica SP5 Confocal Scanning Laser microscope. A representative picture from each staining is shown.

Western blot

Lysate were boiled for 5 minutes and electrophoresed in 10% SDS/polyacrylamide gel. Separated proteins were transferred to nitrocellulose membranes (0.5 A at 100 V; in ice) for 1 hour. Blots were blocked in Tris-Buffered Saline solution containing 0.1% Tween 20 and 5% non-fat dry milk overnight at 4°C, and immune-detection of specific proteins was carried out with primary antibodies: anti-Smad3 antibody (Abcam), phosphorylated Smad2 antibody (Cell signaling Technology) and GAPDH antibody (Sigma) followed by horseradish peroxidase-conjugated anti-mouse or anti-rabbit (GE Healthcare, Chicago, Illinois, USA) secondary antibodies using ECL system (Thermo Fisher Scientific) and quantified using ChemiDoc (Bio-rad).

4.3 Results

Deep sequencing (RNA-seq) analysis conducted (chapter 3) in endothelial progenitors (EYFP+ cells) isolated from regenerating muscle reveals that in addition to endothelial and mesenchymal genes, also Adar1 and Adar2 gene expression is affected by macrophages. When MP are depleted by clodronate treatment the level of Adar1 and Adar2 is reduced by about 50% (Fig.1).

To establish a link between EndMT and Adars we used a HUVEC-immortalized cell line (Ea.hy926), known to be sensitive to TGFβ-induced EndMT (6), to evaluate modulation of Adar expression by ligands belonging to TGFβ family: BMP9, TGFβ3, ActivinA and TNFα for its EndMT-inducing capacity. None of these ligands alters Adar1 or

Adar2 gene expression in wild-type Ea.hy926 cells after 24 hours of treatment (fig. 2a).

Since Adars proteins shuttle out of the nucleus to accomplish different functions, as promoting the activity of Dicer and the assembly of RNA-induced silencing complex (RISC) (1), we checked if TGFβ stimulation can affect Adar translocations (Fig 2B). Starvation has been induced in Ea.hy926 for 6 hours cells by FBS deprivation before TGFβ3 stimulation (45 minutes) to observe change in Adar proteins localization through immunofluorescence in fixed cells. As expected, TGFβ stimulation is followed by traslocation of Smad factor into the nucleus, while Adar proteins do not show appreciable changes in localization upon treatment, which appear to be mainly nuclear (Fig. 2B).

We next interrogated the effects of silencing Adars enzymes in Smad activation. We therefore evaluated the efficiency of different specific short-hairpin RNAs targeting Adar1 or Adar2 proteins (Fig.3). All the constructs were directed against a region shared by all the transcripts of Adar1 or Adar2 reported in literature. As controls we used cells infected with empty (pLKO.1) and Scramble vectors. Adar1 KD does not appear to target Adar2 or to induce a compensatory up-regulating Adar2 mechanism, and the same for Adar2 KD towards Adar1, as expected by literature describing not overlapping editing sites for Adar enzymes.

shAdar1 #4, as demonstrated by Western Blot (Fig.3b) has a low efficiency, while other constructs reach a substantial reduction of Adar proteins. Silencing of Adar1 and Adar2 knock downs were compatible

with Ea.yh926 cells vitality enabling us to stimulate the cells with TGFβ3 for 48 hours (Fig. 4, Fig. 5). Treatment with TGFβ, known to induce EndMT, cause, as expected, the acquirement of a spindle morphology in all conditions (Fig. 4-5), the mesenchymal shape seems to be more pronounced in ShAdar1 #1 KD (Fig. 4, arrows). We therefore wonder if Adars can increase sensitivity to TGFβ hyperactivating Smad factors. Evaluation of Smad2 phosphorylation does not reveal differences among KD and control (Fig. 6). Similarly, TGFβ target genes do not show to be modulated by Adars (Fig.7) after 48 hours of treatment.

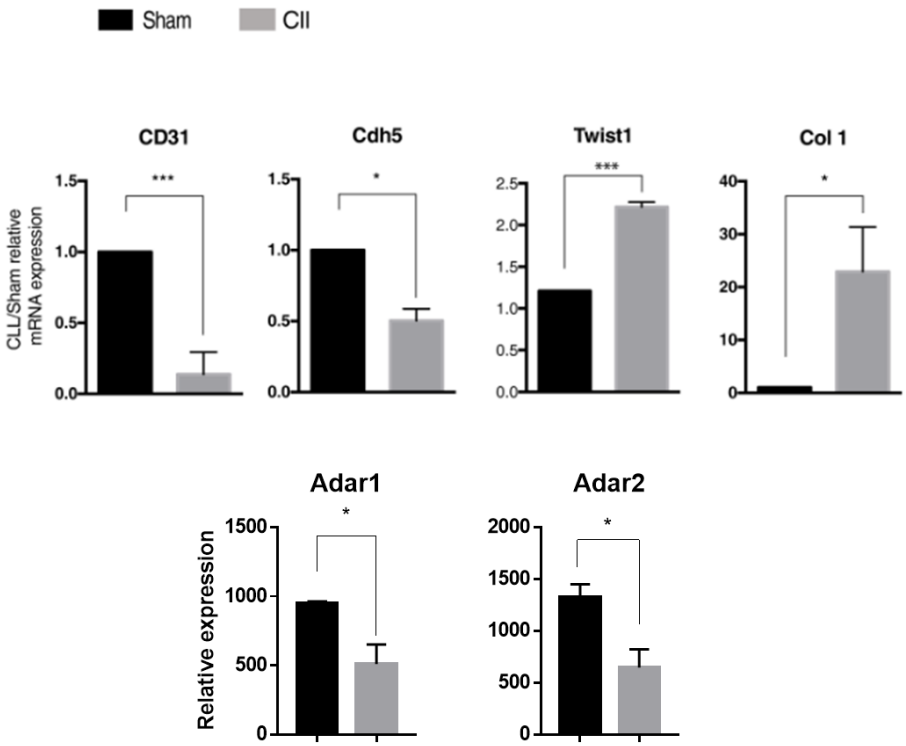

Figure 1. RNA sequencing data analysis on VE-Cad+ cells (Eyfp+) isolated from regenerating muscle 5 days after CTX damage in CII and Sham treated mice. mRNA expression of selected genes. pvalue *<0.05; **<0.01; ***<0.005. Data ± SD (n=5).

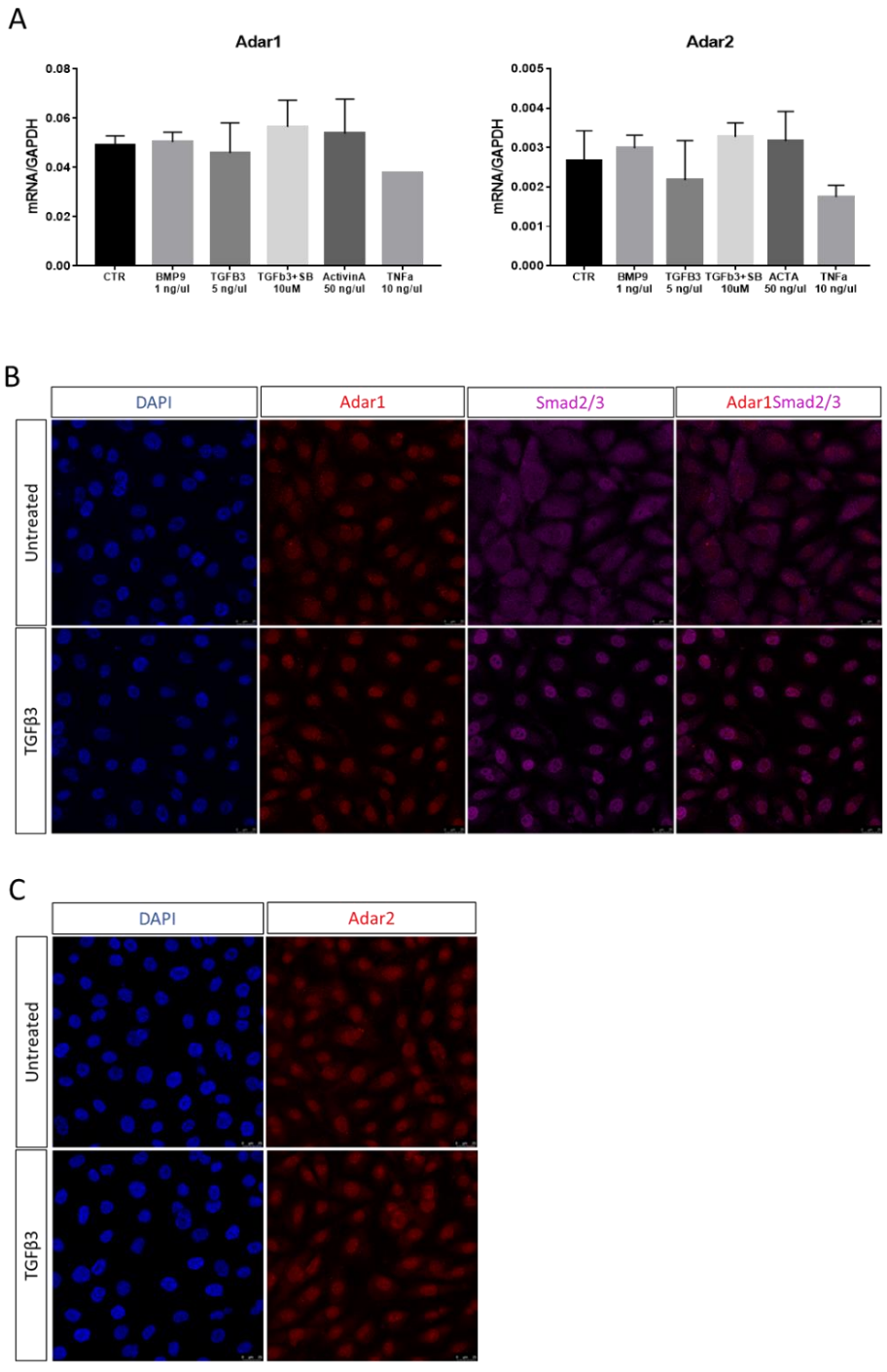

Figure 2. A) RNA expression of Adars enzymes in Ea.hy926 cells after 24h treatement with ligands: BMP9, TNFa, ActivinA (ACTA),TGFβ3, TGFβ3 and TGFβ inhibitor (SB).
B) and C) Ea.hy926 cells treated with 5 ng/µl TGFβ3 for 45 minutes after 6 hours of starvation, stained with anti-Adar1 antibody, anti-Adar2 antibody and anti-Smad2/3 antibody. Magnification 40X.

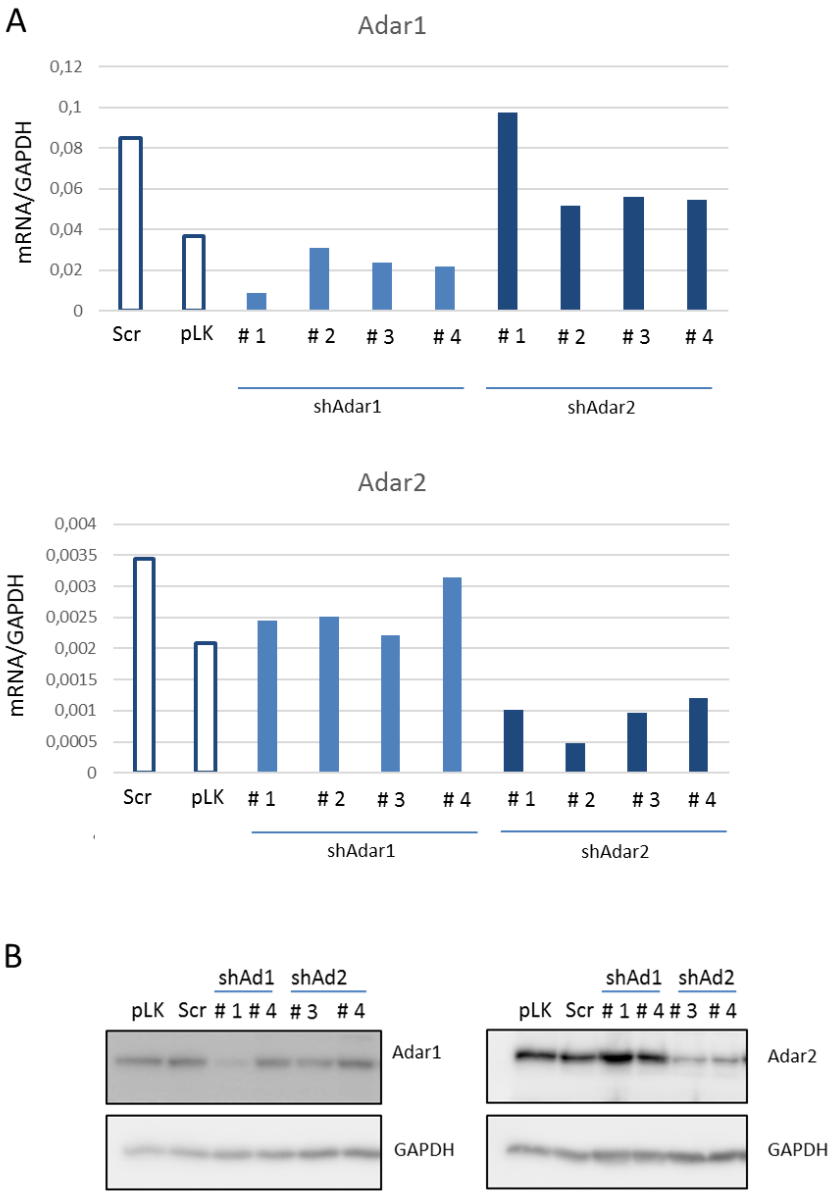

Figure 3 Evaluation of Adars KD in Ea.hy926 cells. A) RNA expression of Adar1 and Adar2, in Ea.hy926 cells stably infected with 4 (# 1-4) short-hairpin RNA to silence the expression of Adar1 and Adar2. Controls: pLKO.1 (empty vector) and Scramble vector. B) Western blot performed on protein extract derived from Adar1 and Adar2 KD Ea.hy926 cells. Incubation with Adar1 or Adar2 antibody. GAPDH is used as loading control

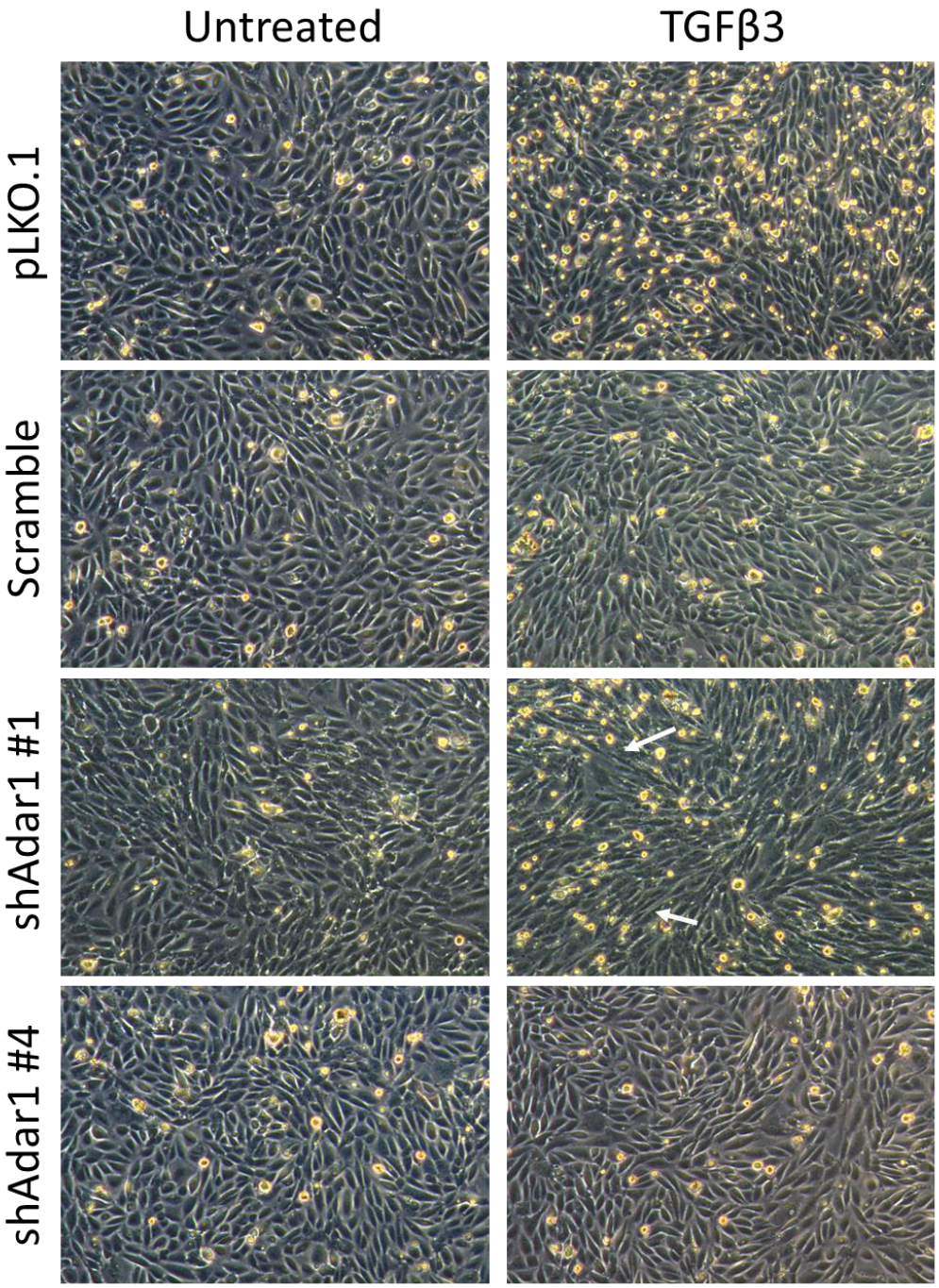

Figure 4. Images of Ea.hy926 cells (controls: pLKO.1 and Scrambled vs Adar1 KD) in untreated conditions and after 48h of TGFβ3 treatment in the presence of 10% of serum. Arrows indicate spindle cells in Ada1 KD #1.

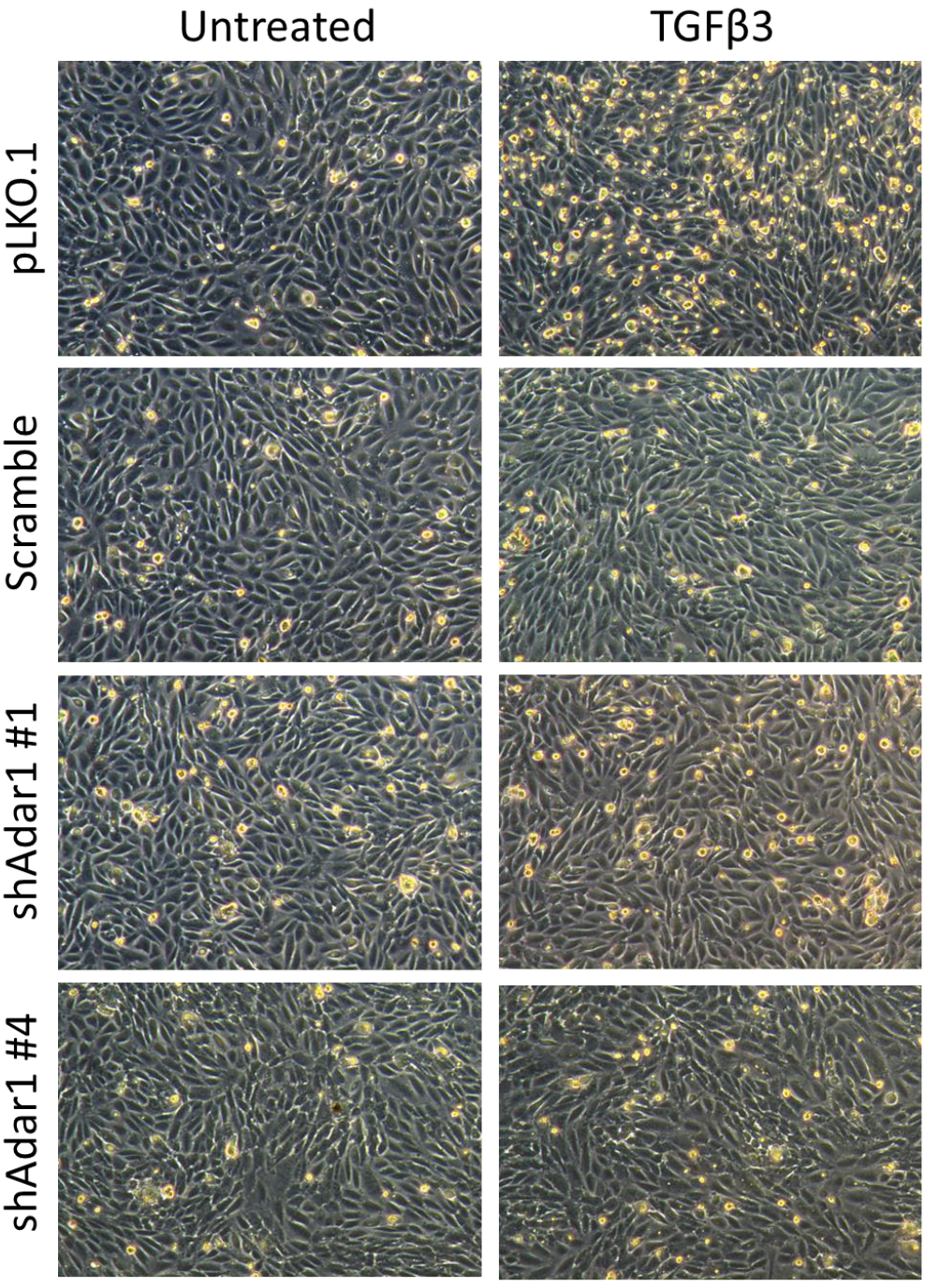

Figure 5 Images of Ea.hy926 cells (controls: pLKO.1 and Scrambled vs Adar2 KD) in untreated conditions and after 48h of TGFβ3 treatment in the presence of 10% of serum.

4.4 **Conclusions**

In conclusion even if Adar enzymes regulate some aspects of endothelial functions (2,3), a direct interplay between Adars and TGFβ signalling has not been demonstrated yet.To understand if the acquirement of spindle morphology depends on TGFβ stimulation and Adar1 KD (#1), further experiments are required. In particular, TGFβ target genes or Smad activation are not increased by reduction of Adar1 protein. Non-canonical TGFβ signalling pathways, including MAP kinase, Rho-like GTPase and phosphatidylinositol-3-kinase/AKT (7) should be studied to evaluate a possible involvement of Adar1 in modulating TGFβ signalling.

Analysis of the effects of non-canonical pathways in Adar1 KD should be carried out using specific pathway inhibitors to verify the effect of TGFβ.

Since Adar enzymes control particular aspects of endothelium (2,3), like angiogenesis, it is possible that the effects of Adar KD cannot be seen in basal conditions and can only be appreciated when endothelial cells are challenged in a specific contest like in sprouting.

Adar1 has a known role of mitigating the intracellular effects of inflammation (2,3) in different cell types, data from non-endothelial cells report that TNFα can induce the expression of Adar1, this effect was not reproduced in our system. This may be related with the specific endothelial cells used in this work (Ea.hy926 cells), since ECFC derived from FOP patients and healthy donors (data not shown) upregulate Adar1 in response to TNFα treatment.

It would be therefore interesting to evaluate how TNFα induced EndMT is affected when Adar1 expression is silenced in another type of endothelial cells.

Endothelial heterogeneity can generate important differences in TGFβ sensitivity and pathways activation (8) explaining why *in vivo* we noted a reduction of Adars level in EndMT inducing conditions not reproduced in our *in vitro* conditions.

Co-culture experiments, using macrophages and EC, can clarify the existence of possible regulating mechanisms of Adar activity between these two cell-types.

4.5 References

1. Nishikura, K. (2016). A-to-I editing of coding and non-coding RNAs by ADARs. *Nat Rev Mol Cell Biol*, *17*, 83-96.
2. Stellos, K., Gatsiou, A., Stamatelopoulos, K., Perisic Matic, L., John, D., Lunella, F.F., Jaé, N., Rossbach, O., Amrhein, C., Sigala, F., Boon, R.A., Fürtig, B., Manavski, Y., You, X., Uchida, S., Keller, T., Boeckel, J.N., Franco-Cereceda, A., Maegdefessel, L., Chen, W., Schwalbe, H., Bindereif, A., Eriksson, P., Hedin, U., Zeiher, A.M., & Dimmeler, S. (2016). Adenosine-to-inosine RNA editing controls cathepsin S expression in atherosclerosis by enabling HuR-mediated post-transcriptional regulation. *Nat Med*, 22, 1140-1150.

3. Welten, S.M., Goossens, E.A., Quax, P.H., & Nossent, A.Y. (2016). The multifactorial nature of microRNAs in vascular remodelling. *Cardiovasc Res*, *110*, 6-22.
4. van der Kwast, R.V.C.T., van Ingen, E., Parma, L., Peters, H.A.B., Quax, P.H.A., & Nossent, A.Y. (2018). Adenosine-to-Inosine Editing of MicroRNA-487b Alters Target Gene Selection After Ischemia and Promotes Neovascularization. *Circ Res*, *122*, 444-456.
5. Zordan, P., Rigamonti, E., Freudenberg, K., Conti, V., Azzoni, E., Rovere-Querini, P., & Brunelli, S. (2014). Macrophages commit postnatal endothelium-derived progenitors to angiogenesis and restrict endothelial to mesenchymal transition during muscle regeneration. *Cell Death Dis*, 5, e1031.
6. Wang, Y., Nakayama, M., Pitulescu, M. E., Schmidt, T. S., Bochenek, M. L., Sakakibara, A., Adams, S., Davy, A., Deutsch, U., Lüthi, U., et al. (2010). Ephrin-B2 controls VEGF-induced angiogenesis and lymphangiogenesis. *Nature* 465, 483-486.
7. Srinivas, S., Watanabe, T., Lin, C. S., William, C. M., Tanabe, Y., Jessell, T. M. and Costantini, F. (2001). Cre reporter strains produced by targeted insertion of EYFP and ECFP into the ROSA26 locus. *BMC Dev Biol* 1, 4.
8. Gao, H., Zhang, J., Liu, T., & Shi, W. (2011). Rapamycin prevents endothelial cell migration by inhibiting the endothelial-to-mesenchymal transition and matrix

metalloproteinase-2 and -9: an *in vitro* study. *Mol Vis*, *17*, 3406-3414.

9. Zhang, Y.E. (2009). Non-Smad pathways in TGFβ signaling. *Cell Res*, *19*, 128-139.
10. Massagué, J. (1998). TGFβ signal transduction. *Annu Rev Biochem*, 67, 753-791.

CHAPTER 5

5. Discussion

5.1 Summary

The results presented in this thesis show that *in vivo* heterotopic ossification is in part caused by EndMT, and the process endochondral ossification can be modulated by inhibitors of BMP signalling and by the cells of the immune system.

In particular we have shown that dipyridamole is able to counteract HO development. Dipyridamole is an ACVR1 modulator, *in vitro* it blocks the chondrocytes and osteoblasts differentiation of two cell lines. The *in vivo* study demonstrated a reduction of ectopic bone volume possibly due to the downregulation of Smad activation.

We have observed indeed that in the muscle niche altered by cardiotoxin damage, endothelial cells are sensitive to the osteogenic stimulus of BMP2 and differentiate into chondrocytes.
Most importantly we demonstrate that altered macrophage infiltration in the damaged muscle is deleterious for two main reasons: i) it increases the number of endothelial progenitors differentiating in chondrocytes leading also to osteoblasts differentiation. ii) it increases the bone ectopic volume and density. Even in this scenario dipyridamole is still able to reduce the extent of osseous lesion.

5.2 Conclusions

When HO takes place in muscle, two opposite events are occurring in the tissue: on the one hand, a new, completely different tissue is developing, on the other hand, the muscle regeneration triggered by trauma fails to heal. In FOP patients indeed, not only we can observe an increased level of ossification, but also uncalcified areas show pathological conditions: a biopsy of masseter muscle reveals the presence fibroblastic cells next to the ossified zone, replacement of muscle with connective tissue, atrophied muscle fibers, dense collagen deposition between muscle fibers. Also the vessel network presents alterations with approximately 70% of these blood vessels showing various degrees of degenerative changes, e.g. artery with collapsed lumen, endothelial fragmentation associated with gaps in the vessel wall, some endothelial cells were dark and showed an almost complete hyalinization of the cell contents. The pericytes were similarly affected (1). These data suggest that, even if ossification is the main pathological manifestation of FOP and the most life-threatening symptom leading to reduced chest mobilization and respiratory insufficiency, the disease includes important defects not directly connected with ossification development. The design of FOP therapy should consider also the restoration of muscle functionality. Only the complete understanding of all cellular dysfunction occurring during HO may pave the way to a successful therapy.

5.2.1 Endothelial cells as players in HO

Endothelial cells participating to the formation of the cartilage analgen exhibit activation of Smad1/5/8 pathway (2), necessary for osteogenic differentiation and loss of endothelial marker CD31, indicating that EndMT is a pathological mechanism concurring to HO development. Contribution of endothelial cells does not show a homogeneous pattern within the ossified sections. 7 days after HO induction it is possible to recognize different areas with Sox9+ cells, some of them co-express EYFP marker, while others do not derive from endothelial precursors. This suggest that osteogenic conversion of endothelial cells may require an additional stimulus, such as a specific concentration of BMP, the presence of particular inflammatory signals or the proximity to specific cell type.

EYFP+ cells take part to HO formation also by assembling vessels within the ectopic lesion: understanding how endothelial cells are committed to vascular or osteogenic differentiation is still to be clarified. A different state of stemness or the heterogeneity of endothelial cells may account for this divergent behaviour: endothelial cells lining the inner wall of blood vessels exhibit diverse subtypes and different ECs have different structural and functional characteristics based on their exposure to distinct microenvironments (3). EC are activated by inflammatory signals and many studies showed that each EC subtype responds differently to different inflammatory stimuli *in vitro* (4). . As described by Scott et al.,(5), response to TNFα is indeed different accordingly to ECs subtype: VCAM-1 expression was only increased in

response to TNFα in HUVECs and glomerular ECs, but not in dermal microvascular ECs . In addition, they (6) reported changes in heterogeneous gene expression in response to TNFα, lipopolysaccharide (LPS), and IL-1β in HUVECs, human pulmonary microvascular ECs, HAECs, carotid artery ECs, coronary artery ECs, subclavian artery ECs, and brachiocephalic artery ECs. TNFα and IL-1β-stimulated organ-specific endothelial heterogeneity has also been reported (7). Also the effects elicited by TGFβ treatment shows variability among EC subtypes. In human coronary artery ECs, both TGFβ1 and TGFβ2 upregulate the expression of the mesenchymal markers α-SMA and SM22α, but only TGFβ1 has an effect on α-SMA expression in human pulmonary microvascular ECs (8). Thus, differential behaviour in response to TGFβ and TNFα stimulus may generate increased or reduced propensity to undergo EndMT.

It has recently been reported evidence that in a mouse FOP model (Acvr1tnR206H/+;R26NG/+;Tie2-Cre mice) endothelial cells do not directly participate to heterotopic ossification, while FAP cells are the main cells contributing to the formation of ectopic bone (9). This discrepancy with our finding can be explained by the use of the different mouse model. In Shepard et al. work (9) the use of Acvr1tnR206H/+;R26NG/+;Tie2-Cre mice, in which FOP mutation is expressed in FAP cells appears to be sufficient to drive the formation of ectopic bone. The *in vivo* effects of the mutation can establish an osteo-inductive environment in which mutated FAP are the most sensitive cells to osteogenic differentiation. These data suggest that,

although acquired and genetic HO show that the process of ossification is phenotypic similar the mechanism governing the cellular differentiation are different.

5.2.2 Macrophages: friends or foe in HO

Correct muscle regeneration requires the presence of macrophages to guide myoblasts differentiation and permit the reconstitution of vessel network, equally important for tissue healing (10,11). In our work, macrophages depletion boosts EndMT and endothelial commitment to osteogenic fate, with an overall increase of calcified area. The molecular explanation of the EndMT and osteogenic stimulation induced by reduction of macrophages is still not completely elucidated. The work of Zordan et al (12), shows that macrophages depletion is associated with increased TGFβ level in the muscle, followed by up-regulation of Snail transcription and reduction of MMP2, MMP13 and MMP14. When BMP is added in the model of cardiotoxin muscle damage and macrophages depletion, we assist, in this work, to a significative up-regulation of BMP6 expression and an increased tendency of BMP4 in non-endothelial cells. In order to clarify if this is a direct effects of macrophages depletion, due for example to macrophages-secreted cytokines, *in vitro* studio are required to challenge macrophages in limiting osteogenic signals present in the muscle niche.

Another possible reason to explain the role of macrophages in counteracting heterotopic ossification is provided by the cross-talk between FAP and macrophages in regenerating muscle. FAP cells in healthy muscle are quiescent but become rapidly activated following injury and they are primary producers of connective tissue in injured muscle, providing a temporary scaffold to the tissue when muscle fibers are destroyed. Proliferation and apoptosis of FAP are regulated by macrophages: the first is induced by M2 macrophages secreting TGFβ, while apoptosis is driven by TNFα released from M1 macrophages (13). Macrophages depletion can therefore increase or reduce the number of FAPs. This double effects of macrophages on FAPs can conciliate the discrepancy on their role in HO arisen in several works where macrophages depletion impairs heterotopic ossification (14).

In our model, we achieved approximately 50% reduction of circulating monocytes that turned into almost 90% macrophages depletion in ossified muscle. Although diminished, a number of macrophages is still present in the lesion, it would be interesting characterize their phenotype regarding M1-M2 markers and comparing the polarization state with the control mice. An *in vitro* study, could also complement and provide more information on eventual differences between M1 and M2 polarization in promoting osteogenic differentiation. This differential capacity of M1-M2 in affecting the differentiation of cells comes true for endothelial cells derived from muscle, we have *in vitro*

evidence (unpublished data) that the state of macrophages polarization can generates difference in EndMT process.

Another unsolved issue about the role of macrophages in HO is how macrophages are affected by HO. It is not known if the occurrence of HO requires intrinsically alterations in immune cells. A bone-marrow transplant in a FOP patient showed that following the transplant no flare-ups occurred, when immunosuppressive therapy for avoiding rejection was suspended the patient underwent new ossification episodes (15). This suggests that also a wild-type immune system can triggers HO, but at the same time studying how immune cells are affected by the mutation can provide useful information since Act A is a powerful cytokine that acts as a key regulator of the immune system in mammals (15), especially in the inflammatory pathways. The work of Del Zotto et al., (16) reveals differences in the profile of immunological markers of FOP patients. Of note DNAM1, an adhesion molecule expressed by both monocyte subpopulations, shows a strong increase in FOP monocytes. Interaction between CD155 and DNAM1 is pivotal in the regulation of monocyte migration by diapedesis through endothelial junctions (17). This finding may suggest the existence of a potential up-regulation of monocyte migration toward the sites of inflammation during the flare-up episodes.

In chapter 2 we showed that dipyridamole is an inhibitor of ACVR1 transcription and can decrease the calcified area, moreover it is effective in reducing the calcified volume in macrophages-depleting conditions. The mechanism for this anti-osteogenic effect has not been elucidated, it has been demonstrated that dipyridamole can reduce the proliferation of several cell types (18). We noted that dipyridamole treatment is associated to a decrease of Smad1/5/8 signalling and it might be a route for the drug to counteract HO development. We can exclude that the effect does not rely on the restoration of macrophages, since the number of monocytes does not appear to be affected by dipyridamole treatment. However, we cannot rule out an effect on macrophages.

5.3 Future perspectives

Up to now, while acquired forms of HO can be treated with surgical resection and anti-inflammatory therapy can limit the occurrence for high-risk procedures such as hip-replacement, the main treatment for FOP is trauma prevention and anti-inflammatory medications (19). If the first option cannot prevent spontaneous flare-ups occurrence and poses serious limits to the life quality, the second one has two main drawbacks: i) side effects and ii) doubtful efficacy of this type of drugs. Since the involvement of inflammation in the pathogenesis of HO, anti-inflammatory drugs are currently use when a new flare-ups appears,

but side effects associated to anti-inflammatory drugs prevent a long-term use.

The nature of the disease and the lack of focused clinical trials arise uncertainties about the effects of these medications (20). The unpredictability of flare-ups evolution makes it hard to evaluate the efficacy, in some cases a flare-ups can spontaneously regress, in other cases symptoms vanish during anti-inflammatory assumption, but when medications are suspended, the flare-ups reappears and progresses through HO development, suggesting a rebound effect of anti-inflammatory drugs (20). The design of BMP inhibitors to block the effects of FOP mutation has revealed its limitation in the lack of specificity (21), both because it is difficult to produce a molecule that acts only on ALK2 without targeting other BMP receptors and because of the multitude and the importance of different physiological events controlled by BMP pathway (22).

The two ongoing clinical trial that are evaluating the efficacy of palovarotene (NCT02521792) and anti-activinA antibody (NCT02870400) arise some concerns about the toxicity of the proposed therapy. The effects of palovarotene in inhibiting HO relies on targeting retinoic acid receptor (23), involved in the chondrogenesis process. The most attractive aspect of this strategy that led to clinical trial was the capacity of palovarotene to permanently derail the differentiation of osteoprogenitors toward a not osteogenic fate, but a recent study has highlighted potential toxicity of palovarotene

mechanism (24), especially for younger people since it exhibits pronounced skeletal toxicity in a mouse model of FOP.

Inhibitors of ActivinA have been already tested for different pathologies and have shown occurrence of bleeding that can potentially endanger FOP patients who present alterations in vasculature network (25). Even if anti-ActivinA antibody has shown tempting results in mice, up to now there is no evidence in patients tissues that can support ActivinA is a driving-HO mechanism in human.

Investigate the signalling induced by ActivinA could open the way to find new therapeutic targets. Some questions about ActivinA need to be addressed. For example is not established yet if ActivinA exerts a direct role on Smad signalling. Analysing the interaction with other BMP receptors might unveil unexpected obligatory partners to elicit intracellular response or the potential modulating effects by type III BMP receptors.

A safer approach to target ActivinA requires study of conformational changes induced by the binding of ActivinA with the mutated receptor. This could lead to the design of inhibitors able to specifically bind the mutated receptor-ActivinA complex. A drug with this characteristic could be theoretically less harmful since it would permit physiological binding and activity of wild-type receptors.

A limiting factor in this field is the reliance of FOP study on mice models, ALK2R206H engineered mice exhibit some divergence between human and mice in ALK2 function. While human embryos

develop quite normally, ALK2 mutation leads to mouse perinatal death. This discrepancy can have also an alternative explanation: since FOP is a very rare disease, affecting one person in two millions, it is legitimate to speculate that some specific genetic backgrounds may be compatible with life while other lead to embryonic death.

Until this question is not addressed it is advisable to study FOP, when it is possible, using patients-derived material. Development of complex *in vitro* system could let make it possible to study interactions of human osteoprogenitors cells with endothelial and immune cells to mimicry *in vivo* environment.

Regarding the pathological role of inflammation in triggering HO, the cross-talk between BMP signalling and immune cells requires further investigation to be elucidated. Each component of the inflammatory cascade should be accurately dissected to analyse the contribution to the pathogenesis of FOP. Understanding if the effect of mutation affects directly immune cells or if generates an aberrant inflammatory response it would be important in order to design a therapy aiming at rebalance the activation of inflammatory response to a physiological state instead of generally turn the immune system off. Even if inhibition of inflammation can abrogate heterotopic ossification, a reduced activation impairs muscle regeneration, limiting the beneficial effects of potential therapy

The role of endothelial cells in HO have been up to now overlooked, their contribution to HO should be investigated beyond the osteogenic differentiation potential induced by EndMT. Bone and vasculature are

two connected systems, influencing their growth, differentiation, development and regeneration in a mutual manner. Bone cells produce VEGF that stimulates angiogenesis (27), fundamental to ensure proper bone vascularization. On the other hand, the work of Kusumbe et al. (28) demonstrates the existence of specialized vessels that control the differentiation of osteogenic precursors. Investigate the involvement of endothelium in the maintenance of bone structure can pave the way to treat late-stage osseous lesions, an issue that none of the approaches developed up to now has taken in consideration. Also new signalling pathways other than TGFβ and TNFα should be considered as therapeutic targets. Adar enzymes are emerging as new regulator of endothelial functions: getting new insights in the role of RNA editing mechanism in vasculature could open new therapeutic strategies for different disorders.

In conclusion, the endothelium is able to define the microenvironment in order to promote tissue regeneration, on the other hand, alteration of endothelial cells can trigger a pathological activation eventually turning into EndMT, endangering the whole tissue integrity and function like in the many reporting of EndMT as a pathological mechanism occurring in several diseases. A deep comprehension of the mechanism governing endothelial biology is determinant to develop efficient therapy in several diseases.

5.4 References

1. el-Labban, N.G., Hopper, C., & Barber, P. (1993a). Ultrastructural finding of vascular degeneration in myositis ossificans circumscripta (fibrodysplasia ossificans). *J Oral Pathol Med*, *22*, 428-431.

2. Provot, S. & Schipani, E. (2005). Molecular mechanisms of endochondral bone development. *Biochemical and Biophysical Research Communications*, *328*, 658-665.

3. Aird, W.C. (2012). Endothelial cell heterogeneity. *Cold Spring Harb Perspect Med*, *2*, a006429.

4. Cho, J.G., Lee, A., Chang, W., Lee, M.S., & Kim, J. (2018). Endothelial to Mesenchymal Transition Represents a Key Link in the Interaction between Inflammation and Endothelial Dysfunction. Front Immunol, 9, 294

5. Scott, D.W., Vallejo, M.O., & Patel, R.P. (2013). Heterogenic endothelial responses to inflammation: role for differential N-glycosylation and vascular bed of origin. *J Am Heart Assoc*, *2*, e000263.

6. Invernici, G., Ponti, D., Corsini, E., Cristini, S., Frigerio, S., Colombo, A., Parati, E., & Alessandri, G. (2005). Human microvascular endothelial cells from different fetal organs demonstrate organ-specific CAM expression. *Exp Cell Res*, *308*, 273-282.

7. Aird, W.C. (2007). Phenotypic heterogeneity of the endothelium: II. Representative vascular beds. *Circ Res*, *100*, 174-190.

8. Massagué, J. (1998). TGFβ-beta signal transduction. Annu Rev Biochem, 67, 753-791.

9. Stellos, K., Gatsiou, A., Stamatelopoulos, K., Perisic Matic, L., John, D., Lunella, F.F., Jaé, N., Rossbach, O., Amrhein, C., Sigala, F., Boon, R.A., Fürtig, B., Manavski, Y., You, X., Uchida, S., Keller, T., Boeckel, J.N., Franco-Cereceda, A., Maegdefessel, L., Chen, W., Schwalbe, H., Bindereif, A., Eriksson, P., Hedin, U., Zeiher, A.M., & Dimmeler, S. (2016). Adenosine-to-inosine RNA editing controls cathepsin S expression in atherosclerosis by enabling HuR-mediated post-transcriptional regulation. *Nat Med*, 22, 1140-1150.

10. Welten, S.M., Goossens, E.A., Quax, P.H., & Nossent, A.Y. (2016). The multifactorial nature of microRNAs in vascular remodelling. *Cardiovasc Res*, *110*, 6-22.

11. Lees-Shepard, J.B., Yamamoto, M., Biswas, A.A., Stoessel, S.J., Nicholas, S.E., Cogswell, C.A., Devarakonda, P.M., Schneider, M.J., Cummins, S.M., Legendre, N.P., Yamamoto, S., Kaartinen, V., Hunter, J.W., & Goldhamer, D.J. (2018a). Activin-dependent signaling in fibro/adipogenic progenitors causes fibrodysplasia ossificans progressiva. Nat Commun, 9, 471.

12. Abou-khalil, R., Mounier, R., & Chazaud, B. (2010). The " ménage à trois " of satellite cells , periendothelial cells and endothelial cells Regulation of myogenic stem cell behavior by vessel cells. *4101*.

13. Tidball, J.G. & Villalta, S.A. (2010). Regulatory interactions between muscle and the immune system during muscle regeneration. *Am J Physiol Regul Integr Comp Physiol*, *298*, R1173-1187.

14. Zordan, P., Rigamonti, E., Freudenberg, K., Conti, V., Azzoni, E., Rovere-Querini, P., & Brunelli, S. (2014). Macrophages commit postnatal endothelium-derived progenitors to angiogenesis and restrict endothelial to mesenchymal transition during muscle regeneration. Cell Death Dis, 5, e1031.

15. Tidball, J.G. (2017). Regulation of muscle growth and regeneration by the immune system. Nat Rev Immunol, 17, 165-178.

16. Convente, M.R., Chakkalakal, S.A., Yang, E., Caron, R.J., Zhang, D., Kambayashi, T., Kaplan, F.S., & Shore, E.M. (2018). Depletion of Mast Cells and Macrophages Impairs Heterotopic Ossification in an Acvr1. J Bone Miner Res, 33, 269-282.

17. Kaplan, F.S., Pignolo, R.J., & Shore, E.M. (2016). Granting immunity to FOP and catching heterotopic ossification in the Act. Semin Cell Dev Biol, 49, 30-36

18. Del Zotto, G., Antonini, F., Azzari, I., Ortolani, C., Tripodi, G., Giacopelli, F., Cappato, S., Moretta, L., Ravazzolo, R., & Bocciardi, R. (2018). Peripheral Blood Mononuclear Cell Immunophenotyping in Fibrodysplasia Ossificans Progressiva Patients: Evidence for Monocyte DNAM1 Up-regulation. *Cytometry B Clin Cytom*, *94*, 613-622.

19. Reymond, N., Imbert, A.M., Devilard, E., Fabre, S., Chabannon, C., Xerri, L., Farnarier, C., Cantoni, C., Bottino, C., Moretta, A., Dubreuil,

P., & Lopez, M. (2004a). DNAM-1 and PVR regulate monocyte migration through endothelial junctions. *J Exp Med*, *199*, 1331-1341.

20. Balakumar, P., Nyo, Y.H., Renushia, R., Raaginey, D., Oh, A.N., Varatharajan, R., & Dhanaraj, S.A. (2014). Classical and pleiotropic actions of dipyridamole: Not enough light to illuminate the dark tunnel? *Pharmacol Res*, *87*, 144-150.

21. Pignolo, R.J., Shore, E.M., & Kaplan, F.S. (2013). Fibrodysplasia ossificans progressiva: diagnosis, management, and therapeutic horizons. Pediatr Endocrinol Rev, 10 Suppl 2, 437-448

22. Kaplan, F.S. (2011). THE MEDICAL MANAGEMENT OF FIBRODYSPLASIA OSSIFICANS PROGRESSIVA: CURRENT TREATMENT CONSIDERATIONS. Clin Proc Intl Clin Consort FOP, 4,1-100

23. Neely, M.D., Litt, M.J., Tidball, A.M., Li, G.G., Aboud, A.A., Hopkins, C.R., Chamberlin, R., Hong, C.C., Ess, K.C., & Bowman, A.B. (2012). DMH1, a highly selective small molecule BMP inhibitor promotes neurogenesis of hiPSCs: comparison of PAX6 and SOX1 expression during neural induction. ACS Chem Neurosci, 3, 482-491.

24. Yuasa, S., Fukuda, K.,.(2008). Multiple roles for BMP signaling in cardiac development. Cardiovascular stem cells

25. Shimono, K., Tung, W.E., Macolino, C., Chi, A.H., Didizian, J.H., Mundy, C., Chandraratna, R.A., Mishina, Y., Enomoto-Iwamoto, M., Pacifici, M., & Iwamoto, M. (2011a). Potent inhibition of heterotopic ossification by nuclear retinoic acid receptor-γ agonists. *Nat Med*, *17*, 454-460.

26. Lees-Shepard, J.B., Nicholas, S.E., Stoessel, S.J., Devarakonda, P.M., Schneider, M.J., Yamamoto, M., & Goldhamer, D.J. (2018).

Palovarotene reduces heterotopic ossification in juvenile FOP mice but exhibits pronounced skeletal toxicity. *Elife*, *7*.

27. Ruckle, J., Jacobs, M., Kramer, W., Pearsall, A.E., Kumar, R., Underwood, K.W., Seehra, J., Yang, Y., Condon, C.H., & Sherman, M.L. (2009). Single-dose, randomized, double-blind, placebo-controlled study of ACE-011 (ActRIIA-IgG1) in postmenopausal women. *J Bone Miner Res*, *24*, 744-752.

28. Dey, D., Bagarova, J., Hatsell, S.J., Armstrong, K.A., Huang, L., Ermann, J., Vonner, A.J., Shen, Y., Mohedas, A.H., Lee, A., Eekhoff, E.M., van Schie, A., Demay, M.B., Keller, C., Wagers, A.J., Economides, A.N., & Yu, P.B. (2016). Two tissue-resident progenitor lineages drive distinct phenotypes of heterotopic ossification. *Sci Transl Med*, *8*, 366ra163.

29. Maes, C. (2013a). Role and regulation of vascularization processes in endochondral bones. *Calcif Tissue Int*, *92*, 307-323.

30. Kusumbe, A.P., Ramasamy, S.K., & Adams, R.H. (2014). Coupling of angiogenesis and osteogenesis by a specific vessel subtype in bone. Nature, 507, 323-328.